AD_____

Award Number: W81XWH-07-1-0250

TITLE: Development of Augmented Leukemia/Lymphoma-Specific T-Cell Immunotherapy for Deployment with Haploidentical, Hematompoietic Progenitor-Cell Transplant

PRINCIPAL INVESTIGATOR: Laurence Cooper, Ph.D.

CONTRACTING ORGANIZATION: University of Texas M.D. Anderson Cancer Center
Houston, TX 77030

REPORT DATE: May 2011

TYPE OF REPORT: Final

PREPARED FOR: U.S. Army Medical Research and Materiel Command
Fort Detrick, Maryland 21702-5012

REPORT DOCUMENTATION PAGE

Form Approved
OMB No. 0704-0188

1. REPORT DATE *(DD-MM-YYYY)*	2. REPORT TYPE	3. DATES COVERED *(From - To)*
01-05-2011	Final	15 APR 2007 - 14 APR 2011

4. TITLE AND SUBTITLE

Development of Augmented Leukemia/Lymphoma-Specific T-Cell Immunotherapy for Deployment with Haploidentical, Hematompoietic Progenitor-Cell Transplant

5a. CONTRACT NUMBER

5b. GRANT NUMBER

W81XWH-07-1-0250

5c. PROGRAM ELEMENT NUMBER

6. AUTHOR(S)

Laurence Cooper, Ph.D.

E-Mail: ljncooper@mdanderson.org

5d. PROJECT NUMBER

5e. TASK NUMBER

5f. WORK UNIT NUMBER

7. PERFORMING ORGANIZATION NAME(S) AND ADDRESS(ES)

University of Texas M.D. Anderson Cancer Center
Houston, TX 77030

8. PERFORMING ORGANIZATION REPORT NUMBER

9. SPONSORING / MONITORING AGENCY NAME(S) AND ADDRESS(ES)

U.S. Army Medical Research and Materiel Command
Fort Detrick, Maryland 21702-5012

10. SPONSOR/MONITOR'S ACRONYM(S)

11. SPONSOR/MONITOR'S REPORT NUMBER(S)

12. DISTRIBUTION / AVAILABILITY STATEMENT

Approved for Public Release; Distribution Unlimited

13. SUPPLEMENTARY NOTES

14. ABSTRACT

This is the final progress report for this grant application and describes our progress to date developing T cells with specificity for CD19.

15. SUBJECT TERMS

Leukemia, Lymphoma, Transplant, Transplantation: bone marrow and stem cell, T-Cell immunotherapy

16. SECURITY CLASSIFICATION OF:			17. LIMITATION OF ABSTRACT	18. NUMBER OF PAGES	19a. NAME OF RESPONSIBLE PERSON
a. REPORT	b. ABSTRACT	c. THIS PAGE			USAMRMC
U	U	U	UU	61	19b. TELEPHONE NUMBER *(include area code)*

"Development of Augmented Leukemia/Lymphoma-Specific T-Cell Immunotherapy for Deployment with Haploidentical Hematopoietic Progenitor-Cell Transplant"

TABLE OF CONTENTS

Development of Augmented Leukemia/Lymphoma-Specific T-Cell Immunotherapy for Deployment with Haploidentical Hematopoietic Progenitor-Cell Transplant

I. INTRODUCTION

Herein is a revision of final report based on 0 9-30-2011 email from Wendy Clevenger (Information management) and James Phillips (Science Officer). This report provides the progress to date regarding the genetic modification and propagation of human T cells that have been rendered specific for CD19, a B-lineage antigen expressed on most B-cell malignancies. We have successfully generated the pre-clinical data to: (1) genetically modify, and (2) numerically expand T cells that have been engineered to express a chimeric antigen receptor (CAR) enabling T cells to recognize and eliminate $CD19^+$ malignancies. This has clinical implications for improving the graft-verses-tumor effect after haploidentical hematopoietic progenitor cell transplantation. In this report we summarize our findings to date with emphasis on the translational implications of our approach. Please refer to prior interim progress reports for additional information.

II. BODY

The original 4-year grant application identified three tasks to improve the potency of genetically modified T cells. All of these tasks relied on the development of a new gene therapy approach to expressing a CAR. This was successfully accomplished and is based on the clinical adaptation of the *Sleeping Beauty* transposon/transposase system. We have demonstrated that the electro-transfer of the *Sleeping Beauty* transposon as a DNA plasmid, to express a CD19-specific CAR, in coordination with the electro-transfer of a h yperactive *Sleeping Beauty* transpose (SB11) can be used to efficiently integrate the CAR (designated CD19RCD28) in the T-cell genome. We have combined this gene transfer approach with an ability to selectively propagate T cells that have stably integrated CAR such that within three to four weeks after electroporation our culture systems can retrieve clinically significant numbers of CD19-specific CAR^+ T cells. These T cells have been shown, in a CAR-dependant fashion, to have the expected redirected specificity for recognition of $CD19^+$ leukemias and lymphomas. This was demonstrated using assays measuring the killing of malignant B cells as well as methodologies to investigate the ability of CAR to provide a fully competent activation signal enabling the T cells to produce cytokines as well as proliferate upon docking to the CD19 antigen. It is these data in aggregate that enabled us to successfully carryout all of the tasks identified in the original grant application. It is emphasized that our approach to the genetic modification and numeric expansion of T cells can now be undertaken in compliance with current good manufacturing practice (cGMP) to undertake Phase I clinical trials.

III. KEY RESEARCH ACCOMPLISHMENT

The statement of work (SOW) pre-identified the following tasks:

Task 1: Development of CD10-specific-IL2 ICK to be used in combination with CD19-specific T cells to improve persistence of infused T cells and to treat B-lineage malignancy

- Develop CD10-specific-IL2 ICK
- Combine with CD19-specific T cells *in vivo*
- Interim analysis

Task 2: Development of CD19-specific CD4+ Th cells to improve the anti-tumor response of CD19-specific CD8+ T cells

- Develop CD4+ CD19-specific T cells
- Combine with CD19-specific CD8+ T cells *in vivo*
- Interim analysis

Task 3: Development of chimeric antigen receptor (CAR) with CD28 co-stimulation to enhance the survival and potency of CD19-specific T cells

- Develop CD19-specific T cells expressing second-generation chimeric antigen receptor
- Evaluate immunobiology of CD19-specific T cells expressing next-generation CAR *in vivo*
- Interim analysis

Task 4: Final analysis

- Report writing

• Preparation of second-generation clinical trial to evaluate the clinical potential of CD19-specific T-cell therapy with augmented therapeutic potential

The major research objectives that have been achieved are as follows.

Task 1

We were able to demonstrate that the therapeutic potential of CD19-specific CAR^+ T cells can be augmented by the addition of an immunocytokine. The immunocytokine we used is a fusion protein combining specificity of antibody for CD20 fused to interleukin (IL)-2, a multi-function cytokine that can provide a proliferative signal to T cells (*e.g.*, Figure 2 of Cancer Res 2007;67:2872-2880, in Appendix). We have demonstrated that the ability of CD19-specific cells to eradicate malignant $CD19^+CD20^+$ B cells is augmented *in vivo* using combination immunotherapy whereby the T cells are combined with the administration of the immunocytokine (*e.g.*, Figure 3 and Figure 5 of Cancer Res 2007;67:2872-2880, in Appendix). This has implications for clinical translation given that the genetically modified T cells have been adapted for human use and similarly the CD20-specific immunocytokine has also been prepared for clinical application. The paper (Cancer Res 2007;67:2872-2880, in Appendix) that reports these data was published on line 03-15-2007, just before the grant was funded. This reflects progress made while the grant was under consideration by the reviewers. As mentioned in prior progress reports, we discontinued work under this task.

Task 2

We were able to substitute the need for immunocytokine through the development of T cells that are capable of providing the T-cell helper function manifested by IL-2. This was accomplished by designing a platform for propagating genetically modified T cells that express CD4. We found that the $CD4^+CAR^+$ T cells were capable by themselves secreting IL-2 in a C AR-dependant manner thereby providing the necessary cytokine milieu in the tumor microenvironment to support persistence and indeed the numeric expansion of CAR^+ T cells (*e.g.*, Figure 3 of Cancer Res 2008;68:2961-2971, in Appendix). To help generate $CD4^+CAR^+$ T cells we adapted the *Sleeping Beauty* system to use a more enzymatically variant of SB11 transposase, termed SB100X (*e.g.*, Figure 2 of Gene Therapy 2011;9:849-856, in Appendix). Task 2 also has clinical implications given that $CD4^+CAR^+$ and $CD8^+CAR^+$ T cells can be retrieved using our propagation technology. In particular the was accomplished by designing artificial antigen presenting cells (aAPC) which were engineered to express desired co stimulatory molecules in addition to expressing CD19. The aAPC can be combined with soluble cytokines such as IL-21 (in addition to IL-2) to support the outgrowth of both $CD4^+$ and $CD8^+$ genetically modified T cells (*e.g.*, Figure 2 of Cancer Res 2011;71:3516-3527, in Appendix). Recognizing that T-cell helper function is desirable as initially envisioned provided by the IL-2 immunocytokine and then adapted through the ability of $CD4^+$ T cells to serve as their own source of IL-2, we went on to explore whether all T cells might be modified to secret this cytokine. This was accomplished by the recognition that the CAR itself could serve as a signaling molecule to trigger T cells to generate IL-2. This enabled us to design and successfully test a second generation CAR molecule that has coordinated signaling through both CD3-zeta (the only signaling molecule in the first generation CAR) with chimeric CD28.

Task 3

The development of this second generation CAR with co-stimulation was the topic of this task. We also recognized that the intrinsic signaling provided through the chimeric CD28 obviates the need for the genetically modified CAR^+ T cells to receive signaling through endogenous CD28. This enabled us to test whether blockade of signaling through endogenous CD28, with continued ability to signal through chimeric CD28, would provide an advantage as we proceed towards the goal to infuse haploidentical T cells in the setting of hematopoietic stem-cell transplantation (HSCT). For, one of the major problems with the adoptive transfer of donor-derived T cells that are HLA-mismatched is that these infused cells can cause graft-verses-host disease (GVHD). Thus, the ability to manipulate the T-cell product before infusion to reduce the potential for GVHD would be highly attractive and have clinical implication. Recognizing that blockade of signaling through endogenous CD28 might induce anergy, we set about to explore this potential in the third task. We demonstrated that the co-stimulatory blockade using soluble molecules to interrupt the binding of CD28 with its ligands (CD80 and CD86) leads to the welcomed emergence of CAR^+ T cells that are selectively depleted of cells that can recognize the disparate HLA molecules (*e.g.*, Figure 3 of Cancer Res 2010;70:3915-3924, in Appendix). What is particularly attractive about this approach is that the agents used to induce the co-stimulatory blockade have been prepared for clinical translation and thus the approach to induce anergy has human application.

Task 4

Based on the encouraging data from the prior three tasks, we have implemented a next-generation clinical trial infusing CD19-specific T cells. This trial has completed all institutional and federal regulatory approvals and is open to accrual.

IV. REPORTABLE OUTCOMES

The major outcomes of the grant application are that we have:

a) Developed a new gene transfer approach based on electro proration of T cells to introduce the *Sleeping Beauty* transposon and transpose plasmids to stability express the CAR to redirect T cells specificity of CD19.
b) Designed aAPC for the purposes of retrieving large numbers of genetically modified CAR^+ T cells that express the immunoreceptor in both CD4 and CD8 subpopulations.
c) Demonstrated that the therapeutic potential of genetically modified T cells can be improved when both CD19 and CD20 are targeted on malignant B cells using combination immunotherapy whereby the CAR^+ T cells are co-administered with an immunocytokine.
d) Shown that the $CD4^+$ subset of T cells is capable of providing IL-2 to augment T cell persistence in a CAR dependent manner.
e) Engineered the CAR to serve as a molecule capable of inducing the production of IL-2 in a CAR-dependant manner.
f) Demonstrated that co stimulatory blockade can be used to induce anergy to disparate HLA molecules.
g) Developed methodologies in keeping with their clinical translation.

V. CONCLUSION

This grant application was successful as we met all the stated tasks. We were able to demonstrate that combination immunotherapy provided increased potency and that genetically modified T cells can be engineered for improve persistence based on an ability to generate IL-2. This was accomplished using a novel gene therapy platform using the *Sleeping Beauty* system used in combination with designer aAPC. We have already moved this technology to the clinical arena. While outside the original grant application, we have now instituted a first-in-human clinical trial whereby the genetically modified T cells based on the *Sleeping Beauty* system and numeric expansion on the aAPC are being used in humans to augment the graft-verses-tumor effect HSCT. Thank you for your support.

VI. REFERENCES

The references in this application are based on the major published reports that have resulted and/or contributed to the work in this grant application. These are summarized below.

1. Singh H, Manuri PR, Olivares S, Dara N, Dawson MJ, Huls H, Hackett PB, Kohn DB, Shpall EJ, Champlin RE, Cooper LJ. Redirecting specificity of T-cell populations for CD19 using the Sleeping Beauty system. Cancer Res. 2008 Apr 15;68(8):2961-71.
2. Singh H, Figliola MJ, Dawson MJ, Huls H, Olivares S, Switzer K, Mi T, Maiti S, Kebriaei P, Lee DA, Champlin RE, Cooper LJ. Reprogramming CD19-Specific T Cells with IL-21 Signaling Can Improve Adoptive Immunotherapy of B-Lineage Malignancies. Cancer Res. 2011 May 15;71(10):3516-27.
3. Jin Z, Maiti S, Huls H, Singh H, Olivares S, Mátés L, Izsvák Z, Ivics Z, Lee DA, Champlin RE, Cooper LJ. The hyperactive Sleeping Beauty transposase SB100X improves the genetic modification of T cells to express a chimeric antigen receptor. Gene Ther. 2011 Mar 31. [Epub ahead of print]
4. Davies JK, Singh H, Huls H, Yuk D, Lee DA, Kebriaei P, Champlin RE, Nadler LM, Guinan EC, Cooper LJ. Combining CD19 redirection and alloanergization to generate tumor-specific human T cells for allogeneic cell therapy of B-cell malignancies. Cancer Res. 2010 May 15;70(10):3915-24.
5. Singh H, Serrano LM, Pfeiffer T, Olivares S, McNamara G, Smith DD, Al-Kadhimi Z, Forman SJ, Gillies SD, Jensen MC, Colcher D, Raubitschek A, Cooper LJ. Combining adoptive cellular and immunocytokine therapies to improve treatment of B-lineage malignancy. Cancer Res. 2007 Mar 15;67(6):2872-80.

VII. APPENDICES

VIII. In these appendices we provide some of the key papers that have resulted from the funding. As previously noted, Cancer Res 2007;67:2872-2880 summarizes data for Task 1 that was undertaken before the grant application was funded. These are:

- Cancer Res 2007;67:2872-2880
  - Combining adoptive cellular and immunocytokine therapies to improve treatment of B-lineage malignancy
- Cancer Res 2008;68:2961-2971
  - Redirecting specificity of T-cell populations for CD19 using the Sleeping Beauty system
- Gene Therapy 2011;9:849-856
  - The hyperactive Sleeping Beauty transposase SB100X
- Cancer Res 2011;71:3516-3527
  - Reprogramming CD19-Specific T Cells with IL-21 Signaling Can Improve Adoptive Immunotherapy of B-Lineage Malignancy
- Cancer Res 2010;70:3915-3924
  - Combining CD19 redirection and alloanergization to generate tumor-specific human T cells for allogeneic cell therapy of B-cell malignancies

IX. SUPPORTING DATA

Please refer to the published papers in the appendices for the relevant data set.

X. FINACIALS

Final information on the allocation of monies from this grant will be provided by our Grants and Contracts department.

DOI:10.1158/0008-5472.CAN-06-2283

Cancer Research

Combining Adoptive Cellular and Immunocytokine Therapies to Improve Treatment of B-Lineage Malignancy

Harjeet Singh, Lisa Marie Serrano, Timothy Pfeiffer, et al.

Cancer Res 2007;67:2872-2880. Published online March 15, 2007.

DOI:10.1158/0008-5472.CAN-06-2283

Research Article

Combining Adoptive Cellular and Immunocytokine Therapies to Improve Treatment of B-Lineage Malignancy

Harjeet Singh,[1,7] Lisa Marie Serrano,[1] Timothy Pfeiffer,[1] Simon Olivares,[1,7] George McNamara,[2] David D. Smith,[3] Zaid Al-Kadhimi,[1,4] Stephen J. Forman,[2,4] Stephen D. Gillies,[6] Michael C. Jensen,[2,4,5] David Colcher,[2] Andrew Raubitschek,[2] and Laurence J.N. Cooper[1,4,5,7]

Divisions of [1]Molecular Medicine, [2]Cancer Immunotherapeutics and Tumor Immunology, [3]Biomedical Informatics, [4]Hematology and Hematopoietic Cell Transplantation, and [5]Pediatric Hematology/Oncology, Beckman Research Institute and City of Hope National Medical Center; [6]EMD Lexigen Research Center, Billerica, Massachusetts; and [7]Division of Pediatrics, The University of Texas M. D. Anderson Cancer Center, Houston, Texas

Abstract

Currently, the lineage-specific cell-surface molecules CD19 and CD20 present on many B-cell malignancies are targets for both antibody- and cell-based therapies. Coupling these two treatment modalities is predicted to improve the antitumor effect, particularly for tumors resistant to single-agent biotherapies. This can be shown using an immunocytokine, composed of a CD20-specific monoclonal antibody fused to biologically active interleukin 2 (IL-2), combined with *ex vivo* expanded human umbilical cord blood–derived $CD8^+$ T cells, that have been genetically modified to be CD19 specific, for adoptive transfer after allogeneic hematopoietic stem-cell transplantation. We show that a benefit of targeted delivery of recombinant IL-2 by the immunocytokine to the $CD19^+CD20^+$ tumor microenvironment is improved *in vivo* persistence of the CD19-specific T cells, and this results in an augmented cell-mediated antitumor effect. Phase I trials are under way using anti-CD20-IL-2 immunocytokine and CD19-specific T cells as monotherapies, and our results warrant clinical trials using combination of these two immunotherapies. [Cancer Res 2007;67(6):2872–80]

Introduction

Malignant B cells express a pattern of cell surface molecules that define their lineage commitment (1–3), and these are the targets of monoclonal antibody (mAb)–based (4–6) and T-cell–based treatment approaches (7–11). However, these immunotherapies may fail to eradicate tumor as a result of an inability of tumor-specific mAb to fully activate the effector functions of the recipient (12–15) and curtailed T-cell persistence after adoptive immunotherapy (16–18). Therefore, strategies that augment mAb function and T-cell survival are predicted to improve the therapeutic effect.

An approach to improve the clinical potential of mAb is to fuse interleukin 2 (IL-2) to a tumor-specific recombinant mAb (e.g., CD20-specific mAb) to deliver this immunostimulatory cytokine to the tumor microenvironment, which leads to recruitment and activation of immune cells that express the cytokine receptor (19–21). *Ex vivo* propagated genetically modified T cells that have been rendered tumor specific are a population of effector cells whose survival is predicted to benefit from this locoregional deposition of IL-2.

To obtain large numbers of clinical-grade, tumor-specific T cells that target B-lineage lymphoma and leukemia, we and others have enforced expression of a CD19-specific chimeric immunoreceptor (designated CD19R), which combines antibody recognition with T-cell effector functions (7, 10, 22). In particular, CD19-specific T cells can be manufactured from umbilical cord blood to augment the graft-versus-tumor effect after allogeneic hematopoietic stem-cell transplantation (23). However, factors that may limit the successful therapeutic use of these *ex vivo* expanded $CD8^+$ T cells include a dependence on exogenous IL-2 to achieve and sustain their proliferative potential after adoptive transfer (24).

With the generation of an anti-CD20-IL-2 immunocytokine (DI-Leu16-IL-2; ref. 25), we now ask if targeted delivery of IL-2 to sites of CD20 binding on malignant B cells could improve the survival and antitumor effect of CD19-specific T cells. In the present study, we show that the anti-CD20-IL-2 immunocytokine binds specifically to $CD20^+$ tumors as well as $IL\text{-}2R^+$ (IL-2 receptor positive) T cells and that infusing a combination of anti-CD20-IL-2 immunocytokine with $CD19R^+$ T cells improves *in vivo* T-cell persistence, which leads to an augmented clearance of $CD20^+CD19^+$ tumor beyond that achieved by delivery of the immunocytokine or T cells alone.

Materials and Methods

Plasmid expression vectors. The plasmid vector CD19R/ffLucHyTK-pMG, described previously, coexpresses the *CD19R* chimeric immunoreceptor gene and the tripartite fusion gene *ffLucHyTK* (22). Truncated CD19, lacking the cytoplasmic domain (26), was expressed in ffLucHyTK-pMG to generate the plasmid tCD19/ffLucHyTK-pMG to coexpress the *CD19* and *ffLucHyTK* transgenes. The bifunctional *hRLucZeo* fusion gene that coexpresses the *Renilla koellikeri* (sea pansy) luciferase hRLuc and the zeomycin-resistance gene (*Zeo*) was cloned from the plasmid pMOD-LucSh (InvivoGen, San Diego, CA) into $pcDNA3.1^+$ (Invitrogen, Carlsbad, CA) to create the plasmid hRLuc:Zeocin-pcDNA3.1.

Propagation of cell lines and primary human T cells. Daudi, ARH-77, Raji, SUP-B15, and K562 cells were obtained from American Type Culture Collection (Manassas, VA). Granta-519 cells were obtained from DSMZ (Braunschweig, Germany). An EBV-transformed lymphoblastoid cell line was kindly provided by Drs. Phillip Greenberg and Stanley Riddell (Fred Hutchinson Cancer Research Center, Seattle, WA). These cells were maintained in tissue culture as described (23). $IL\text{-}2R\beta^+$ TF-1β cells were kindly provided by Dr. Paul M Sondel (University of Wisconsin, Madison, WI; ref. 27). Human T-cell lines were derived from umbilical cord blood mononuclear cells after informed consent and were cultured as previously described (22, 28).

Note: Supplementary data for this article are available at Cancer Research Online (http://cancerres.aacrjournals.org/).

Requests for reprints: Laurence J.N. Cooper, Pediatrics-Research, Unit 907, The University of Texas M. D. Anderson Cancer Center, 1515 Holcombe Boulevard, Houston, TX 77030. Phone: 713-563-3360; Fax: 713-563-0604; E-mail: ljncooper@mdanderson.org.

doi:10.1158/0008-5472.CAN-06-2283

DOI:10.1158/0008-5472.CAN-06-2283

Immunocytokines. The anti-CD20-IL-2 (DI-Leu16-IL-2) immunocytokine was derived from a deimmunized anti-CD20 murine mAb (Leu16). Anti-GD_2-IL-2 (14.18-IL-2), which recognized GD_2 disialoganglioside, served as a control immunocytokine with irrelevant specificity for B-lineage tumor line used in this study (EMD Lexigen Research Center, Billerica, MA; ref. 29).

Nonviral gene transfer of DNA plasmid vectors. OKT3-activated umbilical cord blood–derived T cells were genetically modified by electroporation with CD19R/ffLucHyTK-pMG (23). ARH-77 was electroporated with hRLuc:Zeocin-pcDNA3.1 using the Multiporator device (250V/40 μs, Eppendorf, Hamburg, Germany) and propagated in cytocidal concentration (0.2 mg/mL) of zeocin (InvivoGen).

Flow cytometry. FITC- or phycoerythrin-conjugated reagents were obtained from BD Biosciences (San Jose, CA): anti-TCRαβ, anti-CD3, anti-CD4, anti-CD8, anti-CD25, and anti-CD122. $F(ab')_2$ fragment of FITC-conjugated goat anti-human Fcγ (Jackson Immunoresearch, West Grove, PA) was used at 1/20 dilution to detect cell surface expression of *CD19R* transgene. Leu16 and anti-CD20-IL-2 immunocytokine (100 μg each) were conjugated to Alexa Fluor 647 (Molecular Probes, Eugene OR). Data acquisition was on a FACSCalibur (BD Biosciences) using CellQuest version 3.3 (BD Biosciences), and analysis was undertaken using FCS Express version 3.00.007 (Thornhill, Ontario, Canada).

Chromium release assay. The cytolytic activity of T cells was determined by 4-h chromium release assay (CRA; ref. 22). CD19-specific T cells were incubated with 5×10^3 chromium-labeled target cells in a V-bottomed 96-well plate (Costar, Cambridge, MA). The percentage of specific cytolysis was calculated from the release of ^{51}Cr, as described earlier, using a TopCount NXT (Perkin-Elmer Life and Analytical Sciences, Inc., Boston, MA). Data are reported as mean ± SD.

Immunofluorescence microscopy. $CD19R^+$ T cells (10^6) and $CD19^+$ $CD20^+$tumor cells (10^6) were centrifuged at 200 × *g* for 1 min and incubated at 37°C for 30 min. After gentle resuspension, the cells were sedimented, the supernatant was removed, and the pellet was fixed for 20 min with 3% parafomaldehyde in PBS on ice. After washing, the fixed T cell–tumor cell conjugates were incubated for 30 min at 4°C with anti-CD3-FITC or Alexa Fluor 647–conjugated anti-CD20-IL-2 immunocytokine. Nuclei were counterstained with Hoechst 33342 (Molecular Probes; 0.1 μg/mL). Cells were examined on a Zeiss LSM 510 META NLO Axiovert 200M inverted microscope. Hoechst 33342 was excited at 750 nm using Coherent Ti:Sapphire multiphoton laser, Alexa Fluor 647 at 633 nm using helium-neon laser, and FITC at 488 nm using argon ion laser. Images were acquired with a Zeiss plan-neofluar 20×/0.5 air lens or plan neofluar 40×/1.3 numerical aperture oil immersion lens, and fields of view were then examined using Zeiss LSM Image Browser version 3.5.0.223.

Persistence of adoptively transferred T cells. Before the initiation of the experiment, 6- to 10-week-old female NOD/*scid* (NOD/LtSz-*Prkdcscid*/J) mice (The Jackson Laboratory, Bar Harbor, ME) were γ-irradiated to 2.5 Gy using an external ^{137}Cs source (JL Shepherd Mark I Irradiator, San Fernando, CA) and maintained under pathogen-free conditions at City of Hope National Medical Center (COH) Animal Resources Center. On day −7, the mice were injected in the peritoneum with 2×10^6 $hRLuc^+$ $CD19^+CD20^+$ARH-77 cells. Tumor engraftment was evaluated by biophotonic imaging (see "Biophotonic imaging") and mice with progressively growing tumors were segregated into four treatment groups to receive 10^7 CD19-specific T cells (day 0) either alone or in combination with 75,000 units/injection (equivalent to ~25 μg immunocytokine; ref. 25) of IL-2 (Chiron, Emeryville, CA), 5 μg/injection of anti-CD20-IL-2 immunocytokine (DI-Leu16-IL-2), or 5 μg/injection of anti-GD_2-IL-2 immunocytokine, given by additional separate i.p. injections. Animal experiments were approved by COH institutional committees.

***In vivo* efficacy of combination immunotherapies.** Six- to 10-week-old γ-irradiated NOD/*scid* mice were injected with 2×10^6 $hRLuc^+$ $CD19^+CD20^+$ARH-77 cells in the peritoneum. Sustained tumor engraftment was documented within 7 days of injection by biophotonic imaging. Mice in the four treatment groups received combinations of CD19-specific T cells (10^7 cells in the peritoneum on day 0), anti-CD20-IL-2 immunocytokine, or anti-GD_2-IL-2 immunocytokine (5 μg/injection in the peritoneum).

Biophotonic imaging. Anesthetized mice were imaged using a Xenogen IVIS 100 series system as previously described (30). Briefly, each animal was serially imaged in an anterior-posterior orientation at the same relative time point after 100 μL (0.068 mg/mouse) of freshly diluted Enduren Live Cell Substrate (Promega, Madison, WI), or 150 μL (4.29 mg/mouse) of freshly thawed D-luciferin potassium salt (Xenogen, Alameda, CA) solution injection. Photons were quantified using the software program Living Image (Xenogen). Statistical analysis of the photon flux at the end of the experiment was accomplished by comparing area under the curve using two-sided Wilcoxon rank sum test. Biological T-cell half-life was calculated as $A = I \times (1/2)^{(t/h)}$, where A is flux at time t, I is day 0 flux, and h is rate of decay.

Results

Redirecting T cells specificity for CD19. The genetic modification of umbilical cord blood–derived T cells to render them specific for CD19 was accomplished by nonviral electrotransfer of a DNA expression plasmid designated CD19R/ffLucHyTK-pMG, which codes for the *CD19R* transgene (22) and a recombinant multifunction fusion gene that combines firefly luciferase (*ffLuc*), hygromycin phosphotransferase, and herpes virus thymidine kinase (*HyTK*; ref. 31), permitting *in vitro* selection of $CD19R^+$ T cells with cytocidal concentration of hygromycin B and *in vivo* imaging after infusion of D-luciferin. Genetically modified *ex vivo* expanded T cells were $CD8^+$, expressed components of the high-affinity IL-2R and *CD19R* transgene, as detected by using a Fc-specific antibody (Fig. 1*A*). $CD19R^+$ T cells could specifically lyse leukemia and lymphoma targets expressing CD19 with ~50% to 70% of $CD19^+$ tumor cells killed at an effector to target ratio of 50:1 in a 4 h CRA (Fig. 1*B*). The variability of lysis of the various B-cell lines could be attributed to the expression of various cell surface markers, particularly the adhesion molecules (22). Specific lysis of $CD19^+$ K562 compared with $CD19^-$ K562 cells showed that the killing of $CD19^+$ tumor targets occurred through the chimeric immunoreceptor.

Binding of anti-CD20-IL-2 immunocytokine. The ability of the anti-CD20-IL-2 immunocytokine to bind to both B-lineage tumors and T cells was examined using flow cytometry and confocal microscopy. This immunocytokine bound to $CD20^+$ ARH-77 but not to $CD20^-$ SUP-B15 (data not shown) and K562 cells, consistent with recognition of parental Leu16 mAb for CD20 (Fig. 2*A*; ref. 32). The anti-CD20-IL-2 immunocytokine, but not parental Leu16 mAb, bound to $CD25^+$ genetically modified T cells and TF-1β, a tumor cell line genetically modified to express CD122 (IL-2Rβ; ref. 27), which is consistent with binding of chimeric IL-2 via the IL-2R (Fig. 2*A* and data not shown). The greater median fluorescent intensity (MFI) on T cells, compared with TF-1β, is consistent with binding of the immunocytokine to the high-affinity IL-2R. Immunofluorescence confocal microscopy was done to evaluate the localization of immunocytokine on conjugates of CD19-specific T cells and $CD20^+$ tumors. The confocal micrographs showed cell surface labeling of conjugates of tumor and T cells with Alexa Fluor 647–conjugated anti-CD20-IL-2 immunocytokine (*red*) and T cells labeled with FITC-conjugated anti-CD3 (*green*). Areas of overlapping binding between deposition of immunocytokine and anti-CD3 is depicted by a yellow color (Fig. 2*B*). We hypothesize that T cells show colocalization of CD3 and immunocytokine on their surface initially; however, as they form a synapse with the tumor cell, there seems to be a rearrangement of IL-2R on the T cells toward the synapse leading to the presence of yellow signal extending well outside the synapse and leaving a green pocket opposite the synapse. The Alexa Fluor 647–conjugated parental

DOI:10.1158/0008-5472.CAN-06-2283

anti-CD20 Leu16 mAb, lacking the chimeric IL-2 domain, binds $CD20^+$ tumors, but not the genetically modified T cells (data not shown). In aggregate, these data show that anti-CD20-IL-2 immunocytokine can bind to CD20 molecules on B-lineage tumors and IL-2R on T cells and that this immunocytokine can be deposited at the interface between tumor and T cells.

***In vivo* T-cell persistence given in combination with immunocytokine.** Having determined that the anti-CD20-IL-2 immunocytokine could bind to tumor and T cells, we evaluated whether infusions of anti-CD20-IL-2 immunocytokine could improve the *in vivo* persistence of adoptively transferred genetically modified $CD8^+$ T cells. To achieve sustained locoregional

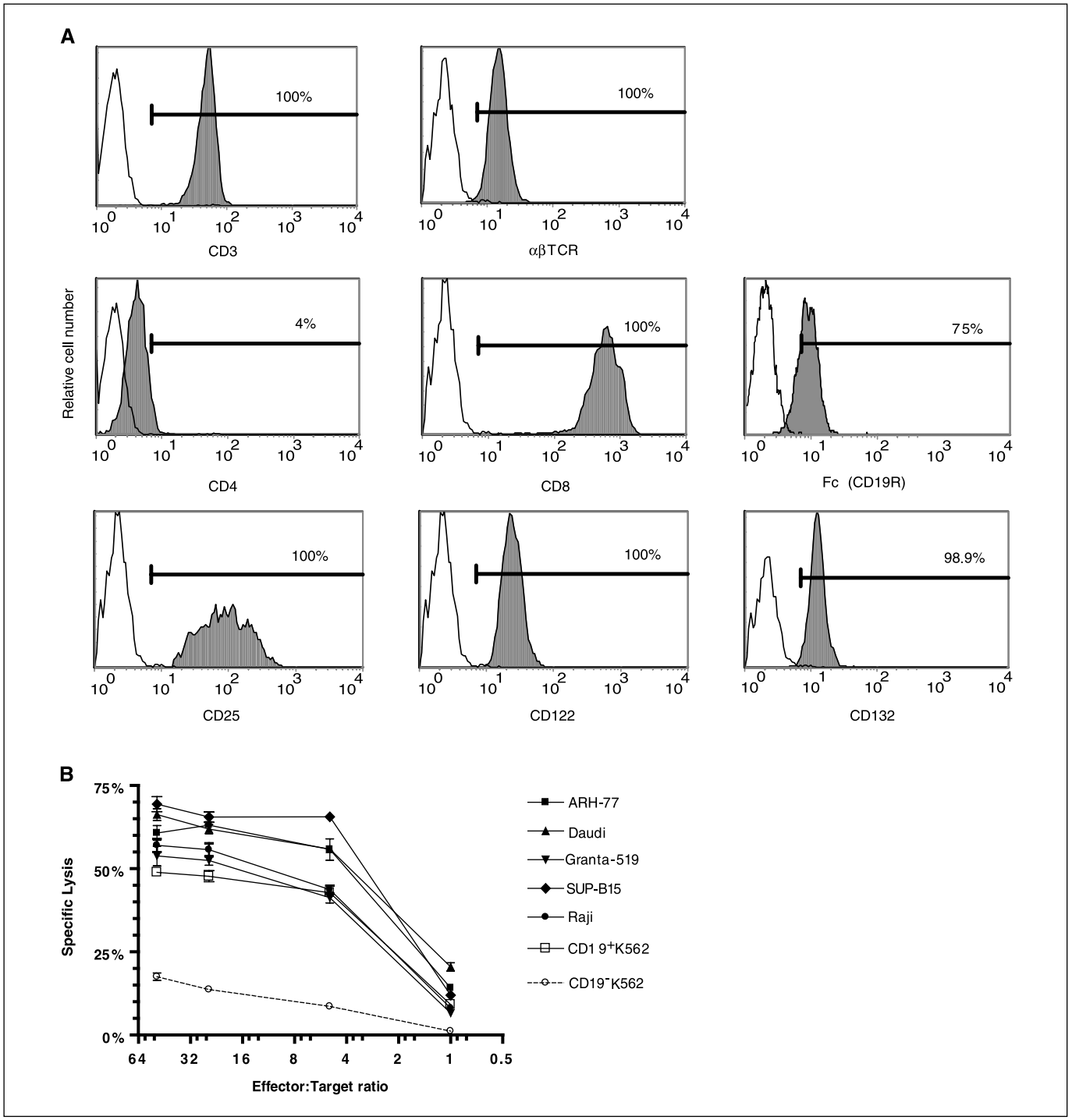

Figure 1. Phenotype and function of genetically modified T cells. *A,* multivariable flow cytometry showing that the genetically modified T cells are predominantly $CD3^+TCR^+CD8^+CD25^+CD122^+CD132^+$. Isotype-matched fluorescent mouse mAb or nonspecific goat control antibody was used to establish the negative gates. The percentage of gated$^+$ cells is shown. *B,* lysis of tumor targets by 4-h CRA. $CD19^+$ B-cell tumor lines are Daudi, ARH-77, SUP-B15, Granta-519, Raji, and genetically modified K562 ($CD19^+$ K562; ref. 30). Background lysis of $CD19^-$ (parental) K562 cells is shown as a control for specificity and endogenous NK-T activity. Spontaneous release of each target was ≤9%. *Points,* mean for triplicate wells at effector to target cell ratios between 50:1 and 1:1; *bars,* ± 1 SD.

DOI:10.1158/0008-5472.CAN-06-2283

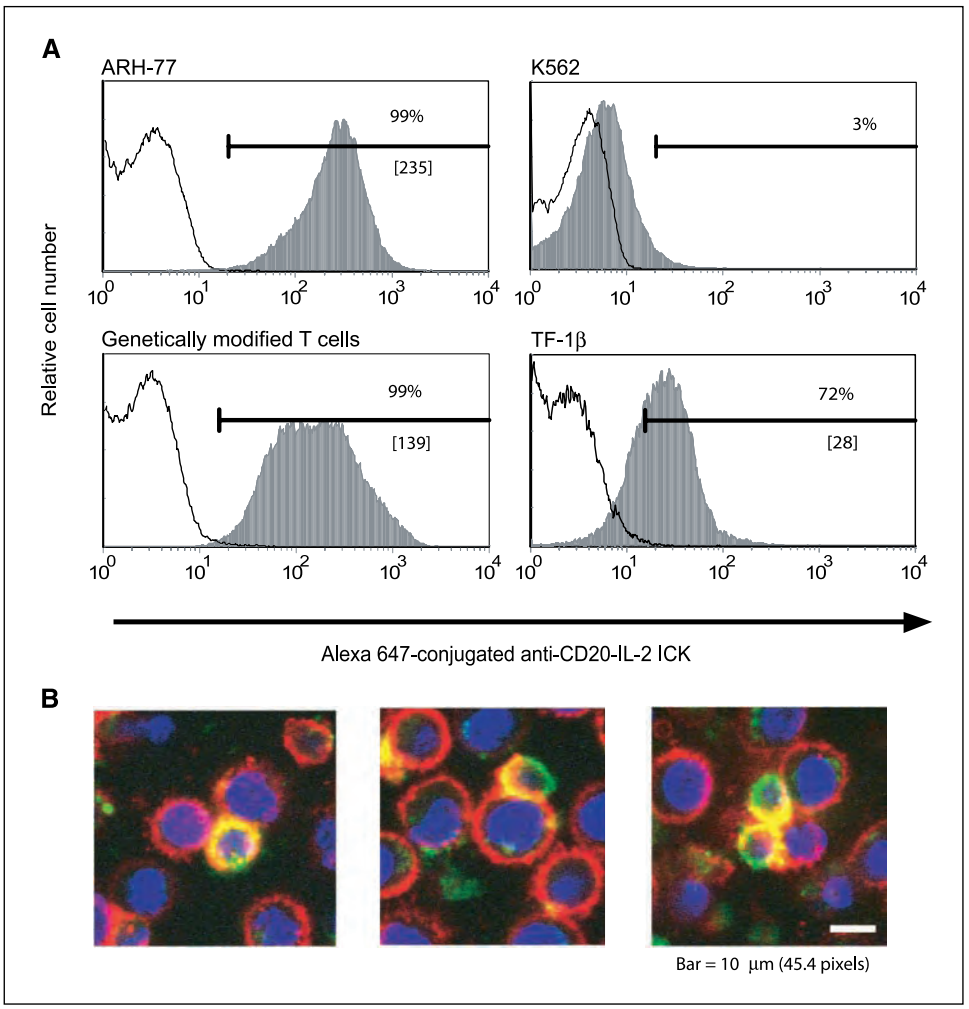

Figure 2. Binding of anti-CD20-IL-2 immunocytokine to B cells and T cells. *A,* flow cytometry analysis of Alexa Fluor 647–conjugated anti-CD20-IL-2 immunocytokine (ICK) binding through CD20 to $CD20^+CD25^-$ ARH-77 and $CD20^-CD25^-$ K562 cell lines; and IL-2 receptors to genetically modified $CD20^-CD25^+$ T cells and $CD20^-CD25^-CD122^+$ TF-1β (*filled histograms*). *Unfilled histograms,* fluorescence of unstained cells. The percentage of gated$^+$ cells and MFI (*in brackets*) are indicated. Alexa Fluor 647 emission (668 nm) was revealed in the APC/Cy5 channel (FL-4). *B,* confocal micrographs of tumor and T-cell conjugates stained with Alexa Fluor 647–conjugated anti-CD20-IL-2 immunocytokine (*red*) and FITC-conjugated anti-CD3 (*green*); cell nuclei were counterstained with Hoechst (*blue*). *Yellow,* areas that show overlapping binding of immunocytokine and anti-CD3 mAb.

depositions of the anti-CD20-IL-2 immunocytokine, we chose the tumor line ARH-77 as a target for immunotherapy because this is relatively resistant to killing by anti-CD20–specific mAb (33), and these results were confirmed *in vivo* in NOD/*scid* mice using rituximab (data not shown). Initially, a dose of immunocytokine was established that could both improve the *in vivo* survival of $CD8^+CD19R^+ffLuc^+$ T cells, compared with adoptive immunotherapy in the absence of immunocytokine, and not statistically alter tumor growth as monotherapy (Fig. 4). We showed that an immunocytokine dose of both 5 and 25 μg could improve the persistence of infused T cells, resulting in a T-cell ffLuc-derived signal detectable above background luminescence measurements ($\leq 10^6$ p/s/cm^2/sr) 14 days after adoptive immunotherapy (Fig. 3*A*). Biological half-life of the infused T cells was determined by calculating the rate of T-cell decay (ffLuc activity) at the end of the experiment and expressed as the number of days required by the cells to achieve half the initial (day 0) flux. Indeed, the biological half-life of the infused T cells was twice as long in mice that received immunocytokine (1.09 days) compared with T cells given alone (0.43 days). As a further indication that infusion of the immunocytokine may enhance the survival of adoptively transferred T cells, we observed an ~300% (3-fold) increase in the ffLuc-derived signal (day 12) compared with day 11 when the immunocytokine was injected in both the groups. As the relative *in vivo* T-cell persistence was similar for both of the immunocytokine doses (P = 0.86), we used 5 μg per immunocytokine injection for subsequent experiments, a dose equivalent to ~15,000 units of human recombinant IL-2 (25).

To determine if the improved T-cell persistence was due to the binding of the immunocytokine in the ARH-77 tumor microenvironment, we used a control immunocytokine (anti-GD_2-IL-2 immunocytokine) that does not bind to GD_2^- ARH-77 (data not shown). Furthermore, we compared the ability of the anti-CD20-IL-2 immunocytokine to potentiate T-cell survival compared with administration of exogenous recombinant human IL-2. Longitudinal measurement of ffLuc-derived flux revealed that the infused T cells persisted longer in mice that received anti-CD20-IL-2 immunocytokine, compared with the untreated (P = 0.01), IL-2–treated (P = 0.02), and control immunocytokine-treated (P = 0.05) groups (Fig. 3*B* and *C*); the biological half-lives of T cells in the groups are 1.7, 0.5, 1.0, and 0.7 days, respectively. There was a difference (P < 0.05) in the *in vivo* persistence of T cells accompanied by IL-2, compared with T cells given without this cytokine, which is consistent with the dependence of these T cells to receive T-cell help in the form of exogenous IL-2 to survive *in vivo*. No apparent difference was observed in the persistence (P = 0.5) or biological half-life (P = 0.2) of adoptively transferred T cells between the mice receiving exogenous IL-2 or control immunocytokine. These data support the hypothesis that the locoregional deposition of the anti-CD20-IL-2 immunocytokine at

DOI:10.1158/0008-5472.CAN-06-2283

the $CD19^+CD20^+$ tumor site significantly augments *in vivo* persistence of $CD8^+$ CD19-specific T cells.

***In vivo* efficacy of immunocytokine in combination with CD19-specific T cell to treat established B-lineage tumor.** We investigated *in vivo* whether the immunocytokine-mediated improved persistence of genetically modified CD19-specific T cells could lead to augmented clearance of established $CD19^+CD20^+$ tumor. A dose of T cells (10^7 cells) was selected because this dose by itself does not control long-term tumor growth (Fig. 4; data not shown). CD19-specific $CD8^+$ T cells were adoptively transferred into groups of mice bearing established $CD19^+CD20^+hRLuc^+$ ARH-77 tumor along with anti-CD20-IL-2 immunocytokine or control anti-GD_2-IL-2 immunocytokine. Tumor growth was serially monitored by *in vivo* bioluminescence imaging of ARH-77 tumor-derived hRLuc enzyme activity. Mice that received both CD19-specific T cells and anti-CD20-IL-2 immunocytokine experienced a reduction in tumor growth, with 75% of mice obtaining complete remission, as measured by bioluminescence imaging, at the end of

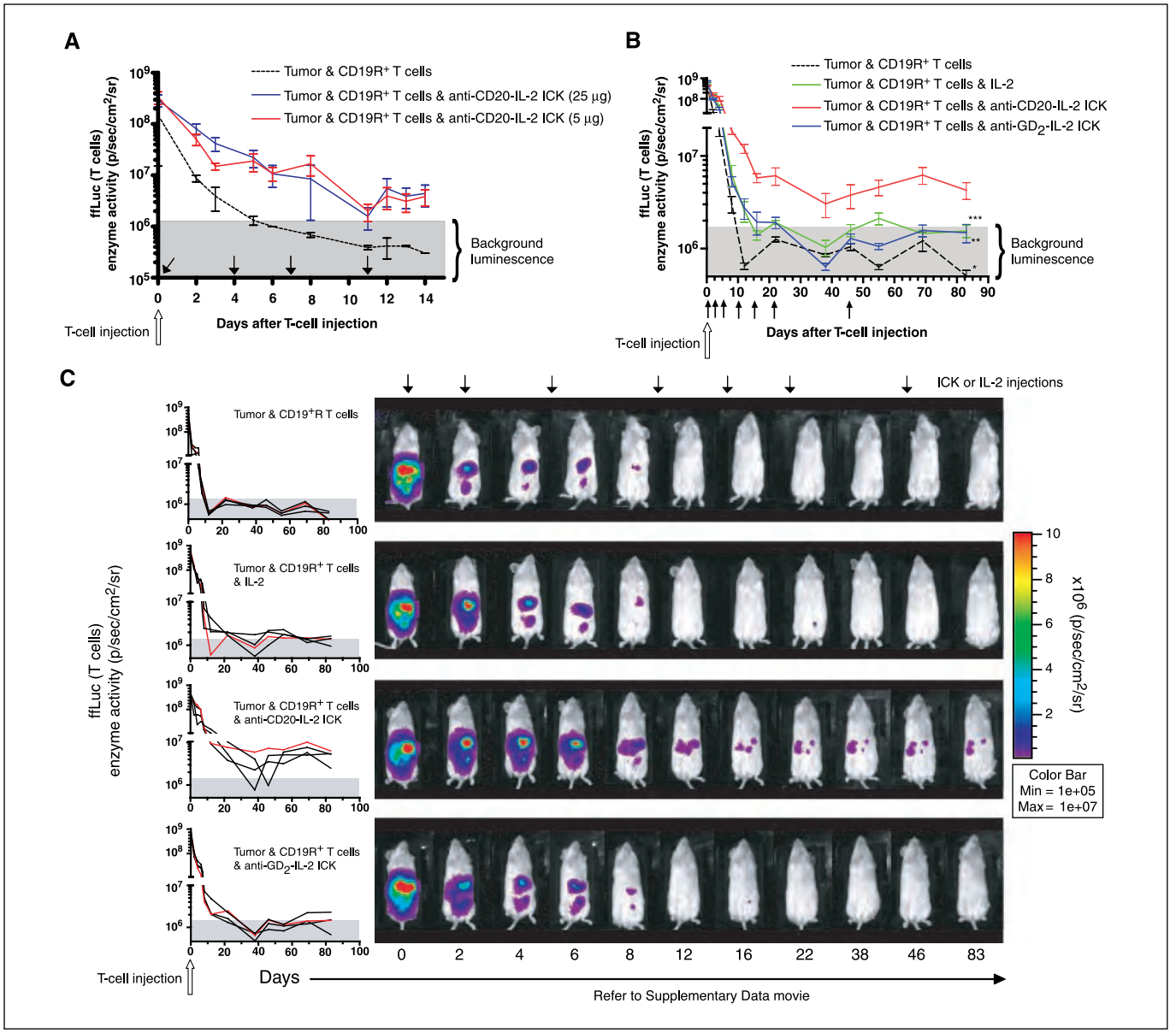

Figure 3. Effect of immunocytokine on persistence of adoptively transferred T cells. NOD/*scid* mice (four mice per group) bearing ARH-77 tumors were treated with 10^7 $CD19R^+ffLuc^+$ umbilical cord blood T-cell clone (day 0, *open arrow*) along with (*A*) anti-CD20-IL-2 immunocytokine (5 and 25 μg; *solid arrows*; on days 0, 4, 7, and 11) or no immunocytokine, or (*B*) anti-CD20-IL-2 immunocytokine/GD_2-IL-2 immunocytokine (5 μg/injection) or rhIL-2 (75,000 units/injection) on days 0, 2, 5, 10, 15, 21, and 45 (*closed arrows*). The persistence of T cells was measured as ffLuc-derived flux from mice and graphed over time (mean flux ± SD is shown in *A* and *B*, and flux for individual mice is shown in *C*). One mouse (*red line*) was selected from each group for the display of sequential bioluminescence images of T cells *in vivo*. Comparison (day 83) between groups receiving combination of T cells and anti-CD20-IL-2 immunocytokine and no treatment (*, $P = 0.01$); T cells and control immunocytokine (anti-GD_2-IL-2 immunocytokine; **, $P = 0.05$); or T cells and IL-2 (***, $P = 0.02$). Background luminescence (*gray area*) was defined from mice that were imaged after receiving D-luciferin along with treatment mice, but which did not receive $ffLuc^+$ T cells. *In vitro* ffLuc activity of the genetically modified T cells was 0.35 ± 0.02 cpm/cell (mean ± SD) compared with 0 ± 0 cpm/cell (mean ± SD) for parental unmodified cells. Supplementary Data contain a movie of the relative *in vivo* T-cell persistence in the four treatment groups.

DOI:10.1158/0008-5472.CAN-06-2283

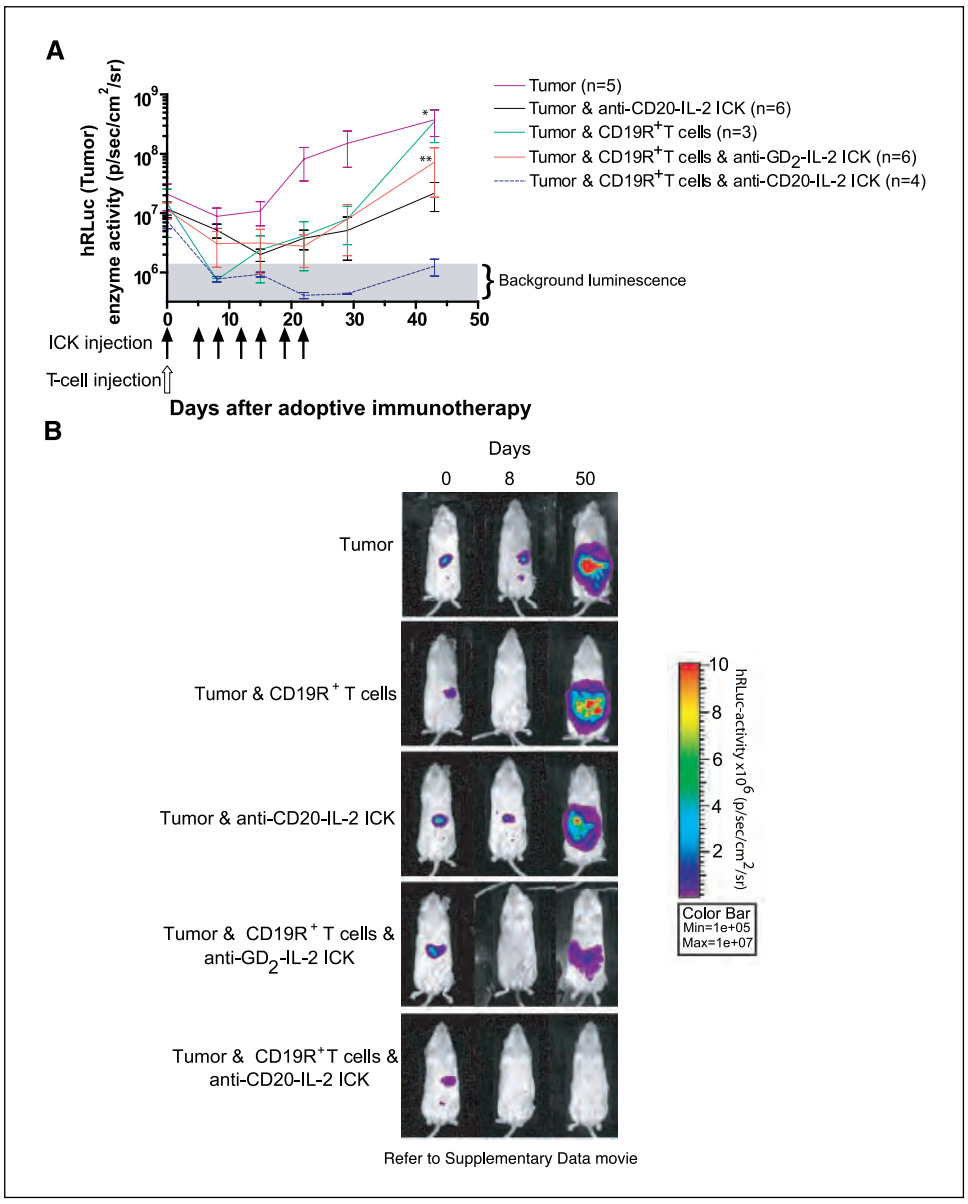

Figure 4. Combined antitumor efficacy of immunocytokine and CD19-specific T cells. *A,* the tumor burden was monitored longitudinally by quantification of ARH-77 tumor-derived hRLuc activity in five groups of NOD/*scid* mice receiving combinations of T cells (10^7 on day 0, *open arrow*); anti-CD20-IL-2 immunocytokine (5 μg/injection); anti-GD_2-IL-2 immunocytokine (5 μg/injection) given on days 0, 5, 8, 12, 15, 19, and 22 (*closed arrows*); and graphed over time as mean flux ± SD. *B,* serial pseudocolor images representing light intensity from hRLuc ARH-77 cells in selected mice before and after immunotherapy. Comparison (day 50) between groups receiving combination of T cells and anti-CD20-IL-2 immunocytokine and no treatment (*, $P = 0.01$), and T cells and control immunocytokine (anti-GD_2-IL-2 immunocytokine; **, $P = 0.03$). Genetically modified ARH-77 (transfected with hRLuc:Zeocin-pcDNA3.1) hRLuc activity *in vitro* was 0.32 ± 0.04 cpm/cell (mean ± SD) compared with 0.004 ± 0.0008 cpm/cell (mean ± SD) for parental unmodified cells. Supplementary Data contain a movie of the relative *in vivo* antitumor effects of immunotherapy in the five mouse groups.

the experiment (50 days after adoptive immunotherapy; Fig. 4). We found that the combination therapy of $CD19R^+$ T cells and anti-CD20-IL-2 immunocytokine was effective in reducing tumor growth compared with no immunotherapy ($P = 0.01$) and T cells given with an equivalent dosing of the control immunocytokine ($P = 0.03$). Although the tumor burden seems to be increasing in the treated group, no visible tumor as seen by hRLuc signal was observed at the end of the experiment, as the flux remained below background level, consistent with a complete antitumor response. Mouse groups receiving T cells alone or T cells with control immunocytokine showed a similar pattern of tumor growth, with an initial reduction around day 8 followed by relapse. All mice in the control group, which received no immunotherapy, experienced sustained tumor growth. We saw similar tumor growth kinetics in mice that did or did not receive anti-CD20-IL-2 immunocytokine in the absence of T cells ($P > 0.05$ through day 50), and this is presumably a reflection of the dose regimen chosen for the immunocytokine in this experiment. Increased doses of T cells or anti-CD20-IL-2 immunocytokine delivered as monotherapies results in a sustained antitumor effect; however, using these doses would preclude our ability to measure the ability of the immunocytokine to potentiate T-cell persistence and improve tumor killing.

The ability to measure both ffLuc and hRLuc enzyme activities in the same mice allowed us to determine whether the persistence of adoptively transferred T cells directly correlated with tumor size for individual mice. This was accomplished by plotting ffLuc-derived T-cell flux versus hRLuc-derived tumor-cell flux from Fig. 3. Both group of mice, which received CD19-specific T cells along with anti-CD20-IL-2 immunocytokine/anti-GD_2-IL-2 immunocytokine, showed a drop in tumor burden at day 8, which is due to the T cells infused. However, the highest numbers of T cells (ffLuc activity; mean flux 4.7×10^6 versus 1.5×10^6 p/s/cm^2/sr) and lowest tumor burden (hRLuc activity; mean flux 1.4×10^7 versus 4×10^7 p/s/cm^2/sr) by day 83 (Fig. 5) was observed in the group receiving anti-CD20-IL-2 immunocytokine when compared with

DOI:10.1158/0008-5472.CAN-06-2283

the control immunocytokine-treated group. This analysis shows that half of the mice achieved an antitumor response (absence of detectable hRLuc activity) after combination immunotherapy with CD19R$^+$ T cells and anti-CD20-IL-2 immunocytokine. We note that there was continued T-cell persistence (ffLuc activity) in the anti-CD20-IL-2 immunocytokine–treated group compared with the control immunocytokine–treated group ($P < 0.05$) at day 83. Although tumor burden (hRLuc activity) was reduced in the CD20 immunocytokine– compared with the control immunocytokine–treated group at day 83, no statistical significance was observed. Thus, we note a trend toward continued T-cell persistence and desired antitumor effect in the anti-CD20-IL-2 immunocytokine–treated group.

We believe that this is the first time that bioluminescence imaging has been used to connect the persistence of genetically modified T cells to an antitumor effect. These data further reveal that the mice that received the tumor-specific immunocytokine control their tumor burden to a greater extent than the mice that received the control immunocytokine (which does not bind the tumor). As a treatment for minimal residual disease in patients undergoing hematopoietic stem-cell transplantation, this combination therapy shows the ability to keep the disease relapse in check for almost 3 months in this mouse model.

In aggregate, these data show that the combination of anti-CD20-IL-2 immunocytokine and CD19R$^+$ T cells results in augmented control of tumor growth, as predicted from the *in vivo* T-cell persistence data.

Discussion

We show that anti-CD20-IL-2 immunocytokine specifically binds to CD20$^+$ tumor, that infusions of the anti-CD20-IL-2 immunocytokine can augment persistence of adoptively transferred CD19-specific T cells *in vivo*, and that this leads to improved control of an established CD19$^+$CD20$^+$ tumor. We believe that these observations are due to the deposition of IL-2 at sites of CD20 binding, which provides a positive survival stimulus to infused CD19R$^+$IL-2R$^+$ effector T cells residing in the tumor microenvironment.

The development of an anti-CD20-IL-2 immunocytokine has implications for future immunotherapy of B-lineage malignancies. Although rituximab has been extensively used to treat CD20$^+$ malignancies (34–36), some patients become unresponsive to this mAb therapy, leading to disease progression (37). The development of an anti-CD20-IL-2 immunocytokine with its ability to activate immune effector cells may rescue these patients, and a clinical trial at COH is under way to determine the safety and feasibility of infusing this immunocytokine. Modifications other than the addition of cytokines (38, 39), such as radionucleotides (40) and cytotoxic agents (41, 42), may also improve the therapeutic potential of unconjugated clinical-grade mAbs. Indeed, combining mAb therapy with therapeutic modalities that exhibit nonoverlapping toxicity profiles is an attractive strategy to improve the antitumor effect without compromising patient safety.

One novel combination therapy for treating B-lineage tumors, described in this report, is to combine immunocytokine with T-cell therapy. The two immunotherapies used, anti-CD20-IL-2 immunocytokine and CD19-specific T cells, have the potential to improve the eradication of tumor because (*a*) the targeting of different cell surface molecules reduces the possibility emergence of antigen-escape variants, (*b*) the mAb conjugated to IL-2 can recruit and activate effector cells (such as CD19-specific T cells) expressing the cytokine receptor in the tumor microenvironment, and (*c*) T cells

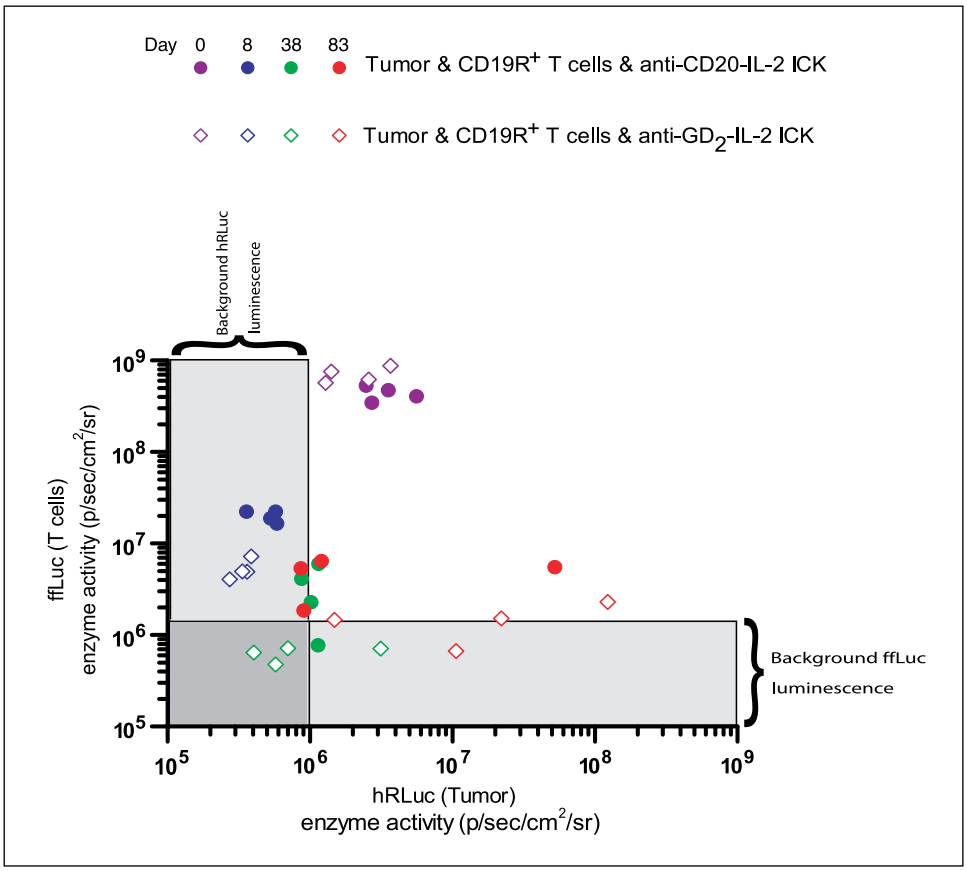

Figure 5. Measurement of both T-cell persistence and antitumor effect of immunotherapies in individual mice. Mice were treated as in Fig. 3*B*, and T-cell persistence (ffLuc signal, *Y axis*) along with tumor burden (hRLuc signal, *X axis*) was measured in the same mouse at the days mentioned. Improved T-cell persistence (ffLuc signal) and reduced tumor burden (antitumor effect, hRLuc signal) in mice that received a combination of CD19-specific T cells and anti-CD20-IL-2 immunocytokine is observed at day 83. *Shaded gray areas,* background fluorescence.

DOI:10.1158/0008-5472.CAN-06-2283

can kill independent of host factors, which may limit the effectiveness of mAb-mediated complement dependent cytotoxicity and antibody-dependent cell cytotoxicity (12–15). These immunotherapies will target both malignant and normal B cells. However, as loss of normal B-cell function has not been an impediment to rituximab therapy and as clinical conditions associated with hypogammaglobulinemia could be corrected with infusions of exogenous immunoglobulin, a loss of B-cell function may be an acceptable side effect in patients with advanced B-cell leukemias and lymphomas receiving CD19- and/or CD20-directed therapies.

Another potential advantage of immunocytokine therapy is that the locoregional delivery of T-cell help in the form of IL-2 may avoid the systemic toxicities observed with i.v. infusion of the IL-2 cytokine (43–45), and this may be particularly beneficial in the context of allogeneic hematopoietic stem-cell transplantation. We have recently described that umbilical cord blood–derived $CD8^+$ T cells can be rendered specific for CD19 to augment the graft-versus-tumor effect after hematopoietic stem-cell transplantation. Moreover, because the immunocytokine improves the *in vivo* immunobiology of umbilical cord blood–derived CD19-specific T cells, this study provides the groundwork for combining these two immunotherapies after umbilical cord blood transplantation.

Alternative immunocytokines and T cells with shared specificities for tumor types other than B-lineage malignancies could also be considered for combination immunotherapy. For example, immunocytokines might be combined with T cells that have been rendered specific by the introduction of chimeric immunoreceptors for breast (46, 47), ovarian (48), colon (49), and brain (50) malignancies. Furthermore, immunocytokines bearing other cytokines might be infused with T cells to deliver IL-7, IL-15, or IL-21 to further augment T-cell function in the tumor microenvironment.

In summary, the clinical testing of anti-CD20-IL-2 immunocytokine and $CD19R^+$ T cells as monotherapy will provide Phase I safety and feasibility data. It is anticipated that the data in this report will be used to justify next-generation clinical trials to evaluate combinations of the immunocytokine and T cells.

Acknowledgments

Received 6/21/2006; revised 12/4/2006; accepted 1/3/2007.

Grant support: CA30206, CA003572, and CA107399; Alliance for Cancer Gene Therapy; Amy Phillips Charitable Foundation; The Leukemia and Lymphoma Society; Lymphoma Research Foundation; National Foundation for Cancer Research; Pediatric Cancer Research Foundation; National Marrow Donor Program; and Marcus Foundation.

The costs of publication of this article were defrayed in part by the payment of page charges. This article must therefore be hereby marked *advertisement* in accordance with 18 U.S.C. Section 1734 solely to indicate this fact.

We thank Adrian Castro and Vanessa Reeves for assistance with animal experiments, COH Animal Resource Center (under the direction of Dr. Richard Ermel), and the Light Microscopy and Flow Cytometry Cores.

References

1. Stamenkovic I, Seed B. CD19, the earliest differentiation antigen of the B cell lineage, bears three extracellular immunoglobulin-like domains and an Epstein-Barr virus-related cytoplasmic tail. J Exp Med 1988;168:1205–10.
2. Tedder TF, Streuli M, Schlossman SF, Saito H. Isolation and structure of a cDNA encoding the B1 (CD20) cell-surface antigen of human B lymphocytes. Proc Natl Acad Sci U S A 1988;85:208–12.
3. Wortis HH. Surface markers, heavy chain sequences and B cell lineages. Int Rev Immunol 1992;8:235–46.
4. Cragg MS, Walshe CA, Ivanov AO, Glennie MJ. The biology of CD20 and its potential as a target for mAb therapy. Curr Dir Autoimmun 2005;8:140–74.
5. Scheuermann RH, Racila E. CD19 antigen in leukemia and lymphoma diagnosis and immunotherapy. Leuk Lymphoma 1995;18:385–97.
6. Weiner GJ, Link BK. Monoclonal antibody therapy of B cell lymphoma. Expert Opin Biol Ther 2004;4:375–85.
7. Brentjens RJ, Latouche JB, Santos E, et al. Eradication of systemic B-cell tumors by genetically targeted human T lymphocytes co-stimulated by CD80 and interleukin-15. Nat Med 2003;9:279–86.
8. Cheadle EJ, Gilham DE, Thistlethwaite FC, Radford JA, Hawkins RE. Killing of non-Hodgkin lymphoma cells by autologous CD19 engineered T cells. Br J Haematol 2005; 129:322–32.
9. Imai C, Mihara K, Andreansky M, et al. Chimeric receptors with 4-1BB signaling capacity provoke potent cytotoxicity against acute lymphoblastic leukemia. Leukemia 2004;18:676–84.
10. Roessig C, Scherer SP, Baer A, et al. Targeting CD19 with genetically modified EBV-specific human T lymphocytes. Ann Hematol 2002;81 Suppl 2:42–3.
11. Rossig C, Pscherer S, Landmeier S, Altvater B, Jurgens H, Vormoor J. Adoptive cellular immunotherapy with CD19-specific T cells. Klin Padiatr 2005;217:351–6.
12. Multani PS, Grossbard ML. Monoclonal antibody-based therapies for hematologic malignancies. J Clin Oncol 1998;16:3691–710.
13. Schmitt CA, Schwaeble W, Wittig BM, Meyer zum Buschenfelde KH, Dippold WG. Expression and regulation by interferon-γ of the membrane-bound complement regulators CD46 (MCP), CD55 (DAF) and CD59 in gastrointestinal tumours. Eur J Cancer 1999;35:117–24.
14. Treon SP, Shima Y, Preffer FI, et al. Treatment of plasma cell dyscrasias by antibody-mediated immunotherapy. Semin Oncol 1999;26:97–106.
15. Zhao S, Asgary Z, Wang Y, Goodwin R, Andreeff M, Younes A. Functional expression of TRAIL by lymphoid and myeloid tumour cells. Br J Haematol 1999; 106:827–32.
16. Dudley ME, Wunderlich JR, Robbins PF, et al. Cancer regression and autoimmunity in patients after clonal repopulation with antitumor lymphocytes. Science 2002; 298:850–4.
17. Klebanoff CA, Finkelstein SE, Surman DR, et al. IL-15 enhances the *in vivo* antitumor activity of tumor-reactive $CD8^+$ T cells. Proc Natl Acad Sci U S A 2004;101: 1969–74.
18. Minamoto S, Treisman J, Hankins WD, Sugamura K, Rosenberg SA. Acquired erythropoietin responsiveness of interleukin-2-dependent T lymphocytes retrovirally transduced with genes encoding chimeric erythropoietin/interleukin-2 receptors. Blood 1995;86:2281–7.
19. King DM, Albertini MR, Schalch H, et al. Phase I clinical trial of the immunocytokine EMD 273063 in melanoma patients. J Clin Oncol 2004;22:4463–73.
20. Lode HN, Xiang R, Becker JC, Gillies SD, Reisfeld RA. Immunocytokines: a promising approach to cancer immunotherapy. Pharmacol Ther 1998;80:277–92.
21. Sondel PM, Hank JA, Gan J, Neal Z, Albertini MR. Preclinical and clinical development of immunocytokines. Curr Opin Investig Drugs 2003;4:696–700.
22. Cooper LJ, Topp MS, Serrano LM, et al. T-cell clones can be rendered specific for CD19: toward the selective augmentation of the graft-versus-B-lineage leukemia effect. Blood 2003;101:1637–44.
23. Serrano LM, Pfeiffer T, Olivares S, et al. Differentiation of naive cord-blood T cells into CD19-specific cytolytic effectors for posttransplantation adoptive immunotherapy. Blood 2006;107:2643–52.
24. Dudley ME, Rosenberg SA. Adoptive-cell-transfer therapy for the treatment of patients with cancer. Nat Rev Cancer 2003;3:666–75.
25. Gillies SD, Lan Y, Williams S, et al. An anti-CD20-IL-2 immunocytokine is highly efficacious in a SCID mouse model of established human B lymphoma. Blood 2005; 105:3972–8.
26. Mahmoud MS, Fujii R, Ishikawa H, Kawano MM. Enforced CD19 expression leads to growth inhibition and reduced tumorigenicity. Blood 1999;94:3551–8.
27. Farner NL, Voss SD, Leary TP, et al. Distinction between γc detection and function in YT lymphoid cells and in the granulocyte-macrophage colony-stimulating factor-responsive human myeloid cell line, Tf-1. Blood 1995;86:4568–78.
28. Riddell SR, Greenberg PD. The use of anti-CD3 and anti-CD28 monoclonal antibodies to clone and expand human antigen-specific T cells. J Immunol Methods 1990;128:189–201.
29. Gillies SD, Reilly EB, Lo KM, Reisfeld RA. Antibody-targeted interleukin 2 stimulates T-cell killing of autologous tumor cells. Proc Natl Acad Sci U S A 1992;89:1428–32.
30. Cooper LJ, Al-Kadhimi Z, Serrano LM, et al. Enhanced antilymphoma efficacy of CD19-redirected influenza MP1-specific CTLs by cotransfer of T cells modified to present influenza MP1. Blood 2005;105: 1622–31.
31. Lupton SD, Brunton LL, Kalberg VA, Overell RW. Dominant positive and negative selection using a hygromycin phosphotransferase-thymidine kinase fusion gene. Mol Cell Biol 1991;11:3374–8.
32. Rentsch B, Bucher U, Brun del Re GP. Biochemical identification of the antigen recognized by the monoclonal pan-B cell antibody Y29/55. Eur J Haematol 1991; 47:204–12.
33. Treon SP, Mitsiades C, Mitsiades N, et al. Tumor cell expression of CD59 is associated with resistance to CD20 serotherapy in patients with B-cell malignancies. J Immunother 2001;24:263–71.
34. Foran JM, Rohatiner AZ, Cunningham D, et al. European phase II study of rituximab (chimeric

DOI:10.1158/0008-5472.CAN-06-2283

anti-CD20 monoclonal antibody) for patients with newly diagnosed mantle-cell lymphoma and previously treated mantle-cell lymphoma, immunocytoma, and small B-cell lymphocytic lymphoma. J Clin Oncol 2000;18:317–24.

35. Maloney DG, Grillo-Lopez AJ, White CA, et al. IDEC-C2B8 (Rituximab) anti-CD20 monoclonal antibody therapy in patients with relapsed low-grade non-Hodgkin's lymphoma. Blood 1997;90:2188–95.

36. Reff ME, Carner K, Chambers KS, et al. Depletion of B cells *in vivo* by a chimeric mouse human monoclonal antibody to CD20. Blood 1994;83:435–45.

37. McLaughlin P, Grillo-Lopez AJ, Link BK, et al. Rituximab chimeric anti-CD20 monoclonal antibody therapy for relapsed indolent lymphoma: half of patients respond to a four-dose treatment program. J Clin Oncol 1998;16:2825–33.

38. Lode HN, Reisfeld RA. Targeted cytokines for cancer immunotherapy. Immunol Res 2000;21:279–88.

39. Penichet ML, Morrison SL. Antibody-cytokine fusion proteins for the therapy of cancer. J Immunol Methods 2001;248:91–101.

40. Jurcic JG, Scheinberg DA. Recent developments in the radioimmunotherapy of cancer. Curr Opin Immunol 1994;6:715–21.

41. Kreitman RJ, Wilson WH, White JD, et al. Phase I trial of recombinant immunotoxin anti-Tac(Fv)-PE38 (LMB-2) in patients with hematologic malignancies. J Clin Oncol 2000;18:1622–36.

42. Pastan I. Targeted therapy of cancer with recombinant immunotoxins. Biochim Biophys Acta 1997;1333:1–6.

43. Chianese-Bullock KA, Woodson EM, Tao H, et al. Autoimmune toxicities associated with the administration of antitumor vaccines and low-dose interleukin-2. J Immunother 2005;28:412–9.

44. Rosenberg SA, Lotze MT, Muul LM, et al. Observations on the systemic administration of autologous lymphokine-activated killer cells and recombinant interleukin-2 to patients with metastatic cancer. N Engl J Med 1985;313:1485–92.

45. Siegel JP, Puri RK. Interleukin-2 toxicity. J Clin Oncol 1991;9:694–704.

46. Gritzapis AD, Mamalaki A, Kretsovali A, et al. Redirecting mouse T hybridoma against human breast and ovarian carcinomas: *in vivo* activity against HER-2/neu expressing cancer cells. Br J Cancer 2003;88:1292–300.

47. Moritz D, Wels W, Mattern J, Groner B. Cytotoxic T lymphocytes with a grafted recognition specificity for ERBB2-expressing tumor cells. Proc Natl Acad Sci U S A 1994;91:4318–22.

48. Parker LL, Do MT, Westwood JA, et al. Expansion and characterization of T cells transduced with a chimeric receptor against ovarian cancer. Hum Gene Ther 2000;11:2377–87.

49. Haynes NM, Snook MB, Trapani JA, et al. Redirecting mouse CTL against colon carcinoma: superior signaling efficacy of single-chain variable domain chimeras containing TCR-ζ vs Fc epsilon RI-γ. J Immunol 2001;166:182–7.

50. Kahlon KS, Brown C, Cooper LJ, Raubitschek A, Forman SJ, Jensen MC. Specific recognition and killing of glioblastoma multiforme by interleukin 13-zetakine redirected cytolytic T cells. Cancer Res 2004;64:9160–6.

DOI:10.1158/0008-5472.CAN-07-5600

Cancer Research

Redirecting Specificity of T-Cell Populations For CD19 Using the *Sleeping Beauty* System

Harjeet Singh, Pallavi R. Manuri, Simon Olivares, et al.

Cancer Res 2008;68:2961-2971. Published online April 15, 2008.

DOI:10.1158/0008-5472.CAN-07-5600

Research Article

Redirecting Specificity of T-Cell Populations For CD19 Using the *Sleeping Beauty* System

Harjeet Singh,[1] Pallavi R. Manuri,[1] Simon Olivares,[1] Navid Dara,[1] Margaret J. Dawson,[1] Helen Huls,[1] Perry B. Hackett,[3] Donald B. Kohn,[4] Elizabeth J. Shpall,[2] Richard E. Champlin,[2] and Laurence J.N. Cooper[1]

Divisions of [1]Pediatrics and [2]Cancer Medicine, University of Texas M. D. Anderson Cancer Center, Houston, Texas; [3]Department of Genetics, Cell Biology and Development, University of Minnesota, St. Paul, Minnesota; and [4]Division of Research Immunology/Bone Marrow Transplantation, Children's Hospital Los Angeles, Los Angeles, California

Abstract

Genetic modification of clinical-grade T cells is undertaken to augment function, including redirecting specificity for desired antigen. We and others have introduced a chimeric antigen receptor (CAR) to enable T cells to recognize lineage-specific tumor antigen, such as CD19, and early-phase human trials are currently assessing safety and feasibility. However, a significant barrier to next-generation clinical studies is developing a suitable CAR expression vector capable of genetically modifying a broad population of T cells. Transduction of T cells is relatively efficient but it requires specialized manufacture of expensive clinical grade recombinant virus. Electrotransfer of naked DNA plasmid offers a cost-effective alternative approach, but the inefficiency of transgene integration mandates *ex vivo* selection under cytocidal concentrations of drug to enforce expression of selection genes to achieve clinically meaningful numbers of CAR$^+$ T cells. We report a new approach to efficiently generating T cells with redirected specificity, introducing DNA plasmids from the *Sleeping Beauty* transposon/transposase system to directly express a CD19-specific CAR in memory and effector T cells without drug selection. When coupled with numerical expansion on CD19$^+$ artificial antigen-presenting cells, this gene transfer method results in rapid outgrowth of CD4$^+$ and CD8$^+$ T cells expressing CAR to redirect specificity for CD19$^+$ tumor cells. [Cancer Res 2008;68(8):2961–71]

Introduction

The most robust example of successful T-cell therapy occurs following allogeneic hematopoietic stem-cell transplantation where the engrafted donor-derived T cells recognize recipient tumor-associated antigens in the context of MHC. However, the graft-versus-tumor effect after allogeneic-hematopoietic stem cell transplantation is incomplete, resulting in relapse as the major cause of mortality. To augment the graft-versus-tumor effect for B-lineage neoplasms, we have previously shown that genetically modified peripheral blood– and umbilical cord blood–derived T cells can be rendered specific for CD19, a molecule constitutively expressed on B-cell malignancies (1, 2). The redirected specificity was achieved by electrotransfer of a linearized DNA plasmid coding for a first-generation chimeric antigen receptor (CAR), designated CD19R, which recognizes CD19 via the scFv of a murine CD19-specific monoclonal antibody (mAb) fused to a chimeric CD3-ζ–derived activation endodomain. A phase I trial (BB-IND1141, clinicalTrials.gov identifier: NCT00182650; ref. 3) is currently evaluating the safety and feasibility of infusing autologous T cells electroporated to coexpress CD19R CAR and the hygromycin phosphotransferase (Hy) and herpes simplex virus-1 thymidine kinase selection/suicide fusion transgene (4).

We anticipated that the therapeutic efficacy of adoptive transfer of CD19-specific T cells would be improved by developing a CAR with a fully competent activation signal and introducing the CAR into central memory (CM) T cells. As a result, a second-generation CAR, designated CD19RCD28, has been developed that provides CD19-dependent signaling through chimeric CD3-ζ and CD28, resulting in improved *in vivo* persistence and antitumor effect, compared with CD19R$^+$ T cells (5). To further optimize the clinical potential of CAR$^+$ T cells, while taking advantage of the cost-efficiency of nonviral gene transfer, we desired a clinically feasible approach to the efficient propagation of CAR$^+$ T-cell populations, including T_{CM}, in the absence of expression immunogenic drug selection genes, such as *Hy*. We reasoned that genetically modified T cells could be selectively propagated, upon activating T cells for sustained proliferation, through the introduced second-generation CAR. To maximize transgene expression, we codon-optimized (CoOp) the CAR as reports have shown that codon optimization of genes toward human consensus codon usage increases protein expression (6, 7).

The focus on developing nonviral gene transfer technologies is justified based on the cost and time savings compared with developing recombinant clinical-grade viral supernatant, which are subject to rigorous regulatory oversight and rely on specialized manufacturing experience of a limited number of production facilities. Although the transfection efficiency of nonviral gene transfer is inferior to viral-mediated transduction, naked DNA plasmids expressing desired transgenes such as CAR can be rapidly produced at a fraction of the cost compared with clinical grade γ-retrovirus and lentivirus. A potential drawback to nonviral gene transfer, compared with viral gene transfer, is the lengthy *ex vivo* manufacturing time to selectively propagate electroporated T cells with stable expression of transgene, during which time the cells may become susceptible to replicative senescence, lose expression of desired homing receptors, and furthermore be cleared *in vivo* due to recognition of immunogenic drug selection transgene (8, 9). What is needed is an approach that when coupled with nonviral gene transfer shortens the culture time to generate T cells with durably expressed transgene and maintains a desired T-cell immunophenotype.

To introduce the CAR, we evaluated whether the efficient transposition and long-lasting transgene expression of the

Requests for reprints: Laurence J.N. Cooper, University of Texas M. D. Anderson Cancer Center, Pediatrics-Research, Unit 907, 1515 Holcombe Boulevard, Houston, TX 77030. Phone: 713-563-3208; Fax: 713-792-9832; E-mail: ljncooper@mdanderson.org.

doi:10.1158/0008-5472.CAN-07-5600

DOI:10.1158/0008-5472.CAN-07-5600

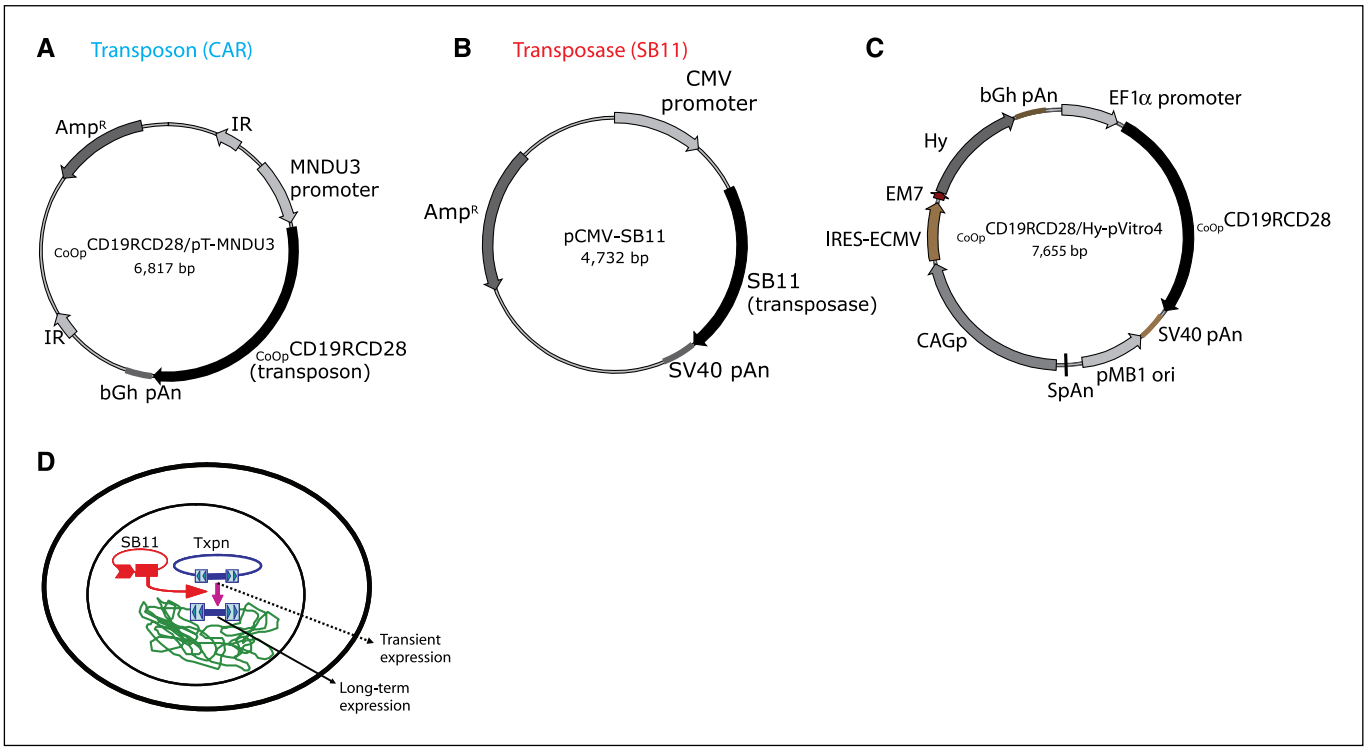

Figure 1. Schematic of the expression plasmids and experimental design. *A,* $_{CoOp}$CD19RCD28/pT-MNDU3 (*Transposon*). *MNDU3 promoter,* the constitutive promoter from the U3 region of the MND retrovirus; *$_{CoOp}$CD19RCD28,* codon-optimized CD19RCD28 CAR; *IR, SB*-inverted/direct repeats; *bGh pAn,* polyadenylation signal from bovine growth hormone; *Amp^R,* ampicillin resistance gene. *B,* pCMV-SB11 (*Transposase*). *SB11, SB*-transposase SB11; *CMV promoter,* CMV enhancer/promoter; *SV40pAN,* polyadenylation signals from SV40. *C,* $_{CoOp}$CD19CD28/Hy-pVitro4. *EF1α promoter,* composite promoter comprising the elongation factor-1α (*EF1α*) core promoter and the R segment and part of the U5 sequence (R-U5′) of the human T-cell leukemia virus type 1 LTR; *pMB1 ori,* a minimal *E. coli* origin of replication; *SpAn,* synthetic pause; *CAGp,* a composite promoter that combines the human CMV immediate-early enhancer and a modified chicken β-actin promoter and first intron; *Hy,* hygromycin B resistance gene (hygromycin phosphotransferase); *bGh pAn,* polyadenylation signal from bovine growth hormone; *EM7*, synthetic prokaryotic promoter. *D,* an expression cassette in a plasmid (*blue*) provides only transient expression unless incorporated into an integrating transposon vector that can be cleaved from the plasmid and integrated into a host genome by a source of transposase (*red*).

Sleeping Beauty (*SB*) DNA transposon derived from *Tc1/mariner* superfamily of transposons (10, 11) can improve transgene transfer efficiency. The *SB* transposable element from a DNA donor plasmid can be adapted for nonviral gene transfer in T cells, using a *SB* transposase supplied *in trans* to mediate integration of a transposon CAR expression cassette flanked by terminal inverted repeats (IR), which each contain two copies of a short direct repeat (DR) that have binding sites for the transposase enzyme (Fig. 1*D*). The *SB* transposase mediates transposition by binding to IRs, excising a precise DNA sequence flanked by the IRs, and inserting the transposon into any of ~200 million TA sites in a mammalian genome (12). Previously, the *SB* system has been used as a nonviral gene delivery into multiple murine and human cell lines, including liver, keratinocytes, endothelial cells, lung, hematopoietic progenitor cells, embryonic stem cells, and tumor cells (11). Of particular relevance is that *SB*-mediated integration has been shown in human T cells (13), signifying the potential application of this technology.

We report that electrotransfer of a two-component DNA *SB* system into primary human T cells from umbilical cord blood and peripheral blood results in efficient and stable CAR gene transfer, which can be numerically expanded to clinically meaningful numbers within 4 weeks on CD19$^+$ artificial antigen-presenting cell (aAPC), without the need for addition of cytocidal concentrations of drug for selection, and with the outgrowth of CD8$^+$ and CD4$^+$ CM and effector CAR$^+$ T-cell subpopulations. This was achieved through the rationale design of (*a*) a next-generation codon-optimized CD19-specific CAR, (*b*) CD19$^+$ aAPC expressing desired costimulatory and cytokine molecules, and (*c*) *SB* DNA plasmids expressing CAR transposon and an improved transposase. The relative ease of DNA plasmid production, electroporation, and outgrowth of stable integrants on a thawed γ-irradiated bank of aAPC can be readily transferred to the facilities operating in compliance with current good manufacturing practice (cGMP) for phase I/II trials. This is predicted to greatly facilitate trial design infusing CD4$^+$ and CD8$^+$ CAR$^+$ T cells that have desired immunophenotype, including T_{CM}.

Materials and Methods

Plasmids. The plasmid pT-MNDU3-eGFP containing salmonid fish–derived *SB* IR flanking the constitutive promoter, derived from the U3 region of the MND retrovirus (14), to drive an eGFP reporter gene (15), was derived from the plasmid pT-MCS (16) that was derived from pT/neo (10). The second-generation CD19RCD28 CAR (5) was human codon optimized (CoOp), substituting codons with those optimally used in mammals (GENEART) without altering anticipated amino acid sequence. The codon-optimized CD19RCD28 ($_{CoOp}$CD19RCD28) CAR was subcloned into pT-MNDU3 DNA plasmid by replacing the eGFP sequence with the CAR to create $_{CoOp}$CD19RCD28/pT-MNDU3 (Fig. 1*A*). The DNA plasmid pCMV-SB11 (Fig. 1*B*) expresses the SB11 transposase (17). Plasmid $_{CoOp}$CD19RCD28/Hy-pVitro4 (Fig. 1*C*) was generated from pVitro4-mcs DNA vector (InvivoGen) by subcloning $_{CoOp}$CD19RCD28 at *Nhe*I in multiple cloning site two and replacing the internal ribosome entry site (IRES) for the foot and mouth disease virus with that of the encephalomyocarditis virus (from pMG vector described; ref. 6). To

DOI:10.1158/0008-5472.CAN-07-5600

generate cell surface–bound human interleukin 15 (IL-15), the granulocyte macrophage colony-stimulating factor signal peptide sequence was fused to the coding sequence of mature human IL-15 at the 5′ end of a modified human IgG4 Fc region (5) fused in frame to human CD4 transmembrane domain and correct assembly was verified by DNA sequence analysis. The membrane-bound IL-15-Fc cytokine fusion gene was subcloned into pIRESpuro3 (Clontech) to obtain IL-15-Fc/pIRESpuro3.

Cell lines and primary human T cells. Daudi (Burkitt lymphoma) and HLA^{null} K562 (erythroleukemia) cells were obtained from American Type Culture Collection. Lymphoblastoid cells (LCL) were a kind gift of Dr. Helen Heslop (Cell and Gene Therapy, Baylor College of Medicine, Houston TX). These cell lines were cultured in HyQ RPMI 1640 (Hyclone) supplemented with 2 mmol/L Glutamax-1 (Life Technologies-Invitrogen) and 10% heat-inactivated defined FCS (Hyclone), referred to as culture medium (1). Human T cells were isolated by density gradient centrifugation over Ficoll-Paque-Plus (GE Healthcare Bio-Sciences AB), from umbilical cord blood or peripheral blood mononuclear cells (PBMC) after consent, and were cultured in culture medium.

Generation of aAPC. As previously reported, K562 cells were electroporated with DNA plasmids to enforce expression of all of the following: truncated CD19, 4-1BBL, and MICA fused to GFP (18). These aAPCs were further modified to express membrane-bound IL-15 to provide a cytokine stimulus at the site of CAR-binding and T-cell costimulation (19).

Electroporation and T-cell coculture with aAPC. On day 0, PBMCs and umbilical cord blood mononuclear cells (10^7) were suspended in 100 μL of Amaxa Nucleofector solution (CD34 kit) and mixed with 5 μg of supercoiled $_{CoOp}$CD19RCD28/pT-MNDU3 and 5 μg pCMV-SB11 DNA plasmids, transferred to a cuvette, and electroporated (Program U-14). After a 10-min room temperature incubation, the cells were transferred to a six-well plate containing 3 to 4 mL incomplete phenol-free RPMI and rested for 2 to 3 h. The cells were cultured overnight in 6 to 7 mL 10% phenol-free RPMI and stimulated the next day (day 1) with γ-irradiated (100 Gy) aAPC at a 1:10 T cell/aAPC ratio. The γ-irradiated aAPC were re-added every 7 d. Recombinant human interleukin 2 (rhIL-2; Chiron) was added to the cultures at 50 units/mL on a Monday-Wednesday-Friday schedule, beginning day 1 of each 7-d expansion cycle. The supercoiled plasmid $_{CoOp}$CD19RCD28/Hy-pVitro4 (expressing CAR under control of EF1α promoter and *Hy* under control of CAG promoter) was electroporated (10 μg) into PBMCs (10^7) using Nucleofector technology and T cells were propagated by cross-linking CD3 using an OKT3-mediated 14-d rapid expansion protocol (REP) as described previously using allogeneic γ-irradiated PBC and LCL feeder cells in the presence of exogenous (soluble) rhIL-2 (20). T cells were enumerated every 7 d, and viable cells were counted based on trypan blue exclusion.

Western blot. Expression of the chimeric 66-kD (CD19R) and 79-kD (CD19RCD28) CD3-ζ was accomplished using a primary mouse anti-human CD3-ζ mAb (1 μg/mL; BD Biosciences) and secondary horseradish peroxidase (HRP)–conjugated goat anti-mouse IgG (1:75,000; Pierce) under reducing conditions, based on methods previously described (20). Protein lysates were transferred onto nitrocellulose membrane using iBlot Dry Blotting System (Invitrogen) and developed with SuperSignal West Femto Maximum Sensitivity substrate (Pierce) per the manufacturer's instructions and chemiluminescence was captured after 1-min exposure using VersaDoc MP 4000 Imaging System (Bio-Rad).

Generation of monoclonal antibody recognizing a CD19-specific CAR. Female BALB/c mice were injected six times in the foot at 3-d intervals with syngeneic NS0 cells expressing CD19R CAR. Three days after the last immunization, mice were sacrificed, popliteal lymph nodes were removed, and cells were fused with P3-8AG-X653 myeloma cells at a ratio of 3:5, using 30% polyethylene glycol 1450 (in serum free RPMI containing 5% DMSO). After 10 d, hybridoma colonies were picked, cloned by limiting dilution in 96-well plates, and 100 μL of supernatants were screened by ELISA for differential binding to round-bottomed 96-plates containing adsorbed (10^5/well) $CD19R^+$ and $CD19R^{neg}$ Jurkat cells as detected by 1:500 dilution of HRP-conjugated goat anti-mouse IgG (Santa Cruz Biotechnology). Detection was achieved by TMB Microwell peroxidase substrate system (KPL). Protein G column (Roche) purified mAb was conjugated to Alexa Fluor 488 (Invitrogen-Molecular Probes) per manufacturer's instructions.

Flow cytometry. Fluorochrome-conjugated reagents were obtained from BD Biosciences: anti-CD4, anti-CD8, anti-CD25, anti-CD27, anti-CD28, anti-CD62L, anti-CD45RA, anti-CD45RO, and anti-CD95. Affinity-purified $F(ab')_2$ fragment of FITC-conjugated goat anti-human Fcγ (Jackson Immunoresearch) was used at 1/20 dilution to detect cell surface expression of CD19-specific CAR. Purified CAR-specific mAb clone 2D3, conjugated to Alexa Fluor 488, was used at a dilution of 1/30, giving a concentration of ~30 μg/mL. In some experiments, binding of this mAb to the Fc region of CAR was blocked (30 min at 4°C) using goat human Fc-specific antiserum (Sigma). Blocking of nonspecific antibody binding was achieved using FACS wash buffer (2% FCS in PBS). T-cell receptor (TCR)-Vβ expression was determined with a panel of 24 TCR-Vβ–specific mAbs (IO TEST Beta Mark TCR-Vβ repertoire kit, Beckman Coulter) used in association with anti-CD3 and appropriate isotype-matched control mAbs. Data acquisition was on a FACSCalibur (BD Biosciences) using CellQuest version 3.3 (BD Biosciences). Analyses and calculation of mean fluorescence intensity (MFI) was undertaken using FCS Express version 3.00.007 (Thornhill).

Intracellular IL-2 cytokine staining. Intracellular IL-2 was assayed using the Intracellular Cytokine Staining Starter Kit (BD PharMingen) per the manufacturer's instructions. Briefly, 10^5 T cells were incubated with 0.5×10^6 stimulator cells in 200 μL culture medium along with protein transport inhibitor (BD Golgi Plug containing Brefeldin A) in a 96-well plate. Following a 4- to 6-h incubation at 37°C, the cells were stained for CAR expression using hybridoma mAb clone 2D3 at 4°C for 30 min. After washing, the cells were fixed and permeabilized (100 μL, Cytofix/Cytoperm buffer) and phycoerythrin-conjugated mAb specific for IL-2 was added. Cells were further washed and analyzed by FACSCalibur. T cells were treated with a leukocyte activation cocktail (phorbol 12-myristate 13-acetate and ionomycin) as a positive control.

Confocal microscopy. Jurkat parental and $CD19R^+$ Jurkat cells were stained with the hybridoma clone mAb 2D3, at a 1:50 dilution for 15 min at 4°C, washed in FACS wash buffer, and fixed with 0.1% paraformaldehyde. After fixing, the cells were washed twice with FACS wash buffer and transferred onto slides, and coverslips were mounted with Prolong Gold anti-fade agent (Invitrogen). Cells were examined under a confocal microscope (Leica TCS SP2-SE) using oil immersion lens (×63 objective). Single-scan images were obtained with a 4.76× zoom in a 1,024 × 1,024 format with a line averaging of 8.

Chromium release assay. The cytolytic activity of T cells was determined by 4-h chromium release assay (1). CD19-specific T cells were incubated with 5×10^3 ^{51}Cr-labeled target cells in a V-bottomed 96-well plate (Costar). The percentage of specific cytolysis was calculated from the release of ^{51}Cr, as described earlier, using a TopCount NXT (Perkin-Elmer Life and Analytical Sciences, Inc.). Data are reported as mean ± SD.

DNA PCR for *SB* transposon and transposase. DNA was isolated from PBMC using the QIAmp DNA mini kit (Qiagen). PCR was carried out using CD19RCD28-specific forward primer 5′-AGATGACCCAGACCACCTCCAGC-3′ and reverse primer 5′-GGTATCCTTGGTGGCGGTGCT-3′ for the transposon. The PCR reaction used 1 μg of DNA/sample in a mix containing 10× PCR buffer, 2.5 mmol/L deoxynucleotide triphosphates, 3 μmol/L $MgCl_2$, and 0.5 units of DNA polymerase (AmpliTaq Gold, Applied Biosystems) in a final volume of 50 μL amplified in a thermal Cycler (PTC-200 DNA Engine Cycler, Bio-Rad). After an initial denaturation at 95°C for 5 min, the samples underwent 34 cycles of 95°C for 30 s, 65°C for 30 s, 72°C for 1 min 15 s, followed by a prolonged extension step at 72°C for 7 min. For the transposase gene, PCR was carried out using SB11-specific forward primer 5′-ATGGGACCACGCAGCCG-3′ and reverse primer 5′-CGTTTCGGGTAGCCTTCCACA-3′. After an initial denaturation at 95°C for 5 min, the samples underwent 34 cycles of 95°C for 15 s, 58°C for 30 s, 74°C for 2 min followed by a prolonged extension step at 74°C for 7 min. The housekeeping gene *GAPDH* was also amplified in the same samples using the forward primer 5′-TCTCCAGAACATCATCCCTGCCAC-3′ and reverse primer 5′-TGGGCCATGAGGTCCACCACCCTG-3′.

DOI:10.1158/0008-5472.CAN-07-5600

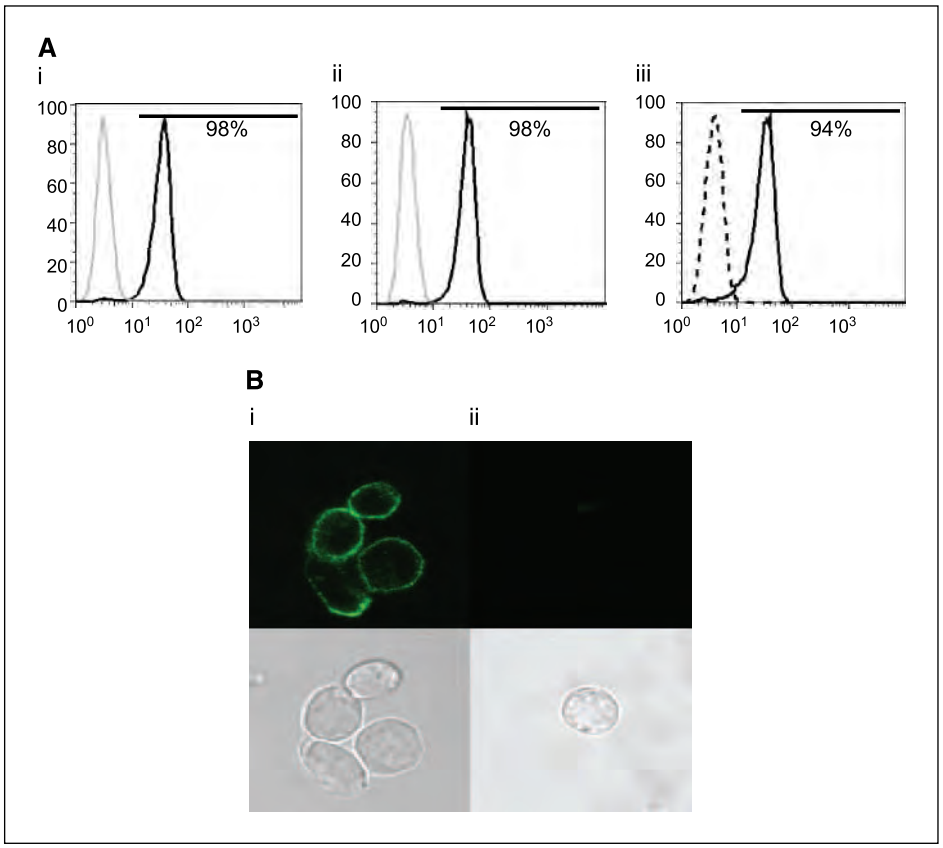

Figure 2. Specificity of mouse-derived CAR-specific mAb (clone 2D3). *A,* Jurkat cells were genetically modified and sorted to express CD19R. Jurkat parental (*gray line*) and CD19R$^+$ (*black line*) cells were stained with (*i*) Alexa 488–conjugated clone 2D3 and (*ii*) F(ab′)$_2$-fragment of goat-derived polyclonal antibody specific for human Fc; *iii,* binding of 2D3 (*solid line*) was blocked by polyclonal Fc-specific antisera (*dashed line*). *B,* cell surface staining of Alexa Fluor 488–conjugated clone 2D3 by confocal microscopy on (*i*) CD19R$^+$ Jurkat cells and (*ii*) Jurkat parental cells. Cells were stained, fixed, and mounted as described in Materials and Methods.

Chromosome banding analysis. Exponentially growing *SB*-transfected T-cell cultures (freshly fed 24 h earlier) were incubated for 2 h at 37°C with colcemid (20 μL of 0.04 μg/mL) per 10 mL medium followed by 0.075 mol/L KCl at room temperature for 15 min, fixed with acetic acid/methanol (1:3), and washed thrice on a glass slide. For Giemsa (G) banding, 5- to 6-d-old slides treated with trypsin were stained with Giemsa stain following standard techniques described previously (21). A total of 15 G-banded metaphases were photographed and 5 complete karyotypes were prepared using a karyotyping system from Applied Imaging Corporation.

Results

We describe a new approach to using nonviral gene transfer of DNA plasmids to efficiently obtain populations of memory and effector T cells with desired specificity (Fig. 1*D*). The system we have devised provides for robust antigen-driven expansion of CD4$^+$ and CD8$^+$ CAR$^+$ T cells to clinically meaningful numbers.

Monoclonal antibody with specificity for CD19-specific CAR. The cell surface expression of the introduced CAR was predicted to increase with outgrowth of T-cell populations that have undergone CAR-mediated numerical expansion on CD19$^+$ aAPC. Currently, the only-commercially available flow cytometry reagents that recognize our CARs are polyclonal anti-Fc antibodies raised in goat, but we desired a homogeneous monoclonal product for use in the release of CAR$^+$ T cells for clinical trials. To longitudinally follow the transgene expression, we developed a CAR-specific mAb by immunizing mice with syngeneic NS0 cells expressing CD19R. A hybridoma mAb clone 2D3 (IgG1) was selected by flow cytometry that selectively bound to CD19R$^+$ Jurkat cells, but not parental Jurkat cells. The binding of 2D3 can be blocked using a Fc-specific antibody (Fig. 2*A*). The 2D3 clone bound a CD20-specific CAR that shares the IgG4 Fc region with CD19R and CD19RCD28 (data not shown). The pattern of staining by confocal microscopy showed 2D3 binding to CAR on the cell surface (Fig. 2*B*). These data are consistent with a mAb binding specifically to the CD19-specific CAR and recognizing the modified human IgG Fc region. Of note, the production of this mAb avoided the need to purity recombinant CAR protein as the immunogen was genetically modified NS0 cells and the ELISA screening used genetically modified Jurkat cells.

Electrotransfer of *SB* two-plasmid DNA system. We have used a nonviral gene transfer approach to introduce codon optimized DNA expression plasmids because these expression vectors can be readily and cheaply manufactured to clinical grade. Although codon modification of TCR genes has been shown to enhance expression of transgenic TCR in primary human T cells (22), we now show the usage of a codon optimized second-generation CAR. Previously, our electroporation approach based on the Multiporator (Eppendorf; refs. 23, 24) used T cells that had been stimulated to proliferate by cross-linking CD3 with OKT3 to allow access of the introduced naked DNA to the nucleus after dissolution of the nuclear envelope during prometaphase. However, T cells nonspecially activated to proliferate, such as by cross-linking CD3 as occurs in the REP (25), would preclude subsequent immediate antigen-mediated propagation and thus directed outgrowth of CAR$^+$ T cells. Nucleofector technology has been used to electroporate nonreplicating cells by direct transfer of DNA to the nucleus (26). Thus, we investigated whether this electrotransfer system could be used to genetically modify circulating T cells from peripheral blood and umbilical cord blood, which are in a

DOI:10.1158/0008-5472.CAN-07-5600

Table 1. Percent CAR expression in T cells after electroporation of CAR transposon with or without SB11 transposase plasmid

DNA plasmid(s)	Day 1						Day 28					
	$CD4^+CAR^+$		$CD8^+CAR^+$		Total CAR^+		$CD4^+CAR^+$		$CD8^+CAR^+$		Total CAR^+	
	PBMC	UCB	PBMC	UCB	PBMC	UCB	PBMC	UCB	PBMC	UCB	PBMC	UCB
No DNA	0.6	1.0	0.2	0.1	1.6	1.3						
SB11	0.9	1.1	0.8	0.2	1.2	1.4						
Txpn*	15.9	10.7	9.5	1.0	27.0	11.8	0.07	0.8	0.5	0.3	0.8	3.5
Txpn* and SB11	13.3	4.9	7.9	0.8	22.0	5.4	27.5	24.8	13.5	1.9	38.9 †	29.7 ‡

Abbreviation: UCB, umbilical cord blood.

*Txpn (transposon) = $_{CoOp}$CD19RCD28/pT-MNDU3.

† When *SB* transposase is electroporated with transposon, there is 49-fold improved CAR expression.

‡ When *SB* transposase is electroporated with transposon, there is 8.4-fold improved CAR expression.

quiescent state. To assist with subsequent translation to clinical practice, the Nucleofector solution is available for use in cGMP.

Both the *SB* transposase and IR have been independently manipulated to improve efficiency of transposition, but changes to both do not generally seem to be additive. In preliminary experiments, we too compared the relative transposition efficiency of the SB10 (10, 16) and SB11 transposases (the latter exhibiting improved enzymatic activity; ref. 17) in a two-by-two matrix using the Amaxa 96-well Shuttle system to introduce these transposases and pT (15, 16) and pT2 transposons (the latter exhibiting improved transposition; ref. 27) into Jurkat T cells. As observed with other cell lines, we found a similar increase in transposition using SB11 with pT and using SB10 with pT2 (27) although, as reported, overproduction of transposase inhibited transposition (13, 17). When the pT2-improved transposon was combined with SB11, no further increase in transgene expression was observed over that achieved when these components were used with SB10 or pT, respectively. In the present study, a combination of pT transposon (for integration) and SB11 transposase (for transient expression) was used for experiments with primary T cells.

Generation of $CD19^+$ aAPC. We determined whether peripheral blood and umbilical cord blood–derived T cells could be selectively propagated by stimulating through an introduced immunoreceptor. This experiment would evaluate our underlying hypothesis of whether the presence of the *SB* transposase would improve efficiency of CAR transposon integration in T cells. Our initial attempts at CAR-dependent T-cell propagation after electrotransfer of the *SB* system used allogeneic LCL because these are widely available as master cell banks (including at M. D. Anderson Cancer Center) manufactured in compliance with cGMP for phase I/II trials. However, these LCL resulted in nonspecific outgrowth of CAR^{null} T cells that had undergone electrotransfer of *SB* plasmids, independent of CAR expression (data not shown), presumably due to outgrowth of alloreactive T cells. Because our *SB* transposon by design does not include a drug resistance gene, we avoided nonspecific propagation of T cells using K562 as aAPC because these do not express classical HLA molecules. K562 cells are widely recognized as a platform suitable for the numerical expansion of lymphocytes because they (*a*) can be cultured in compliance with cGMP, (*b*) express desired endogenous T-cell costimulatory molecules, (*c*) secrete pro-inflammatory cytokines, and (*d*) can be readily modified to enforce the expression of antigen and desired endogenous T-cell costimulatory molecules (28, 29). To provide an IL-15–mediated growth stimulus coordinated with recognition of CD19 antigen, the aAPC expressing tCD19, 4-1BBL, and MICA were further modified to express the IL-15 cytokine on the cell surface (IL-15-Fc; Fig. 2*A*). Membrane-bound IL-15 has been used before to propagate natural killer (NK) cells on K562 (19). The ability of these K562 aAPCs to propagate CAR^+ T cells after electrotransfer of *SB* transposon and transposase plasmids is described in the next section.

***SB*-mediated gene transfer of CAR transposon in primary T cells.** After using the Nucleofector to import plasmid DNA into quiescent T cells, we observed that peripheral blood– and umbilical cord blood–derived electroporated $CD4^+$ and $CD8^+$ T cells readily expressed the CAR transposon (Table 1; Fig. 3*A*). Not surprisingly, the presence of the plasmid expressing the SB11 transposase did not increase transposon expression when measured 24 hours after electroporation (22% and 27% CAR expression with and without transposase, respectively), as this early time point for assessing transgene expression records transient nonintegrated CAR expression (Fig. 3*A*). The genotoxicity reported with excess expression of *SB* transposase (17) was apparently controlled in our two-plasmid system using a 1:1 ratio of transposon and transposase. To obtain peripheral blood– and umbilical cord blood–derived T cells with integrated transposon, the genetically modified cells were cocultured with γ-radiated aAPC (K562 genetically modified to express tCD19, 4-1BBL, MICA, IL-15-Fc) at a ratio of 1:10 (T cell to aAPC). After 5 weeks of continuous coculture (γ-radiated aAPC re-added every 7 days), the percentage of peripheral blood–derived T cells expressing CAR increased in the transposase-containing group (43%), whereas the CAR expression was lost (0.7%) when transposon was electrotransferred in the absence of transposase (Fig. 3*A*). Thus, after 28 to 35 days, the efficiency of two DNA plasmid *SB*-mediated gene transfer improved CAR expression by ~49 to 60-fold, compared with a single plasmid transposon control (Table 1). The expression of the CAR was confirmed by Western blot of whole-cell lysates of propagated T cells probed using a mAb specific for CD3-ζ chain revealed the 79-kDa chimeric ζ chain in addition to the 21-kDa endogenous ζ chain (Fig. 3*C*). To monitor for the presence or absence of the integrated CD19RCD28 transgene, DNA from the

DOI:10.1158/0008-5472.CAN-07-5600

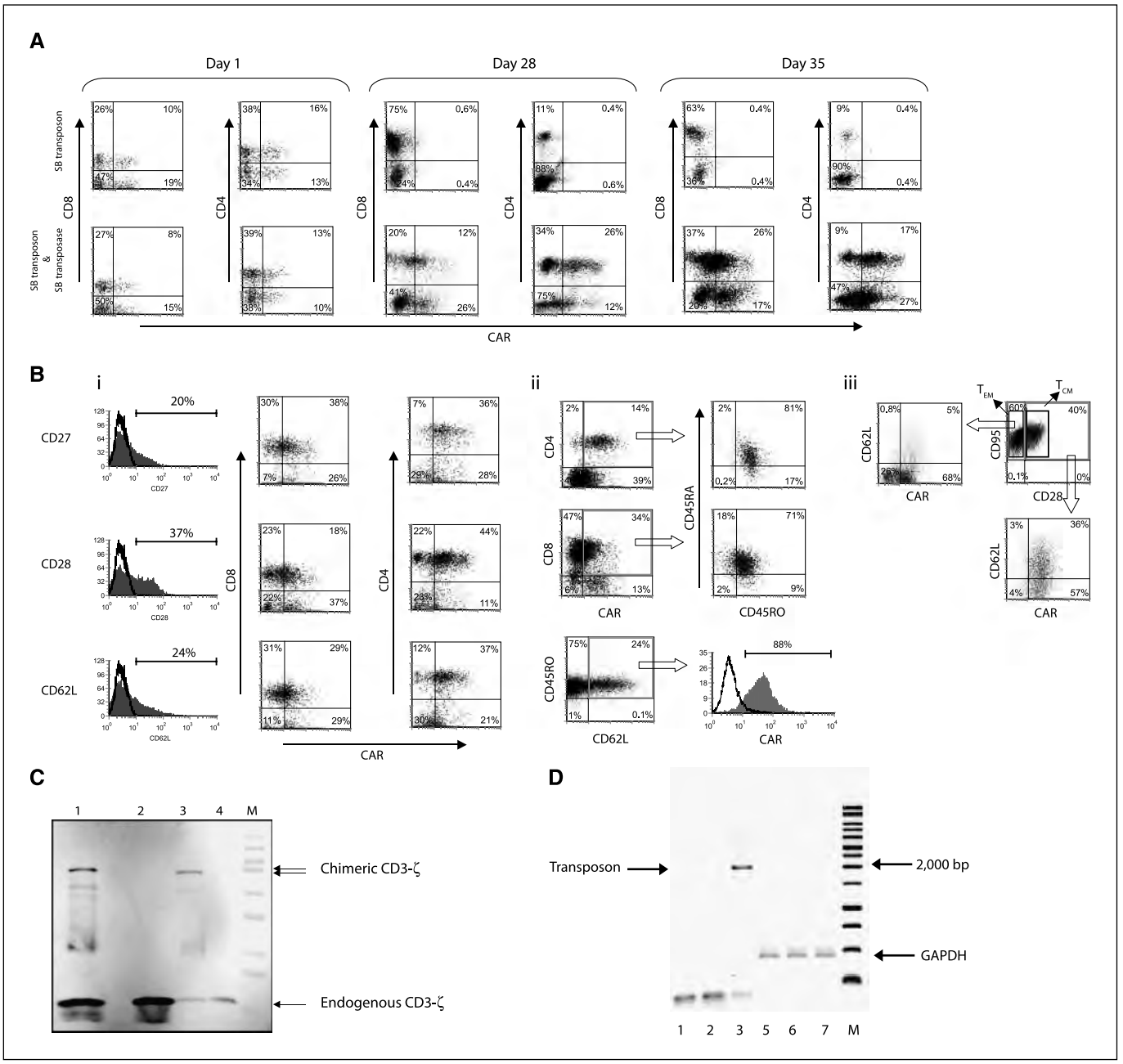

Figure 3. Characterization of CAR expression on peripheral blood–derived T cells after electrotransfer of *SB* plasmid system. *A,* expression of CAR on $CD8^+$ and $CD4^+$ T cells after electrotransfer of *SB* transposon with or without SB11 transposase at 24 h, and 4 and 5 wk of coculture on γ-irradiated K562-derived aAPC expressing tCD19, IL-15-Fc, MICA, and 4-1BBL. *B, i,* immunophenotype of memory cell markers (CD27, CD28, CD62L) on genetically modified T cells generated after 5 wk of coculture on aAPC. The gray-filled histograms reveal the percentage of T cells expressing CD27, CD28, and CD62L in the lymphocyte-gated population. Those expressing the memory cell markers were analyzed for coexpression of CAR (detected by mAb clone 2D3) and CD8 or CD4. *ii,* expression of CD45RO, CD45RA, and CD62L on T cells generated after coculture. CAR^+ CD4 or CD8 cells were analyzed for the expression of CD45RA and CD45RO. The MFI of the unmanipulated T cells was 867/50 (CD45RA/CD45RO) compared with 28/38 for the SB-transfected T cells. CD45RO and CD62L double-positive cells were also analyzed for coexpression of CAR. *iii,* T_{CM}, defined as double-positive for CD28 and CD95 (T_{EM}, $CD28^{neg}CD95^{pos}$), were analyzed for coexpression of CD62L and CAR. *C,* Western blot analysis of CAR expression detected by mAb specific for CD3-ζ. Whole-cell protein (20 μg) lysates from primary T cells genetically modified with $_{CoOp}$CD19RCD28 (*lane 1,* ~79 kDa chimeric protein) or no plasmid control (*lane 2*); $CD19R^+$ Jurkat cells (*lane 3,* ~66 kDa chimeric protein) or parental Jurkat (*lane 4*) were resolved by SDS-PAGE under reducing conditions. *D,* integration of $_{CoOp}$CD19RCD28 by PCR. DNA was isolated from T cells after mock electroporation (no DNA, *lanes 1* and *4*), from T cells 28 d after electroporation with *SB* transposon in the absence of transposase (*lanes 2* and *5*), and from T cells 28 d after electroporation with transposon in the presence of SB11 transposase (*lanes 3* and *6*). PCR was accomplished using transposon-specific primers (*lanes 1–3*) or GAPDH-specific primers (*lanes 4–6*). The data showing *SB* system in peripheral blood/cord blood are from a representative experiment.

numerically expanded T cells, electroporated with and without SB11, were PCR amplified using CAR-specific primers. A 1,900-bp band corresponding to the CD19RCD28 transgene was observed in T cells electroporated using the *SB* two-plasmid system, whereas no similar band was observed in cells electroporated with *SB* transposon in the absence of transposase, which is consistent with improved SB11-mediated transposition in T cells expressing CAR protein (Fig. 3*D*).

DOI:10.1158/0008-5472.CAN-07-5600

Propagation of CAR$^+$ T cells. The K562-derived aAPC was calculated to give a 20-fold growth of genetically modified T cells at the end of 4 weeks with continued and accelerated expansion thereafter (Fig. 4*A*). A subset analysis revealed that populations of both CD4$^+$CAR$^+$ and CD8$^+$CAR$^+$ T cells could be propagated (Table 1). Initially, the rates of CD4$^+$ and CD8$^+$ T-cell growth on aAPC were similar, but after ~8 weeks there was an outgrowth of CD4$^+$CAR$^+$ T cells (Fig. 4*B*). Thus, continued time in tissue culture could be used to derive CAR$^+$ T cells with an increased CD4 to CD8 ratio. We also followed the percentage expression and density of the CAR on the T-cell surface by flow cytometry. With coculture, there was outgrowth of percentage of T cells expressing the CD19-specific CAR (22% on day 1 and peaking at 99% on day 70). However, as the percentage of CAR$^+$ T cells increased, there was a decrease in the density of CAR expression, as the MFI dropped from a peak of 109 arbitrary units at 21 days, early in the coculturing process, and then declined over culture time. The amount of CAR for the population peaked at ~70 days after electroporation (percentage expression multiplied by MFI). Thus, adding a fixed ratio of aAPC (with a fixed density of CD19 antigen) to T cells seems to have supported the growth for populations of T cells that either expressed high density of CAR or high percentage of CAR.

Immunophenotype of CAR$^+$ memory T cells. Previously, T cells from healthy donors electroporated to express a CD19-specific CAR and nonspecifically activated for proliferation by cross-linking CD3 with OKT3 using REP have shown a predominant phenotype consistent with differentiated effector CD8$^+$ T cells (20). In contrast, after electrotransfer of *SB* plasmids and numerical expansion on aAPC, T cells exhibited a heterogeneous immunophenotype and apparently included populations of CAR$^+$ T_{CM}. We showed that the CAR$^+$ T cells expressed memory cell markers (CD27, CD28, CD62L; refs. 30–32) as well as determinants of an effector-cell phenotype (Fig. 3*Bi*). For example, over half of CD27$^+$, CD28$^+$, and CD62L$^+$ T cells expressed CAR. Indeed, as a marker for T_{CM}, 88% of the CD62L$^+$CD45RO$^+$ cells expressed the CAR (Fig. 3*Bii*; ref. 33). Upon

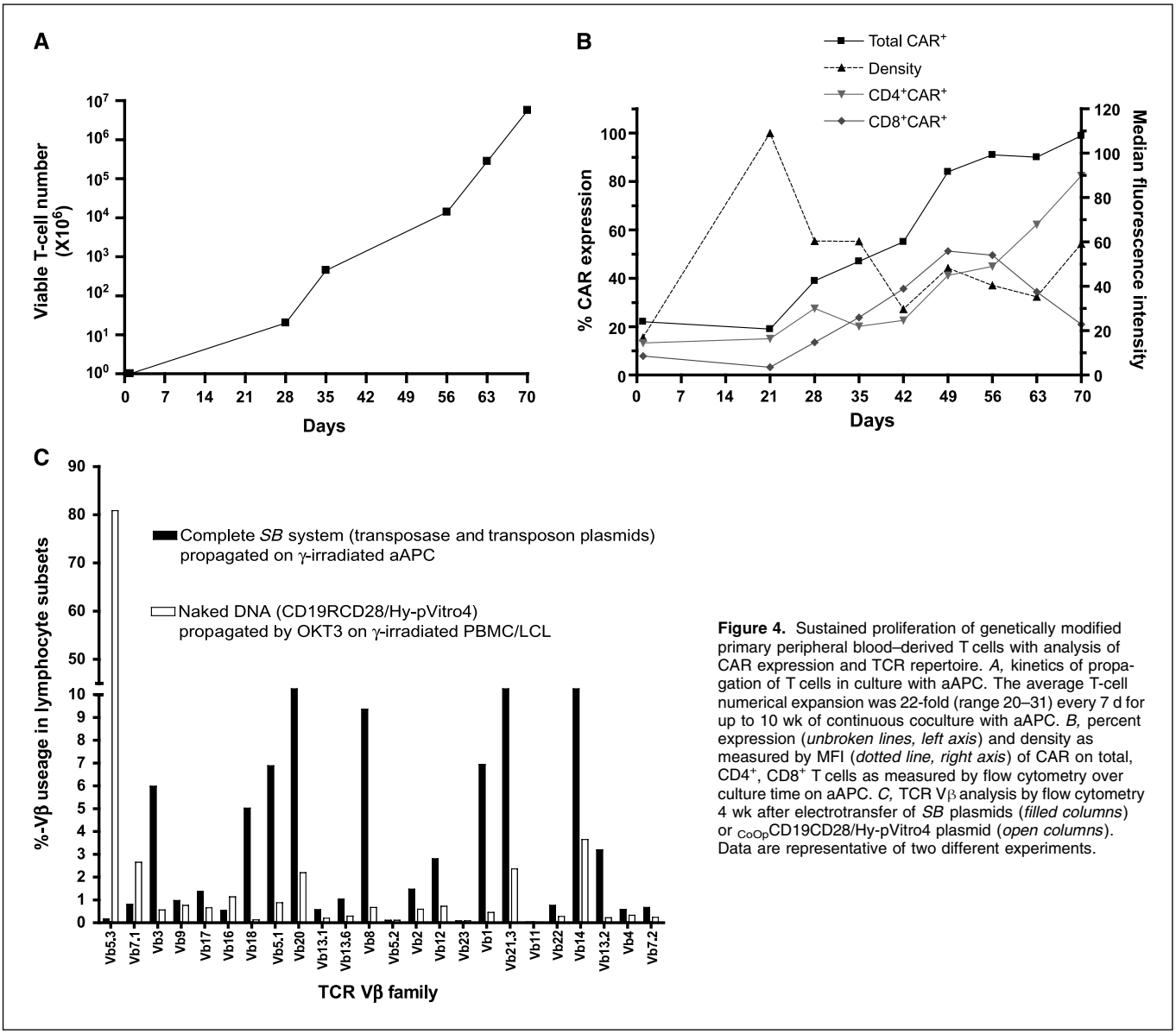

Figure 4. Sustained proliferation of genetically modified primary peripheral blood–derived T cells with analysis of CAR expression and TCR repertoire. *A,* kinetics of propagation of T cells in culture with aAPC. The average T-cell numerical expansion was 22-fold (range 20–31) every 7 d for up to 10 wk of continuous coculture with aAPC. *B,* percent expression (*unbroken lines, left axis*) and density as measured by MFI (*dotted line, right axis*) of CAR on total, CD4$^+$, CD8$^+$ T cells as measured by flow cytometry over culture time on aAPC. *C,* TCR Vβ analysis by flow cytometry 4 wk after electrotransfer of *SB* plasmids (*filled columns*) or $_{CoOp}$CD19CD28/Hy-pVitro4 plasmid (*open columns*). Data are representative of two different experiments.

DOI:10.1158/0008-5472.CAN-07-5600

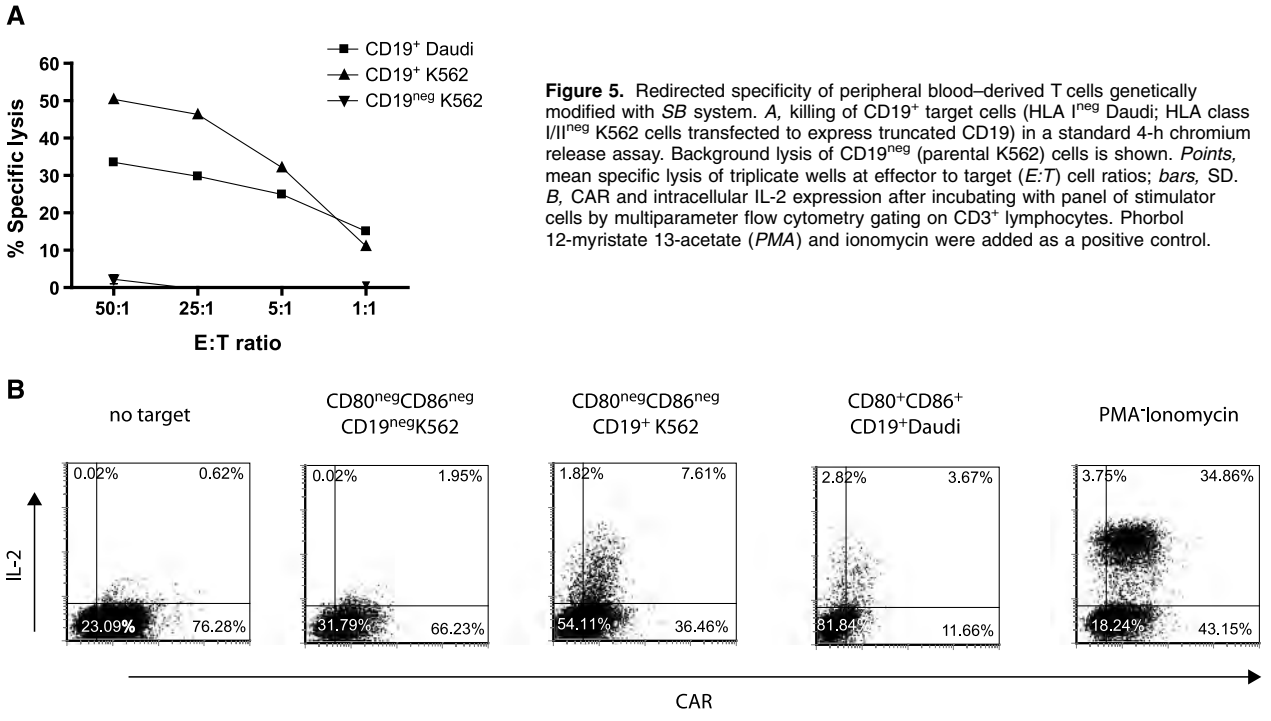

Figure 5. Redirected specificity of peripheral blood–derived T cells genetically modified with *SB* system. *A,* killing of $CD19^+$ target cells (HLA I^{neg} Daudi; HLA class I/II^{neg} K562 cells transfected to express truncated CD19) in a standard 4-h chromium release assay. Background lysis of $CD19^{neg}$ (parental K562) cells is shown. *Points,* mean specific lysis of triplicate wells at effector to target (*E:T*) cell ratios; *bars,* SD. *B,* CAR and intracellular IL-2 expression after incubating with panel of stimulator cells by multiparameter flow cytometry gating on $CD3^+$ lymphocytes. Phorbol 12-myristate 13-acetate (*PMA*) and ionomycin were added as a positive control.

gating $CD45RO^+$ cells, we observed a preferential expansion of T cells with this memory-cell marker in the cultured *SB*-transfected T cells (90%; MFI, 38) compared with unmanipulated T cells obtained directly from PBMC (36%; MFI, 50). T_{EM} and T_{CM} have also been distinguished based on relative expression of CD28 and Fas (34). Using these markers, we were able to identify that genetically modified and propagated T_{CM} constituted ~40% of the total cell population and $CD28^{neg}CD95^+$ T_{EM} represented the remainder of the propagated T cells. Multiparameter flow cytometry further revealed that 39% of $CAR^+CD28^+CD95^+$ T_{CM} expressed CD62L. In comparison, only 7% of the CAR^+ T_{EM} expressed CD62L (Fig. 3*Biii*). These data reveal that CAR^+ T cells are present in T cells that express markers consistent with T_{CM}. Preferential expansion of T cells in tissue culture with an apparent memory phenotype can also be inferred by from the ratio of CD45RA/CD45RO, which decreased from 2.75 in unmanipulated freshly derived PBMC to 0.9 for SB-transfected and *ex vivo* propagated T cells (Fig. 3*Bii*). The relative percentage increase of observed $CD45RO^+$ cells, or the decrease in CD45RA/CD45RO ratio, is presumably due to the repetitive antigenic stimulation of cultured T cells resulting in down-regulation of the high molecular weight CD45RA isoform and reciprocal up-regulation of the low molecular weight isoform CD45RO during time in culture. Coexpression of both CD45RA and CD45RO has been associated with the phenotype of effector T cells (35) but as in circulating peripheral blood–derived T cells express both CD45RA and CD45RO, the markers are presumably also present on memory cells. These data have implications for improved *in vivo* efficacy as T_{CM} are associated with long-term persistence after adoptive transfer.

TCR Vβ repertoire. We tracked the expression of TCR Vβ usage by flow cytometry over time with the hypothesis that an improvement in DNA-plasmid integration would be reflected by maintenance of a broad pre-electroporation TCR Vβ repertoire. The pattern of TCR Vβ usage observed after electrotransfer of the two DNA *SB* plasmids and propagation on aAPC was much broader than when T cells were electroporated using the single $_{CoOp}$CD19RCD28/Hy-pVitro4 plasmid and expanded by REP by cross-linking CD3 with OKT3 in cytocidal concentrations of hygromycin B. We observed that ~80% of the T cells electroporated with $_{CoOp}$CD19RCD28/Hy-pVitro4 plasmid expressed a single TCR Vβ family (Vβ5.3). In contrast, ~80% of the T cells electroporated with the complete *SB* system expressed 30% of the TCR Vβ families (Fig. 4*C*). This is consistent with less efficient integration of the $_{CoOp}$CD19RCD28/Hy-pVitro4 plasmid compared with the *SB* system. These data have implications for design of adoptive immunotherapy trials as maintaining a broad TCR diversity is desired to restore immune reconstitution after myeloablative preparative regimens.

Redirected function of CAR^+ T cells after electrotransfer of *SB* plasmids. The numerically expanded T cells were evaluated for redirected killing. The genetically modified T cells were able to lyse $CD19^+$ targets, and specificity of killing was shown by the background lysis of $CD19^{neg}$ K562 cells (Fig. 5*A*). We showed a 25-fold increase in specific lysis of $CD19^+$ K562 at effector-to-target ration of 50:1. The lack of killing of $CD19^{neg}$ K562 is consistent with absence of resident NK cell function in the culture, as these target cells are sensitive to NK cell–mediated lysis. Because the CAR contains a CD28 endodomain, we investigated whether T cell–derived IL-2 could be produced when CAR contacted CD19 antigen in the absence of binding CD80 or CD86. An intracellular cytokine assay showed that IL-2 could be detected in the CAR^+ T cells only when cultured with $CD19^+$ stimulator cells and not with $CD19^{neg}$ cells (Fig. 5*B*). There was an ~4-fold increase in IL-2 expression when CAR^+ T cells were stimulated by $CD19^+CD80^{neg}CD86^{neg}$ K562 cells compared with $CD19^{neg}$ K562 parental controls. No significant

DOI:10.1158/0008-5472.CAN-07-5600

IL-2 production was observed when T cells were cultured in absence of stimulator cells. These data are consistent with activation of T cells for killing and IL-2 cytokine production through the CAR.

Lack of integration of SB11 transposase in propagated T cells. Continued presence of the SB11 transposase in genetically modified T cells may cause genotoxicity. We evaluated for the presence of integrated transposase plasmid by genomic PCR. No band corresponding to the SB11 transposase gene (size ~830 bp) was detected in T cells that were electroporated with the *SB* transposon and transposase and had undergone 4 weeks of coculture with aAPC (Fig. 6*A*), which is consistent with the rapid loss of transposase expression activity over the first few days postdelivery in mice (36). These results indicate that the SB11 transposase was not integrated into the genome of cells stably expressing the CD19RCD28 CAR.

Karyotype of genetically modified T cells. As a measure of global genotoxicity associated with undesired and continued transposition, we evaluated the integrity of the chromosome structure. G-banding analysis of the *SB*-transfected T cells showed a normal female karyotype, 46, XX with no apparent numerical or structural chromosome alterations (Fig. 6*B*). Although this does not exclude chromosomal damage below the limit of detection of this technique, it supports the premise that *SB* transposition in T cells is not associated with translocations and chromosomal aberrations.

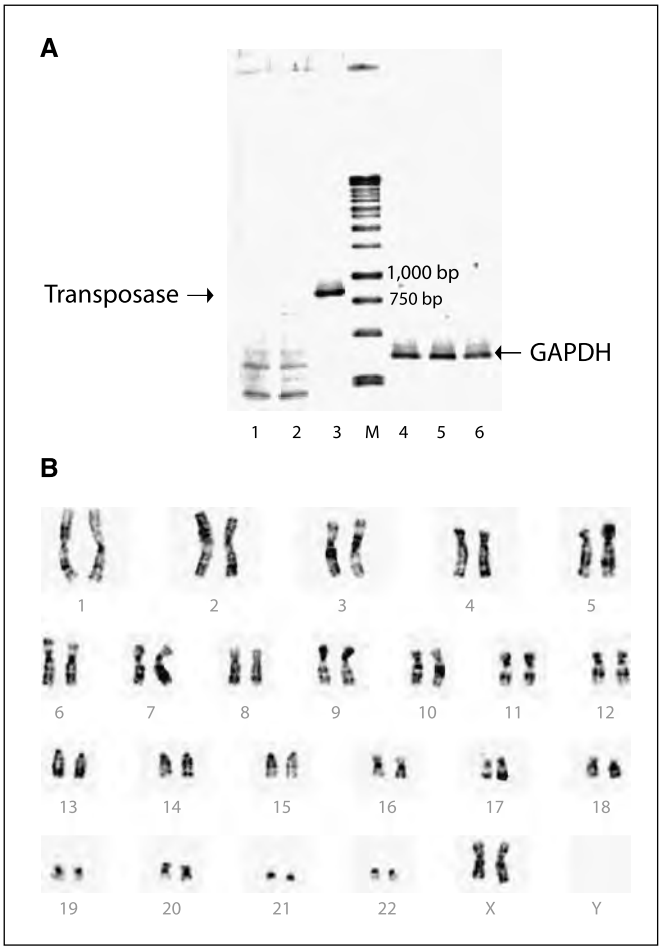

Figure 6. Safety issues regarding SB transposase and chromosomal aberrations. *A,* lack of integration of SB11 transposase by genomic PCR from genetically modified and propagated peripheral blood–derived T cells. DNA was isolated from T cells after mock electroporation (no DNA, *lanes 1* and *4*), from T cells 28 d after electroporation with the two-plasmid *SB* system (*lanes 2* and *5*), or from T cells 1 d after electroporation with the two-plasmid *SB* system (*lanes 3* and *6*). PCR was accomplished using transposase-specific primers (*lanes 1–3*) or GAPDH-specific primers (*lanes 4–6*). *B,* idiogram of a G-banded karyotype of the *SB*-transfected peripheral blood–derived T cells showing no apparent numerical or structural chromosome alterations.

Discussion

We have previously showed that peripheral blood– and umbilical cord blood–derived T cells can be rendered specific for CD19, based on using a CAR capable of providing a fully competent activation signal, development of aAPC-expressing antigen, and desired costimulatory signals. In this report, we describe the use of *SB* transposon/transposase plasmids to introduce CD19-specific CAR leading to efficient outgrowth of CAR^+ T cells on aAPC with preservation of $CD4^+$, $CD8^+$, central memory, and effector-cell immunophenotypes. This is expected to be of widespread interest as many institutions are evaluating the clinical potential of genetically modified T cells with redirected specificity. The majority of these programs use recombinant viral vectors, which, although efficient at gene transfer, are generally cost-prohibitive to manufacture to clinical grade and still permit incremental changes to clinical trial design. Yet, at this early stage of gene therapy planning with clinical grade T cells, what is needed, and is provided here, is a cost-effective gene transfer system that encourages reiterative changes to expression vector and/or CAR design to be used in proof-of-concept clinical trials that support hypothesis testing from the bench to the bedside and back again. The approximate cost for manufacture and release of a clinical grade plasmid DNA is between $20,000 and $40,000 depending on supplier and degree of release testing needed. This release testing typically requires restriction enzyme analyses, sequencing, and measures of (*a*) homogeneity/purity/contamination (protein, RNA, and other DNA) and (*b*) sterility including endotoxin. For early-phase proof-of-concept trials, this pricing compares favorably with the relatively high cost of recombinant retrovirus, including lentivirus as manufacture and release of clinical grade viruses may exceed 10 times the cost of DNA-plasmid production. Furthermore, there is downward pressure on the unit cost for DNA because there are many vendors worldwide with the capability to produce clinical grade plasmids. The manufacture/release of recombinant retrovirus is highly specialized, requiring the expertise of a small number of GMP facilities that contributes to high cost and can introduce delays to production and thus availability for clinical use.

Previously, the relatively low levels of nonviral gene transfer efficiency to introduce naked DNA plasmid coding CAR transgene, compared with viral-mediated transduction, has been compensated by lengthy periods of *ex vivo* tissue culture to select-out T cells expressing drug-metabolizing enzymes. Thus, an attractive feature of the *SB* gene transfer system to introduce CAR into T cells is avoidance of the need to express immunogenic section genes, such as bacteria-derived *Hy* transgene. Some human-derived drug-resistant transgenes are available for use in hematopoietic cells (37, 38), but they typically incorporate amino acid changes from the native protein sequence that may compromise their inability to remain nonimmunogenic and the continued presence of chemoselective drugs may slow kinetics of *ex vivo* numerical expansion and alter T-cell function.

Coupling electrotransfer of *SB* system with selective propagation of CAR^+ T cells was made possible using K562 cells that had been

DOI:10.1158/0008-5472.CAN-07-5600

genetically modified to express costimulatory molecules to function as aAPC. We have previously shown that the presence of 4-1BBL and MICA on $CD19^+$ K562 could propagate $CD19R^+$ T cells (18). However, sustained antigen-driven numerical expansion of genetically modified T cells on aAPC has required the presence of rhIL-15 (18). In our current experiments, we found that the exogenous addition of this soluble cytokine led to nonspecific stimulation of T cells after electrotransfer, especially because there was no concomitant drug selection, resulting in the outgrowth of T cells that did not maintain CAR expression (data not shown). This could be corrected by expression of IL-15 at the interface between aAPC and T cells, using membrane-bound IL-15, as has been shown for the survival/propagation of NK cells (19, 39). This approach of expressing IL-15 on the cell surface has the further advantage of avoiding rhIL-15 protein that is not yet readily/widely available for use in clinical trials. Allogeneic LCL are another source of $CD19^+$ aAPC to propagate CD19-specific T cells and are available to many centers operating facilities in compliance with cGMP as a master cell bank. However, the presence of HLA led to stimulation of T cells through activation of allospecific TCR and subsequent outgrowth of T cells that lacked CAR expression. This alloimmune response could be avoided using the K562 as aAPC, as these cells lack endogenous class I and II MHC (29).

Next-generation clinical trials using genetically modified T cells are expected to infuse predefined populations of T cells with defined characteristics such as the inclusion of both $CD4^+$ and $CD8^+$ T cells and T_{CM}. There is convincing clinical data that the presence of $CD4^+$ T-helper cells improves the persistence of $CD8^+$ antigen-specific T cells (40). Furthermore, clinical trials using melanoma-specific T cells have shown *in vivo* long-term persistence of subpopulations of infused $CD28^+$ memory T cells (41) and human experience has shown a preference for the selective survival of autologous HIV-specific $CD27^+$ versus $CD27^{neg}$ adoptively transferred T cells (31). These data are supported by nonhuman experiments in which adoptive transfer of *ex vivo* propagated macaque $CD28^+CD95^+CD62L^+$ T_{CM} resulted in longer *in vivo* persistence compared with infusion of numerically expanded effector T cells (34). We note that the electrotransfer of *SB* plasmids and subsequent CAR-mediated propagation on aAPC supports the outgrowth of T cells with these desired phenotypes as our CAR^+ T cells maintain expression of CD27, CD28, CD45RO, CD95, and CD62L. Clinical trials will be needed to determine whether adoptive transfer of these CAR^+ T cells with an apparent central memory immunophenotype ($CD28^+CD95^+CD62L^+$) results in long-term *in vivo* persistence of genetically modified T cells or whether these cells, despite being maintained for weeks in culture, will differentiate after infusion into effector T cells with limited *in vivo* survival. Clinical experience will also be needed to assess whether the presence of CD62L (L-selectin) on genetically modified T cells enables CAR^+ T cells to traffic to sites of minimal residual disease for B-lineage malignancies, such as secondary lymphoid organs (42, 43).

Although there are a variety of transposase/transposon expression vectors available, we elected to combine the improved enzymatic activity of the SB11 transposase with pT IR sequences, rather than less efficient SB10 transposase with pT2 plasmid containing IR with improved IR activity. This was based on (*a*) the observation that integrated SB11 transposase could not be detected after T-cell culture on aAPC and (*b*) the assumption that because the CAR transposon with flanking IR is to be integrated, we wished to reduce the potential for introducing an element with increased potential for retransposition and potential deleterious chromosomal rearrangement. We note that the majority of viral vectors currently used in human gene therapy trials also contain elements flanking transgene to be integrated, such as the long terminal repeat (LTR) termini of recombinant retrovirus, with binding sites for enzymes with integrase activity. The transfer of retroviral-derived LTR has not been associated with deleterious host genome chromosome rearrangements, especially in T cells (44), and the low risk of genotoxicity due to the integrated presence of *SB* IR should be on par with retrovirally mediated transduction.

A gene transfer event with stable integration could result in deleterious insertional mutagenesis, but for *SB* transposition this seems to be less than retrovirally mediated transduction given the observed preference for random chromosomal integration at TA-dinucleotide base pairs areas. Although the safety of *SB* transposition can only be adequately addressed in clinical trials, we have not seen major chromosomal aberrations after electrotransfer of *SB* plasmids. Furthermore, to safeguard against the emergence of genetically modified T cells with autonomous growth, we routinely culture T cells after electroporation without aAPC and we are yet to observe evidence of antigen-independent proliferation. The risks for first-in-human trials using *SB* system would seem to be ameliorated when using T cells, rather than hematopoietic progenitor cells and in the setting of high-risk malignancies in which patients are expected to succumb to underlying relapsed malignancies. The risks of genotoxicity may be reduced in the future using a transposase with directed integration (45, 46), coupling persistent transposase activity with a transgene mediating conditional suicide, or introducing mRNA (47) rather than DNA coding for the transposase.

The future for clinical therapy infusing genetically modified T cells with redirected specificity looks promising. There are published reports on the therapeutic effect of T cells genetically modified to express full-length αβTCR (48) and clinical studies using T cells expressing chimeric receptors to redirect specificity have been reported or are under way (35, 49, 50). With the results of the first in-human trial infusing CD19-specific T cells being reported (3), the next step (the so-called second translational hurdle) will be expanding these single-institution experiences to multi-institution trials powered for efficacy. The platform we describe for producing CAR^+ T cells should be appealing to investigators undertaking single-site as well as multisite trials using gene transfer of immunoreceptor(s) to redirect the specificity of T cells, including T_{CM}. The system we have developed uses technology that is readily accessible and practiced in compliance with cGMP for phase I/II trials because we use (*a*) DNA plasmids, (*b*) electroporation using a commercial device, (*c*) weekly addition of irradiated immortalized aAPC feeder cells derived from K562 (which are available for use in cGMP), and (*d*) addition of exogenous rhIL-2 purchased through pharmacy stores.

In conclusion, we report a new gene transfer approach for the clinical application of T cells with redirected specificity for desired antigens. It is anticipated that this approach will be of interest not just for generating clinical grade T cells with specificity for CD19, but for genetically modifying T cells to express CAR with alternative specificities as well as for introducing TCR transgenes. Most adoptive immunotherapy trials that have shown therapeutic efficacy, e.g., to melanoma, CMV, EBV, and adenoviral antigens, have all used an *in vitro* antigen-driven proliferation step to propagate antigen-specific T cells before infusion. We have now incorporated *ex vivo*

DOI:10.1158/0008-5472.CAN-07-5600

CAR-dependent proliferation to derive genetically modified T cells and will evaluate the CD19-specific T cells, using *SB* transposition and aAPC, in a next-generation clinical trial.

Acknowledgments

Received 9/21/2007; revised 12/19/2007; accepted 1/17/2008.

Grant support: Cancer Center Core Grant CA16672; RO1 CA124782 and CA120956; R21 CA129390 and CA116127; Department of Defense grant PR064229; The Alliance for Cancer Gene Therapy; The Alex's Lemonade Stand Foundation; The Carl C. Anderson, Sr. and Marie Jo Anderson Charitable Foundation; The Gillson Longenbaugh Foundation; The J.P. McCarthy Fund Developmental Grant Program; The Leukemia and Lymphoma Society; The Lymphoma Research Foundation; The Miller Foundation, The National Foundation for Cancer Research; The National Marrow Donor Program; and The Pediatric Cancer Research Foundation.

The costs of publication of this article were defrayed in part by the payment of page charges. This article must therefore be hereby marked *advertisement* in accordance with 18 U.S.C. Section 1734 solely to indicate this fact.

We thank Dr. Mark Kay at Stanford School of Medicine, Stanford, CA, for providing the pT plasmid; Dr. John Rossi at City of Hope Cancer Center, Duarte, CA, for his valuable suggestions; Karen Ramirez and David He from Flow Cytometry Core Laboratory (NIH grant 5P30CA016672-32) for their help with flow cytometry; Jim Wygant and Dr. Brad McIntrye in the Immunology Core for their help with the monoclonal antibody production; and Dr. Asha Multani from T.C. Hsu Molecular Cytogenetics Core for her assistance with G-banding.

References

1. Cooper LJ, Topp MS, Serrano LM, et al. T-cell clones can be rendered specific for CD19: toward the selective augmentation of the graft-versus-B-lineage leukemia effect. Blood 2003;101:1637–44.
2. Serrano LM, Pfeiffer T, Olivares S, et al. Differentiation of naive cord-blood T cells into CD19-specific cytolytic effectors for posttransplantation adoptive immunotherapy. Blood 2006;107:2643–52.
3. Jensen MC, Popplewell L, DiGiusto DL, et al. A first-n-human clinical trial of adoptive therapy using CD19-specific chimeric antigen receptor re-directed T cells for recurrent/refractory follicular lymphoma. Mol Ther 2007;15:S142.
4. Lupton SD, Brunton LL, Kalberg VA, Overell RW. Dominant positive and negative selection using a hygromycin phosphotransferase-thymidine kinase fusion gene. Mol Cell Biol 1991;11:3374–8.
5. Kowolik CM, Topp MS, Gonzalez S, et al. CD28 costimulation provided through a CD19-specific chimeric antigen receptor enhances *in vivo* persistence and antitumor efficacy of adoptively transferred T cells. Cancer Res 2006;66:10995–1004.
6. Cid-Arregui A, Juarez V, zur Hausen H. A synthetic E7 gene of human papillomavirus type 16 that yields enhanced expression of the protein in mammalian cells and is useful for DNA immunization studies. J Virol 2003;77:4928–37.
7. Patterson SS, Dionisi HM, Gupta RK, Sayler GS. Codon optimization of bacterial luciferase (lux) for expression in mammalian cells. J Ind Microbiol Biotechnol 2005;32:115–23.
8. Berger C, Huang ML, Gough M, Greenberg PD, Riddell SR, Kiem HP. Nonmyeloablative immunosuppressive regimen prolongs *in vivo* persistence of gene-modified autologous T cells in a nonhuman primate model. J Virol 2001;75:799–808.
9. Jung D, Jaeger E, Cayeux S, et al. Strong immunogenic potential of a B7 retroviral expression vector: generation of HLA-B7-restricted CTL response against selectable marker genes. Hum Gene Ther 1998;9:53–62.
10. Ivics Z, Hackett PB, Plasterk RH, Izsvak Z. Molecular reconstruction of Sleeping Beauty, a Tc1-like transposon from fish, and its transposition in human cells. Cell 1997;91:501–10.
11. Izsvak Z, Ivics Z. Sleeping beauty transposition: biology and applications for molecular therapy. Mol Ther 2004;9:147–56.
12. Geurts AM, Hackett CS, Bell JB, et al. Structure-based prediction of insertion-site preferences of transposons into chromosomes. Nucleic Acids Res 2006;34:2803–11.
13. Huang X, Wilber AC, Bao L, et al. Stable gene transfer and expression in human primary T cells by the Sleeping Beauty transposon system. Blood 2006;107:483–91.
14. Robbin PB, Yu XJ, Skelton DM, et al. Increased probability of expression from modified retroviral vectors in embryonal stem cells and embryonal carcinoma cells. J Virol 1997;71:9466–74.
15. Holli RP, Nightingal SJ, Wan X, et al. Stable gene transfer to human CD34(+) hematopoietic cells using the Sleeping Beauty transposon. Exp Hematol 2006;34:1333–43.
16. Yan SR, Meus L, Chi W, Ivic Z, Izsva Z, Ka MA. Somatic integration and long-term transgene expression in normal and haemophilic mice using a DNA transposon system. Nat Genet 2000;25:35–41.
17. Geurts AM, Yang Y, Clar KJ, et al. Gene transfer into genomes of human cells by the sleeping beauty transposon system. Mol Ther 2003;8:108–17.
18. Numbenjapon T, Serrano LM, Singh H, et al. Characterization of an artificial antigen-presenting cell to propagate cytolytic CD19-specific T cells. Leukemia 2006;20:1889–92.
19. Imai C, Iwamoto S, Campana D. Genetic modification of primary natural killer cells overcomes inhibitory signals and induces specific killing of leukemic cells. Blood 2005;106:376–83.
20. Cooper LJ, Al-Kadhimi Z, Serrano LM, et al. Enhanced antilymphoma efficacy of CD19-redirected influenza MP1-specific CTLs by cotransfer of T cells modified to present influenza MP1. Blood 2005;105:1622–31.
21. Pathak S. Chromosome banding techniques. J Reprod Med 1976;17:25–8.
22. Scholten KB, Kramer D, Kueter EW, et al. Codon modification of T cell receptors allows enhanced functional expression in transgenic human T cells. Clin Immunol 2006;119:135–45.
23. Cooper LJ, Ausubel L, Gutierrez M, et al. Manufacturing of gene-modified cytotoxic T lymphocytes for autologous cellular therapy for lymphoma. Cytotherapy 2006;8:105–17.
24. Jensen MC, Clarke P, Tan G, et al. Human T lymphocyte genetic modification with naked DNA. Mol Ther 2000;1:49–55.
25. Riddell SR, Greenberg PD. The use of anti-CD3 and anti-CD28 monoclonal antibodies to clone and expand human antigen-specific T cells. J Immunol Methods 1990;128:189–201.
26. Gresch O, Engel FB, Nesic D, et al. New non-viral method for gene transfer into primary cells. Methods 2004;33:151–63.
27. Cui Z, Geurts AM, Liu G, Kaufman CD, Hackett PB. Structure-function analysis of the inverted terminal repeats of the sleeping beauty transposon. J Mol Biol 2002;318:1221–35.
28. Butler MO, Lee JS, Ansen S, et al. Long-lived antitumor CD8+ lymphocytes for adoptive therapy generated using an artificial antigen-presenting cell. Clin Cancer Res 2007;13:1857–67.
29. Suhoski MM, Golovina TN, Aqui NA, et al. Engineering artificial antigen-presenting cells to express a diverse array of co-stimulatory molecules. Mol Ther 2007;15:981–8.
30. Bachmann MF, Wolint P, Schwarz K, Jager P, Oxenius A. Functional properties and lineage relationship of $CD8^+$ T cell subsets identified by expression of IL-7 receptor α and CD62L. J Immunol 2005;175:4686–96.
31. Ochsenbein AF, Riddell SR, Brown M, et al. CD27 expression promotes long-term survival of functional effector-memory $CD8^+$ cytotoxic T lymphocytes in HIV-infected patients. J Exp Med 2004;200:1407–17.
32. Sallusto F, Lenig D, Forster R, Lipp M, Lanzavecchia A. Two subsets of memory T lymphocytes with distinct homing potentials and effector functions. Nature 1999;401:708–12.
33. Baron V, Bouneaud C, Cumano A, et al. The repertoires of circulating human CD8(+) central and effector memory T cell subsets are largely distinct. Immunity 2003;18:193–204.
34. Berger C, Jensen MC, Lansdorp PM, Gough M, Elliott C, Riddell SR. Adoptive transfer of effector CD8 T cells derived from central memory cells establishes persistent T cell memory in primates. J Clin Invest 2008;118:294–305.
35. Park JR, Digiusto DL, Slovak M, et al. Adoptive transfer of chimeric antigen receptor re-directed cytolytic T lymphocyte clones in patients with neuroblastoma. Mol Ther 2007;15:825–33.
36. Bell JB, Aronvovich EL, Schriefels JM, Clifford AM, Hoekstra ND, Whitley CB, Hackett PB. Duration of expression of Sleeping Beauty transposase in mouse liver following hydrodynamic delivery. Mol Ther 2006;13 Suppl 1:S150.
37. Sato T, Neschadim A, Konrad M, Fowler DH, Lavie A, Medin JA. Engineered human tmpk/AZT as a novel enzyme/prodrug axis for suicide gene therapy. Mol Ther 2007;15:962–70.
38. Yam P, Jensen M, Akkina R, et al. *Ex vivo* selection and expansion of cells based on expression of a mutated inosine monophosphate dehydrogenase 2 after HIV vector transduction: effects on lymphocytes, monocytes, and $CD34^+$ stem cells. Mol Ther 2006;14:236–44.
39. Wittnebel S, Da Rocha S, Giron-Michel J, et al. Membrane-bound interleukin (IL)-15 on renal tumor cells rescues natural killer cells from IL-2 starvation-induced apoptosis. Cancer Res 2007;67:5594–9.
40. Rooney CM, Smith CA, Ng CY, et al. Infusion of cytotoxic T cells for the prevention and treatment of Epstein-Barr virus-induced lymphoma in allogeneic transplant recipients. Blood 1998;92:1549–55.
41. Powell DJ, Jr., Dudley ME, Robbins PF, Rosenberg SA. Transition of late-stage effector T cells to $CD27^+$ $CD28^+$ tumor-reactive effector memory T cells in humans after adoptive cell transfer therapy. Blood 2005;105:241–50.
42. Galkina E, Florey O, Zarbock A, et al. T lymphocyte rolling and recruitment into peripheral lymph nodes is regulated by a saturable density of L-selectin (CD62L). Eur J Immunol 2007;37:1243–53.
43. Mitoma J, Bao X, Petryanik B, et al. Critical functions of N-glycans in L-selectin-mediated lymphocyte homing and recruitment. Nat Immunol 2007;8:409–18.
44. Bonini C, Bondanza A, Perna SK, et al. The suicide gene therapy challenge: how to improve a successful gene therapy approach. Mol Ther 2007;15:1248–52.
45. Ivics Z, Katzer A, Stuwe EE, Fiedler D, Knespel S, Izsvak Z. Targeted sleeping beauty transposition in human cells. Mol Ther 2007;15:1137–44.
46. Yant SR, Huang Y, Akache B, Kay MA. Site-directed transposon integration in human cells. Nucleic Acids Res 2007;35:e50.
47. Wilber A, Wangensteen KJ, Chen Y, et al. Messenger RNA as a source of transposase for Sleeping Beauty transposon-mediated correction of hereditary tyrosinemia type I. Mol Ther 2007;15:1280–7.
48. Morgan RA, Dudley ME, Wunderlich JR, et al. Cancer regression in patients after transfer of genetically engineered lymphocytes. Science 2006;314:126–9.
49. Kershaw MH, Westwood JA, Parker LL, et al. A phase I study on adoptive immunotherapy using gene-modified T cells for ovarian cancer. Clin Cancer Res 2006;12:6106–15.
50. Lamers CH, Langeveld SC, Groot-van Ruijven CM, Debets R, Sleijfer S, Gratama JW. Gene-modified T cells for adoptive immunotherapy of renal cell cancer maintain transgene-specific immune functions *in vivo*. Cancer Immunol Immunother 2007;56:1875–83.

Gene Therapy (2011), 1–8

www.nature.com/gt

ENABLING TECHNOLOGIES

The hyperactive *Sleeping Beauty* transposase SB100X improves the genetic modification of T cells to express a chimeric antigen receptor

Z Jin[1], S Maiti[1], H Huls[1], H Singh[1], S Olivares[1], L Mátés[2], Z Izsvák[2,3], Z Ivics[2,3], DA Lee[1], RE Champlin[4] and LJN Cooper[1]

Sleeping Beauty (SB[3]) transposon and transposase constitute a DNA plasmid system used for therapeutic human cell genetic engineering. Here we report a comparison of SB100X, a newly developed hyperactive SB transposase, to a previous generation SB11 transposase to achieve stable expression of a CD19-specific chimeric antigen receptor (CAR[3]) in primary human T cells. The electro-transfer of SB100X expressed from a DNA plasmid or as an introduced mRNA species had superior transposase activity in T cells based on the measurement of excision circles released after transposition and emergence of CAR expression on T cells selectively propagated upon CD19[+] artificial antigen-presenting cells. Given that T cells modified with SB100X and SB11 integrate on average one copy of the CAR transposon in each T-cell genome, the improved transposition mediated by SB100X apparently leads to an augmented founder effect of electroporated T cells with durable integration of CAR. In aggregate, SB100X improves SB transposition in primary human T cells and can be titrated with an SB transposon plasmid to improve the generation of CD19-specific CAR[+] T cells.
Gene Therapy advance online publication, 31 March 2011; doi:10.1038/gt.2011.40

Keywords: chimeric antigen receptor; T cells; *Sleeping Beauty*; SB11; SB100X; CD19

INTRODUCTION

To overcome immune tolerance, T cells can be genetically modified to express chimeric antigen receptors (CARs) to redirect specificity to tumor-associated antigens, such as CD19 (ref. 1). These transgenes can be introduced into T cells *ex vivo* using virus-based vectors and non-viral systems. Viral-based vectors are widely used in research and clinical trials as they provide stable transduction of target cells.[2,3] However, retroviruses' non-random patterns of integration, at least in hematopoietic stem cells, could potentially activate/inactivate oncogenes/tumor suppressor genes leading to deleterious autonomous T-cell proliferation.[4] Non-viral gene transfer systems based on transposable elements are an alternative approach to transduction to introduce desired transgenes into the genome.[5,6] The *Sleeping Beauty* (SB) transposon system, which integrates at TA dinucleotides apparently randomly across the genome, can be adapted for genetic engineering of T cells.[7–9] This is a result of the stable and efficient integration of an electro-transferred SB transposon by the enzymatic activity of an SB transposase, which is typically introduced as a separate DNA plasmid *in trans* from the DNA plasmid expressing the transposon. SB11 is a hyperactive SB transposase reported to achieve about 100-fold higher integration rates than those achieved by DNA plasmids without transposase activity that use illegitimate recombination to achieve integration.[10] On the basis of the SB11 transposase, we are undertaking gene therapy clinical trials (INDs no. 14193 and no. 14577) infusing CD19-specific T cells that have been electroporated to introduce SB transposon and transposase to generate CAR[+] T cells, which can be selectively propagated on CD19[+] artificial antigen-presenting cells (aAPC[3]).[11,12] Using this approach, clinically sufficient numbers of T cells can be obtained within a few weeks after electroporation of the SB DNA plasmids.

Improvements to the efficiency of transposition may augment our ability to generate CAR[+] T cells. Therefore, we investigated the integration efficiency of a CD19-specific CAR transposon, designated CD19RCD28, using a new mutant of SB transposase termed SB100X,[13] which had been systematically engineered to have increased enzymatic activity in mammalian cells. Follow-up studies have validated the superiority of SB100X transposase activity in mouse embryonic stem cells and human hematopoietic stem cells.[5,14] In preparation for a next-generation trial using the SB system, we compare for the first time the ability of SB11 and SB100X to generate CAR[+] T cells from human peripheral blood mononuclear cells (PBMC). Our data reveal that SB100X results in 10 to 100 times more transposition events than SB11, as determined by the excision of transposon from DNA plasmid, which resulted in three to four times more efficient outgrowth of CD19-specific CAR[+] T cells within 28 days after electroporation, and with approximately one copy of CAR transposon per T-cell genome. This apparent increase in enzymatic activity of SB100X is highlighted by our ability to achieve superior outgrowth of CAR[+] T cells using just one-tenth the amount of DNA plasmid coding for SB100X compared with SB11.

[1]Division of Pediatrics, Children's Cancer Hospital, The University of Texas Graduate School of Biomedical Sciences, The University of Texas MD Anderson Cancer Center, Houston, TX, USA; [2]Max Delbrück Center for Molecular Medicine, Berlin, Germany; [3]University of Debrecen, Debrecen, Hungary and [4]Stem Cell Transplantation and Cellular Therapy, University of Texas MD Anderson Cancer Center, Houston, TX, USA
Correspondence: Dr LJN Cooper, Division of Pediatrics, The University of Texas Graduate School of Biomedical Sciences, The University of Texas MD Anderson Cancer Center, Unit 907, 1515 Holcombe Boulevard, Houston, TX 77030, USA.
E-mail: ljncooper@mdanderson.org
Received 4 August 2010; revised 28 December 2010; accepted 31 January 2011

RESULTS

Measuring SB transposition by quantifying excision circles

It has been reported that SB100X results in improved transposition in mouse and human cells.[14,18] Therefore, we determined the relative ability of SB100X versus SB11 to mediate a transposition event by quantitative-polymerase chain reaction (Q-PCR) adapted to measure DNA fragments (excision circle)[19] that are the expected by-product produced when CAR transgene (transposon) integrates into the T-cell genome, as schematically shown in Figure 1a. The DNA plasmids used to introduce SB transposase in this study are shown in Figures 1b and c.

SB100X transposase improves frequency of transposition

To assess directly the ability of SB100X to improve the frequency of transposition compared with SB11 transposase, we serially measured the formation of non-integrated excision circles (products) by real-time Q-PCR after electroporation of T cells from PBMC. The transient accumulation of excision circles represents the enzymatic activities of the two SB transposases, whereas measurement of the electro-transferred SB transposon and subsequent expression of CD19RCD28 CAR indicates the overall integration efficiency of the non-viral gene transfer process. To account for variations in electro-transfer efficiency, we normalized the excision circle data to the amount of DNA transposon recovered after electroporation (excision circle to CD19RCD28 ratio). This revealed the individual SB transposase's enzymatic activities and adjusted for possible difference in electroporation efficacy between different samples. Measurement of RPPH1, a subunit of RNase P,[20] which is present at one copy on chromosome 14q11.2, was used as internal control in real-time Q-PCR for both quantification of excision circles and transposon DNA species. By varying the relative amounts of DNA plasmids coding for the transposases, SB100X reached peak activity at a concentration of 5 μg per electroporation (Figure 2b). However, at 10 μg per electroporation, SB100X resulted in significant loss of PBMC viability (data not shown). This decrease in excision products when 10 μg of SB100X DNA plasmid was used per electroporation could be due to DNA toxicity, although this was not observed with SB11, but is more likely due to over-production inhibition. SB11 also showed maximal activity at 5 μg per electroporation (Figure 2a), but the amount of excision circles produced was significantly less than that achieved with SB100X.

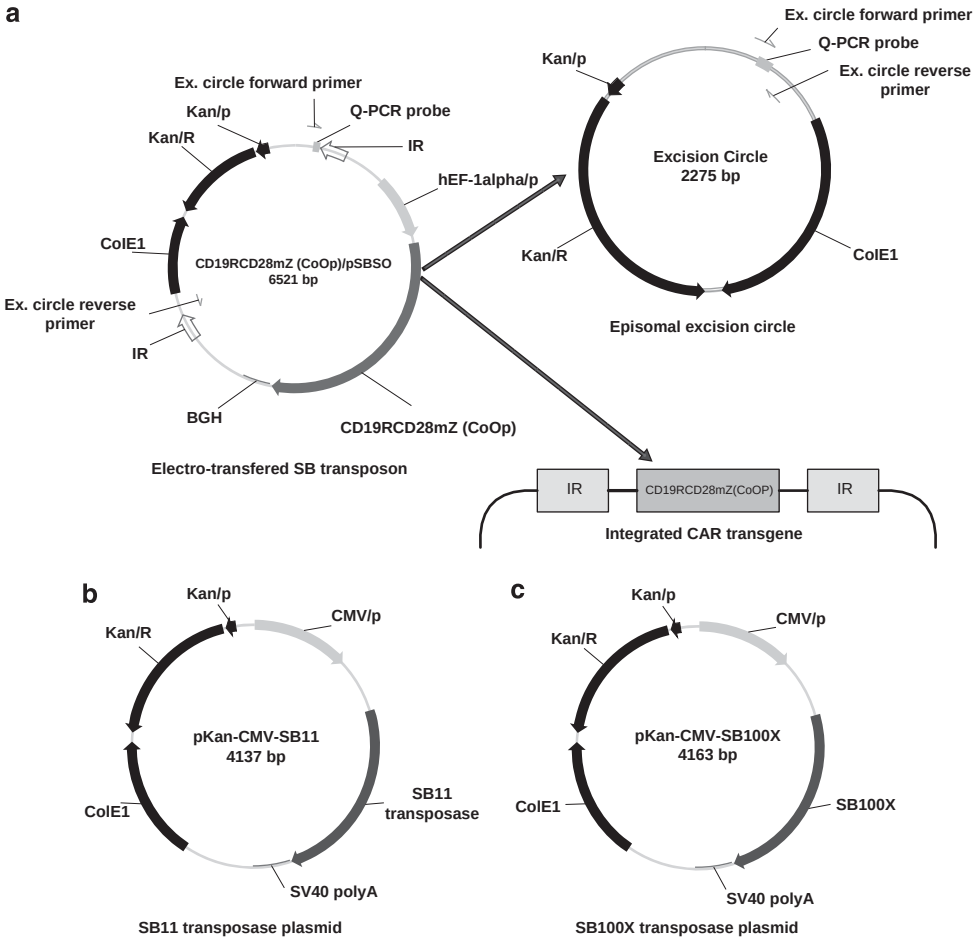

Figure 1 Schematic showing the formation of excision circles and integration of transgene using DNA plasmids from SB system. (**a**) The transgene (transposon) to be integrated is flanked by two IR and mobilized from the CD19RCD28mZ(CoOp)/pSBSO plasmid by SB transposase. Upon SB transposition, the CAR transposon (CD19RCD28) is inserted into the T-cell genome, whereas the non-integrated DNA forms an episomal excision circle. The PCR to detect a released excision circle reveals a 77 base pair band, whereas the same primers bound to sites in the CD19RCD28mZ(CoOp)/pSBSO plasmid are 4298 base pairs apart. (**b**) Schematic of DNA plasmids expressing SB11 transposase and (**c**) SB100X transposase. BGH, bovine growth hormone polyadenylation signal sequence; CDS, coding sequence of gene; CMV/p, cytomegalovirus promoter; ColE1, colicin E1 (origin of replication); hEF-1α/p, human elongation factor-1α hybrid promoter; IR, inverted repeats; Kan/R, kanamycin resistance gene; Kan/P, kanamycin resistance gene promoter; SV40 poly A, Simian virus 40 polyadenylation signal sequence.

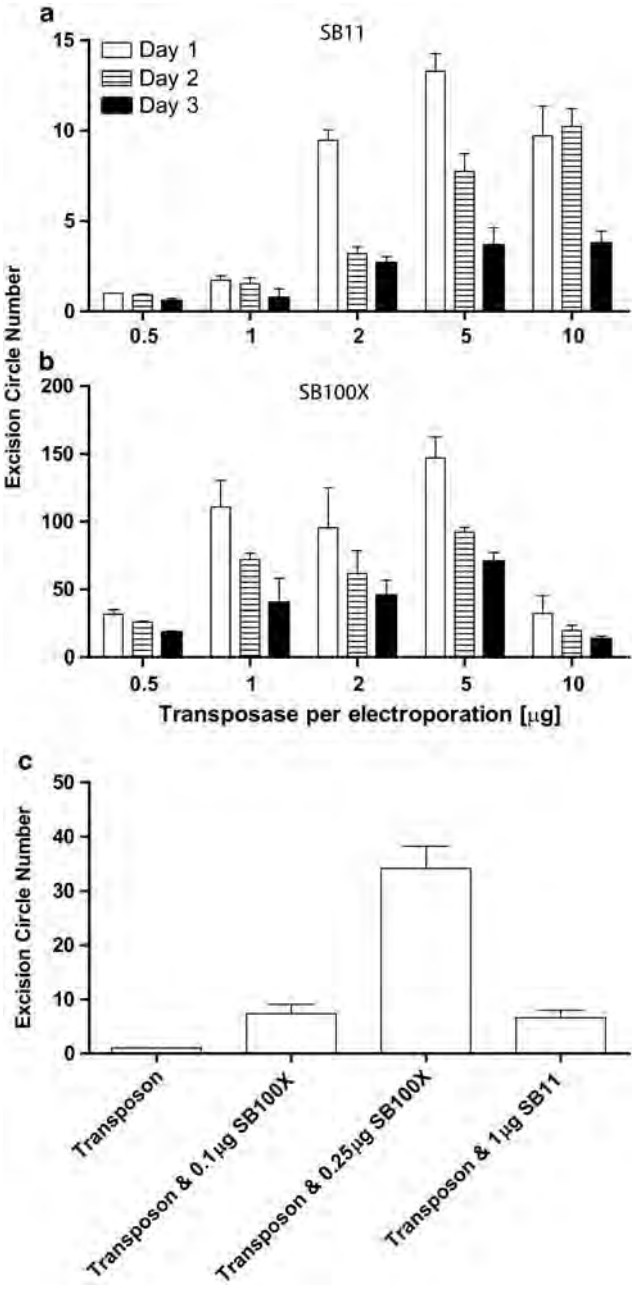

Figure 2 Evaluation of transposase activity by detecting excision-circle formation after SB transposition event. Excision circle to CD19RCD28 ratio is based on the amount of (**a**) SB11 and (**b**) SB100X transposase as detected by Q-PCR at days 1 to 3 after electroporation. The DNA transposon plasmid (CD19RCD28mZ(CoOp)/pSBSO) to express CD19RCD28 CAR was used at 15 μg per electroporation. (**c**) Excision circle to CD19RCD28 ratio after electro-transfer of mRNA coding for SB100X and SB11, combined with SB DNA transposon plasmid, on day 1 after electro-transfer.

Overall, SB100X was apparently 10 to 100 times more active compared with SB11. As expected, the episomal excision circles are lost to detection as the T cells propagate on the aAPC. To avoid the possibility that the SB transposases could integrate, we assessed whether improved transposition could also be achieved by mRNA coding for SB100X. The two transposases were electro-transferred as mRNA species along with a fixed amount of SB DNA transposon into T cells pre-activated by crosslinking CD3 with the monoclonal antibody OKT3. We observed that the introduction of SB100X mRNA at 0.1 μg per electroporation was as active as 10× the amount of SB11. When SB100X mRNA was used at 0.25 μg per electroporation, there was a higher transposition activity compared with SB11 at 1 μg per electroporation (Figure 2c). These data indicate the superior activity of SB100X in primary T cells whether this transposase is expressed from electro-transferred DNA or mRNA.

Generation of CAR+ T cells by SB transposition

Primary human T cells from PBMCs were electro-transferred on day 0 of cell culture with SB transposon (CD19RCD28mZ(codon optimized (CoOp))/pSBSO) and one of the two DNA plasmids, pKAN-CMV-SB11 and pKAN-CMV-SB100X, coding for SB11 or SB100X, respectively. The T cells were subsequently propagated for up to 28 days on γ-irradiated CD19+ aAPC, added every 7 days in the presence of soluble recombinant interleukin-2 (IL-2) cytokine (Figure 3a). Our approach to generating clinical-grade CAR+ T cells uses 5 μg of pKAN-CMV-SB11 along with 15 μg of CD19RCD28mZ(CoOp)/pSBSO in the electroporation of 2×10^7 PBMC per cuvette; therefore, this was used as a starting point to assess the ability of SB100X to improve the rate of transposition and subsequent outgrowth of CAR+ T cells. However, when we electroporated T cells with the DNA plasmid coding for SB100X at 5 μg per electroporation with 15 μg per electroporation of the DNA plasmid coding for CAR transposon, this accentuated cell death the day after electro-transfer, as shown by Trypan blue staining and failure to propagate CAR+ T cells. However, the electro-transfer of DNA plasmid coding for SB100X at decreased amounts did not compromise cell viability as the genetically modified T cells could be readily propagated on aAPC. Indeed, upon reducing the concentration of the DNA plasmid coding for this transposase to 0.1 and 0.5 μg per electroporation, SB100X successfully integrated the transposon to support the outgrowth of CAR+ T cells. When using 10-fold less (0.5 μg per electroporation) than the input concentration of SB11 (5 μg per electroporation), we calculate that SB100X was about 3.6 times more efficient than SB11 in generating CAR+ cells as assessed at day 28 of co-culture with CD19+ aAPC (based on dividing the number of CAR+ T cells associated with SB100X with the number of CAR+ T cells associated SB11, in two independent experiments). Indeed, even 0.1 μg per electroporation of the DNA plasmid coding for SB100X was almost as efficient as 5 μg per electroporation of SB11 when the number of CAR+ T cells were counted at 28 days of tissue culture (Figures 3b and c). Expression of the CAR on electroporated and propagated T cells was documented by flow cytometry (Figure 3d). Thus, transposition mediated by SB100X results in improved outgrowth of CAR+ T cells.

CAR+ T cells can be generated using SB100X mRNA

As SB transposase coded by mRNA species was capable of accomplishing SB transposition, we determined if CAR+ T cells could be selectively propagated on aAPC after electro-transfer of DNA plasmid coding for CD19RCD28 and mRNA coding for SB100X or SB11. We adapted our propagation method to generate CAR+ T cells (Figure 4a), so that T cells were pre-activated with OKT3 to improve uptake of and expression from mRNA. As shown in Figure 4b, 0.25 μg per electroporation of SB100X and 1 μg per electroporation of SB11 successfully produced CAR+ T cells that could be propagated on CD19+ aAPC. The superiority of the SB100X transposase to support the outgrowth of CAR+ T cells was apparently not due to differences in integrity of the mRNA (Figure 4c).

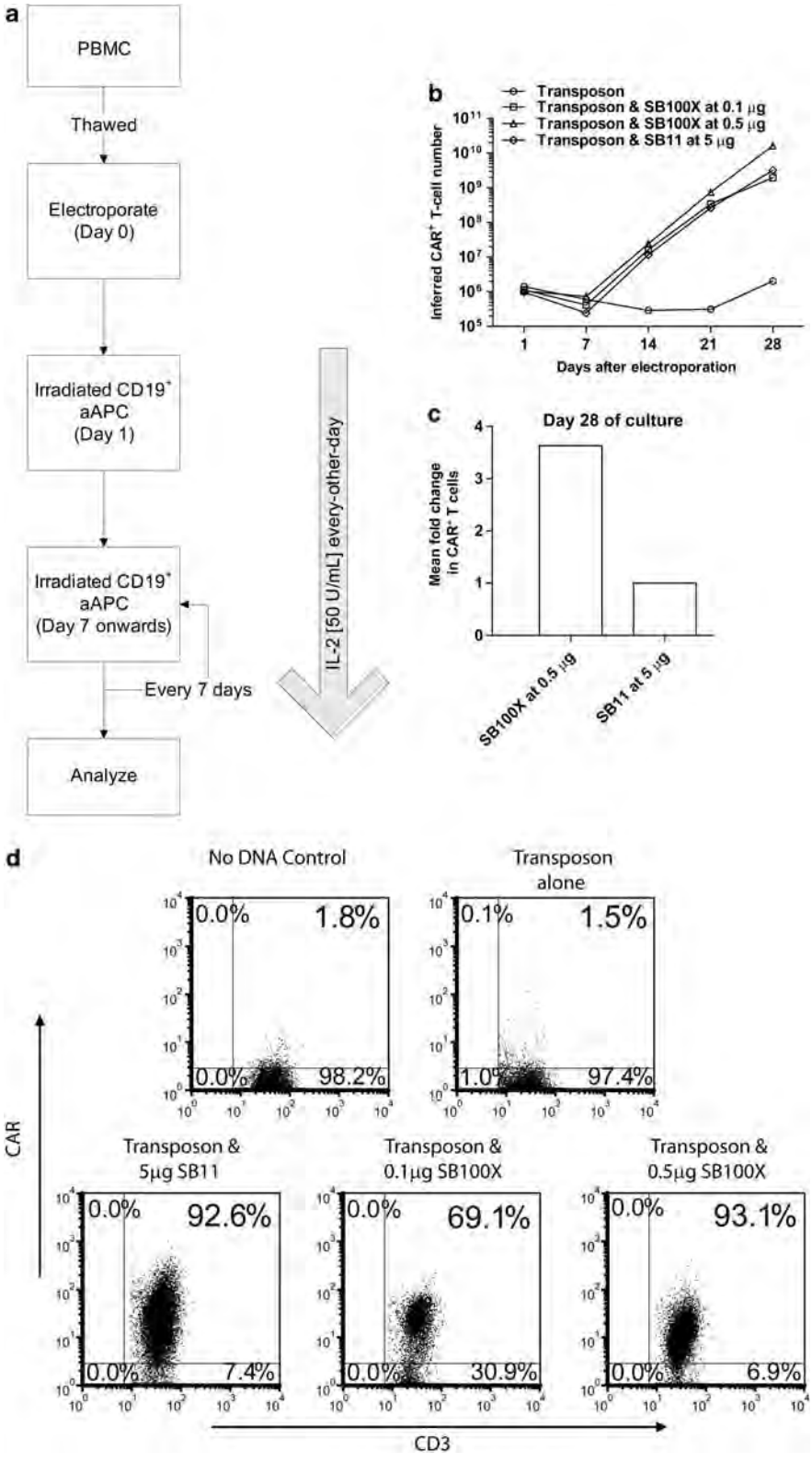

Figure 3 Selective outgrowth of CD19-specifc CAR+ T cells after transposition with SB100X versus SB11 transposases. (**a**) Schematic outlining co-culture process to generate CD19-specifc CAR+ T cells. A total of 10^5 CAR+ T cells from PBMC were stimulated with γ-irradiated CD19+ aAPC (clone no. 4) every 7 days at a 1:2 (CAR+ aAPC) ratio in the presence of soluble IL-2. (**b**) Kinetics of CAR+ T-cell numeric expansion by repetitive co-culture with CD19+ aAPC. T cells were electroporated on day 0 with SB DNA plasmid transposon expressing CD19RCD28 and graded doses of DNA plasmids expressing SB100X or SB11. (**c**) Fold change in the number of CAR+ T cells sampled at day 28 of co-culture on aAPC from two independent experiments. (**d**) Expression of CAR (CD19RCD28) on CD3+ T cells by flow cytometry at day 28 of culture.

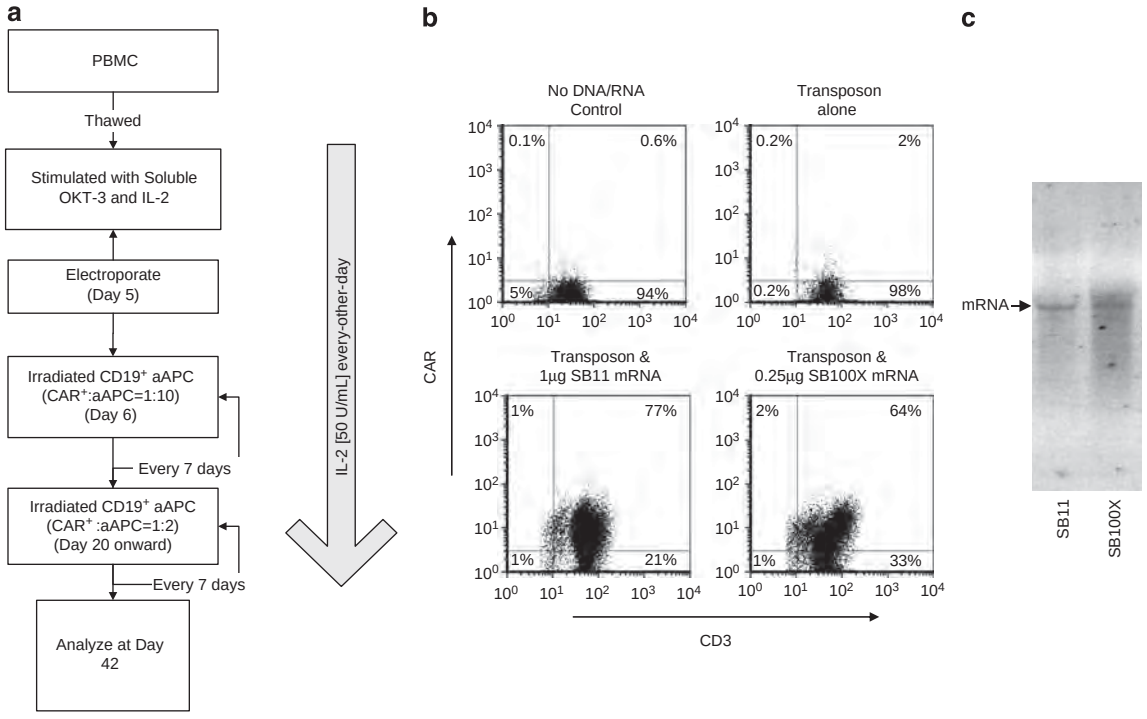

Figure 4 CAR+ T cells generated by electro-transfer of mRNA coding for SB transposases and DNA plasmid coding for CD19RCD28 CAR transposon. (**a**) Schematic used to generate CAR+ T cells. (**b**) Expression of CAR on numerically expanded CD3+ T cells at day 42 of co-culture with aAPC. The SB100X mRNA was used at 0.25 μg per electroporation, whereas the SB11 mRNA concentration was at 1 μg per electroporation. The DNA plasmid expressing CD19RCD28 was used at 10 μg per electroporation. (**c**) Integrity of mRNA species after *in vitro* transcription used to express SB11 and SB100X.

Transposition using SB100X and SB11 result in comparable number of integration events per T cell

Given that SB100X gives rise to a greater number of transposition events compared with SB11, we investigated whether this enzyme resulted in multiple integration events. To evaluate the number of integration events per electroporated and propagated T cell, we measured the copy number of CD19RCD28 transpose relative to the copy number of RNase P gene by real-time Q-PCR. The calculated transgene copy per T cell is 0.95 ± 0.068 gene (mean ± s.e.m.) for 0.5 μg per electroporation SB100X and 0.80 ± 0.033 (mean ± s.e.m.) for 5 μg per electroporation SB11, respectively (Figure 5a). This difference is not statistically significant (P=0.185) when measured at a time point when sufficient (clinical grade) CAR+ T cells are available that can be harvested from cultures for adoptive immunotherapy. These data revealed that the number of integrated copies of CAR is approximately 1 per T-cell genome upon transposition with both SB100X and SB11.

SB100X DNA cannot be detected in electroporated and propagated T cells

To establish that SB100X or SB11 DNA is not present in propagated T cells, we developed a Q-PCR assay to reveal integrated transposase plasmid. Our data show that after 28 days of *in vitro* culture, the SB100X transposase, as well as that of SB11, are absent in the cultured cells (Figure 5b). The standard curves associated with this assay are in the Supplementary Data.

CAR+ T cells generated by SB transposition with SB100X exhibit redirected killing for CD19+ tumor cells

We have previously shown that CAR+ T cells genetically modified with SB11 transposase specifically lyse B-cell tumor cells.[8] The electroporated and propagated T cells generated using SB100X transposase (using 0.1 μg per electroporation) were evaluated for their ability to be activated for effector functioning in a CAR-dependent manner. We showed by chromium release assay that CAR+ T cells exhibited redirected specific lysis of a genetically modified EL4 target expressing 92% human CD19 (Figure 6a). T cells not genetically modified, but propagated by crosslinking CD3 using γ-irradiated aAPC loaded with OKT3 did not appreciably lyse CD19− EL4 cells (Figure 6b).

DISCUSSION

We and others have used transposon and transposase systems to improve integration efficiency of DNA plasmids expressing immunoreceptors.[8,9,17,21,22] Building upon these data, we have adapted the SB system for human application[11] to use the SB11 transposase to integrate CAR into TA dinucleotide repeats across the genome of populations of human T cells.

The development of SB100X raised the possibility that we could use this new SB transposase to improve the integration frequency of CAR transposon in T cells. We were able to show that SB100X had up to 100 times higher rates of transposition compared with SB11 based on the release of excision circles. This is attributed to improved enzymatic activity, but the improved transposition efficiency may also be due to different translational efficiencies as well as post-translational modifications. The efficiency of transposition was dependent on the amount of electro-transferred transposase, but an elevated input concentration of SB100X led to cell death. The reasons for this toxicity are not known, however, it is apparent that overexpression of transposase can lead to inhibition of SB transposition.[6,16] This highlights the need to titrate the input DNA plasmid concentrations between the transposon and the transposase. By reducing the amount of SB100X relative to SB11, we were able to show its superior activity.

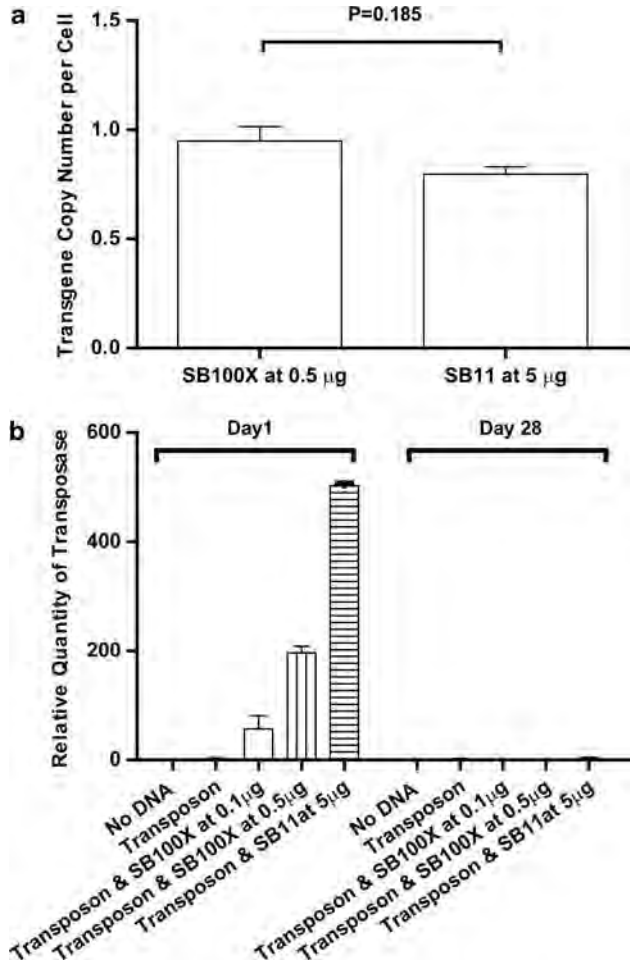

Figure 5 Measurement of the number of copies of integrated CAR transgene and detection of SB transposases. (**a**) Copy number of CAR transgene, normalized to RNase P, at day 28 of co-culture on CD19+ aAPC after SB transposition with SB100X or SB11. Q-PCR using CAR-specific primers revealed CD19RCD28 copy numbers at 0.95 and 0.80 transgene per T-cell genome after electro-transfer of 0.5 μg DNA plasmid coding for SB100X, and 5 μg DNA plasmid coding for SB11, respectively. There was no statistical difference between the copy number of integrated CAR transgenes. (**b**) Measurement by Q-PCR using transposase-specific primers at day 1 (day after electroporation) and at day 28 of co-culture of genetically modified T cells on CD19+ aAPC. Transposon was added at 15 μg per electroporation along with graded doses of DNA plasmids coding for SB100X and SB11 transposases.

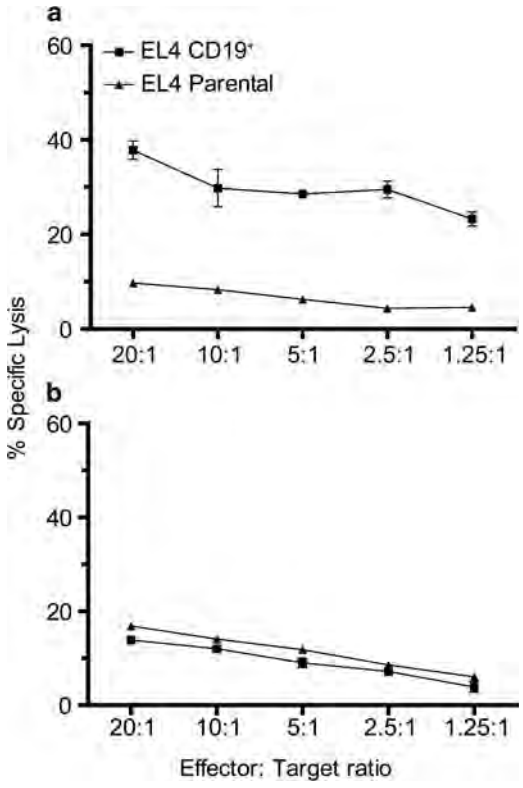

Figure 6 Killing of tumor cells by genetically modified T cells. Lysis by chromium release assay of CD19+ EL4 tumor cells compared with CD19− parental EL4 cells by (**a**) T cells genetically modified with SB100X and propagated on aAPC for 28 days. (**b**) CAR^{neg} T cells that were not genetically modified were numerically expanded on OKT3-loaded aAPC and these cells failed to lyse the EL4 targets.

The ability of SB100X to augment the selective propagation of CAR+ T cells on CD19+ aAPC raised the possibility that this transposase led to the insertion of multiple copies of the transposon per cell. Indeed, multiple integrations have been observed after SB100X-mediated transposition in other cells.[6,13] However, this was disproved when we found that on average, there was approximately one copy of the CAR transgene per T cell, which was similar to the integration efficiency associated with SB11. Our lower number of integrants per genome compared with the published reports of SB100X activity may be due to an intrinsic property of the T-cell genome, genotoxicity leading to loss of viability of T cells carrying multiple copies of the transposon, a reduced amount of SB100X DNA plasmid electro-transferred, and/or a reflection of the selective pressure provided by the aAPC to selectively propagate CAR+ T cells bearing just one copy of the transposon.

That SB100X has intrinsically improved transposase activity is revealed by the release and detection of more excision circles when SB100X was used compared with SB11. Presumably, the release of the excision circles from a population of electroporated T cells is correlated with the stable integration of the CAR transgene, which is measured per T cell. Thus, it appears that the superior enzymatic activity of SB100X results in an improved efficiency of transposon integration and a beneficial founder effect leading to the subsequent improved outgrowth of CAR+ T cells upon *in vitro* propagation on aAPC. This finding pertains to the safety of SB100X for, as with SB11, it does not lead to multiple insertions of the CAR transgene when T cells are electroporated and co-cultured on aAPC.

The increased enzymatic activity of SB100X was also evident when we reduced the amount of transposase DNA plasmid needed to accomplish the integration of CAR into T cells. Indeed, we could achieve superior numeric expansion of CAR+ T cells on CD19+ aAPC using 0.5 μg per electroporation of SB100X compared with 10 times as much DNA plasmid coding for SB11. This also has implications for improved safety of SB system in human trials as a decrease in the amount of SB transposase delivered by DNA plasmid presumably decreases the chance of inadvertent integration of the transposase into the genome and the potential for re-mobilization of the inserted transposon. When we evaluated for the presence of integrated plasmid expressing SB100X, we did not detect a signal by Q-PCR, which curtails the possibility of a re-hopping event after SB-mediated transposition. However, it is possible that DNA for SB transposase was present in the genome at a level below the limit of detection by

this assay. To exclude the possibility that SB100X can integrate into the T-cell genome, we showed that electro-transfer of mRNA species coding for this integrase could mediate transposition, and further that the efficiency of integration was again higher than SB11. Previously, it has been shown that SB11 transposase coding by mRNA can mediate transposition.[23] Furthermore, viral vectors have been used to deliver SB transposase to improve the pattern of integration of an integrase-deficient lentivirus to achieve a more random pattern of integration than can be achieved with lentiviral integrase.[24,25]

We are currently undertaking the first clinical applications of the SB system, which has successfully received Investigational New Drug Applications from the Food and Drug Administration, to electro-transfer the SB11 transposase to express CD19RCD28 transposon in autologous and allogeneic T cells for infusion in patients with B-lineage lymphoma. With the development of SB100X, our data show that this transposase may be a desirable alternative transposase to the use of SB11 for use in future clinical trials to adoptively transfer CAR^+ T cells.

MATERIALS AND METHODS

Plasmids

The SB transposon contains the CoOp second-generation CD19RCD28 CAR, specific for human CD19, flanked by the SB inverted repeats. This CAR has been described previously.[15] In brief, the ampicillin resistance gene (*AmpR*) and origin of replication from the plasmid CoOpCD19RCD28/pT-MNDU3 was replaced with a DNA fragment encoding the kanamycin resistance gene (*KanR*) and origin of replication (ColE1) from the pEK Vector.[8] The human elongation factor-1α promoter from pVitro4 vector (InvivoGen, San Diego, CA, USA) was swapped with MNDU3 promoter to generate the DAN plasmid CD19RCD28mZ(CoOp)/pSBSO (Figure 1a). The pKan-CMV-SB11 DNA plasmid (Figure 1b), coding for the SB11 transposase, was constructed by digesting pCMV-SB11 (kindly provided by Dr Perry Hackett, University of Minnesota, Minneapolis, MN, USA)[16] with *Pvu*II, harvesting the fragment coding for SB11 transposase and ligating to the *Ase*I and *Pac*I fragment, which contained the *KanR* and *ColE1* origin of replication from pEK vector. pKan-CMV-SB100X (Figure 1c), coding for SB100X transposase, was built by digesting both the pKan-CMV-SB11 plasmid and pCMV(CAT)T7-SB100X plasmid[13] with *Ava*I and *Psi*I, and then annealing the fragment coding for SB100X with the backbone of pKan-CMV-SB11 plasmid. All DNA plasmids were purified using Qiagen (Valencia, CA, USA) endotoxin-free reagents. The integrity of the DNA plasmids coding SB100X and SB11 transposase was assessed by Experion automatic electrophoresis station (Bio-Rad, Hercules, CA, USA).

Cells

After obtaining consent, PBMC from healthy donors were isolated by density gradient centrifugation over Ficoll-Paque-Plus (Pharmacia Biotech, Piscataway, NJ, USA) and stored in liquid nitrogen. K562 were transduced with lentivirus to express CD64, CD86, CD137L and membrane-bound IL-15 and were cloned (clone no. 4, kindly provided by Dr Carl June, University of Pennsylvania, Philadelphia, PA, USA). The construction of $CD19^+$ K562 aAPC was reported previously.[17] The parental murine immortalized EL4 T-cell line (catalog no. TIB-39; ATCC, Manassas, VA, USA) and human $CD19^+$ EL4 transfectants were cultured in RPMI 1640 medium (Hyclone, Logan, UT, USA), supplemented with 2 mM Glutamax-1 (Gibco-Invitrogen, Carlsbad, CA, USA) and 10% heat-inactivated fetal calf serum (FCS).

Generation of CAR^+ T cells by transposition with SB DNA plasmids coding for CAR and transposases

On day 0, PBMCs were thawed at 37 °C, washed once with phenol-free RPMI 1640 and rested for 2 h at 37 °C. A total of 2×10^7 PBMC/cuvette were resuspended in Human T Cell Nucleofector buffer (Lonza Inc., Basel, Switzerland) along with 15 μg CD19RCD28mZ(CoOp)/pSBSO plasmid coding for CD19RCD28 CAR and graded doses of DNA plasmids coding for SB100X or SB11. After electroporation with Nucleofector II (Lonza Inc.) using program U14, the cells were washed once with phenol-free RPMI 1640 and resuspended in 1 ml of phenol-free RPMI 1640 (without FCS) and cultured in a 12-well plate at 37 °C for 4 h. Then, 1 ml of phenol-free RPMI 1640 with 20% of FCS was added. The next day, 3×10^5 cells were harvested for DNA extraction and immunophenotyping. The remaining cells were stimulated by 1:2 (CAR^+ T cells:aAPC) weekly additions of γ-irradiated (100 Gy) $CD19^+$ aAPC (clone no. 4) for 28 days of continuous co-culture in RPMI 1640 supplemented with 2 mM Glutamax-1 and 10% heat-inactivated FCS. Recombinant human interleukin 2 (50 IU ml^{-1}; Novartis Pharmaceuticals Corporation, East Hanover, NJ, USA) was added every other day beginning at day 1.

In vitro transcription to generate mRNA coding for SB100X and SB11

Twenty micrograms of the SB transposase plasmids were digested with *Spe*I and purified with Qiaquick gel extraction kit (Qiagen) and the DNA concentration was measured. Ten micrograms of the linearized plasmid DNA was used to synthesize mRNA with T7 RiboMAX Express Large Scale RNA Production System (Promega, Madison, WI, USA). A PolyA tail was added to the newly synthesized mRNA molecule with Poly(A) Tailing Kit (Ambion, Austin, TX, USA). After quantification, the mRNA was analyzed by gel electrophoresis, aliquoted and stored in Nalgene cryogenic vials (Thermo Fisher Scientific, Waltham, MA, USA) at −80 °C for future use.

Generation of CAR^+ T cells by transposition with SB DNA plasmid coding CAR and mRNA coding for transposases

PBMC were resuspended in RPMI 1640 with 5% heat-inactivated AB human serum (Invitrogen) along with 50 ng ml^{-1} of OKT3 monoclonal antibody (eBioscience, San Diego, CA, USA) and 50 U ml^{-1} of IL-2, which was re-added to the culture every other day. After 5 days, 10^7 cells per cuvette were electroporated using 10 μg DNA plasmid (CD19RCD28mZ(CoOp)/pSBSO) coding for CD19RCD28 and graded amounts of SB transposase mRNA. The propagation of the T cells was achieved using 1:10 (CAR^+ T cells to aAPC) ratio of γ-irradiated $CD19^+$ aAPC for first 2 weeks and 1:2 ratio thereafter. aAPC clone no. 4 were added every 7 days and IL-2 every other day beginning at day 1.

Flow cytometry

Cells were first incubated with 1:200 diluted APC-labeled goat anti-human immunoglobulin G Fc (category (cat.) no. 12-0569-42; Jackson ImmunoResearch Laboratories Inc., West Grove, PA, USA), then washed once, and finally incubated with 1:50 anti-CD3-FITC (cat. no. 349201; BD Biosciences, Los Angeles, CA, USA) and 1:50 anti-CD56-PE (cat. no. 12-0569; eBiosciences). After staining, all cells were resuspended in 100 μl fluorescence-activated cell Sorting buffer (2% FCS and 0.1% sodium azide in phosphate-buffered saline) and live/dead cells were differentiated upon the addition of propidium iodide (catalog no. P4864; Sigma-Aldrich, St Louis, MO, USA), and then analyzed with flow cytometry (FACSCalibur; BD Biosciences).

Real-time Q-PCR

All of the primers, probes and TaqMan Gene Expression Master Mix were purchased from Applied Biosystem (Foster City, CA, USA). The Q-PCR reactions were performed in a Steponeplus Real-time PCR system (Applied Biosystem) with TaqMan real-time Q-PCR technique as recommended. To measure excision circles, the forward primer (5′-TCCCAGTCACGACGTTG TAAAA-3′) and probe (5′-CCAGTGAATTCGAGCTC-3′) bound 5′ of the CAR cassette and the reverse primer (5′-CGTTGGCCGATTCATTATCG-3′) bound 3′ of the CAR cassette in the SB transposon DNA plasmid CD19RCD28mZ (CoOp)/pSBSO as illustrated in Figure 1a. A positive PCR reaction reveals a 77 base pair band that is generated only after the CAR transposon was excised. To measure CD19RCD28 CAR, the primer sequences are as follows: forward primer, 5′-CAGCGACGGCAGCTTCTT-3′; reverse primer, 5′-TGCATCACG-GAGCTAAA-3′; and probe, 5′-AGAGCCGGTGGCAGG-3′. To measure SB transposases, a common primer and probe set were designed to target the plasmid backbone shared by pKan-CMV-SB100X and pKan-CMV-SB11. These sequences are as follows: forward primer, 5′-AAGGCCAGGAACCGTAAAAAG-3′; reverse primer, 5′-GGCGGAGCCTATGGAAAAA-3′; and probe, 5′-CCGCGT TGCTGGC-3′. RNase P primer and probe set of TaqMan RNase P Control Reagents Kit (cat. no. 4316844; Applied Biosystem) were used as Q-PCR internal control.

Analysis of Q-PCR results

An RNase P C_T versus cell number standard curve (Curve A, Supplementary Figure 1s 1a) was achieved by a serial dilution (200, 20 and 2 ng) of genomic DNA from a genetically modified Jurkat T-cell clone bearing one copy of CAR transgene based on Southern blotting (Maiti *et al.*, in preparation). As one cell has about 7 pg of DNA, 200 ng total DNA is equivalent to approximately 28 570 cells. C_T represents the threshold circle where the Q-PCR was deemed positive. With Curve A, we calculated the cell number from corresponding RNase P C_T value. In parallel, a CD19RCD28 transgene C_T versus transgene number curve (Curve B, Supplementary Figure 1s 1b) was generated to compute the number of integrated transgenes. Twenty nanograms of sample genomic DNA from genetically modified and propagated primary T cells could then be analyzed by Q-PCR. The RNase P C_T was used to calculate cell numbers with Curve A and the integrated transgene copy number was deduced from transgene C_T with Curve B. The copy numbers per cell were calculated with the following formula:

$$\text{Copy number per cell} = \frac{\text{Tg}\,N}{\text{Cell}\,N}$$

TgN is the number of integrated transgenes and Cell$N$ represents the cell number deduced from RNase P C_T. Quantification of excision circle was achieved with comparative C_T method provided by the Steponeplus real-time PCR system (Applied Biosystem).

Chromium release assay

The redirected specificity of the genetically modified T cells was determined by chromium release assay using ^{51}Cr-labeled EL4 cells as targets. The T cells (effectors) were harvested 28 days following stimulation with aAPC, washed and plated in V-bottom microtiter plates (Costar, Cambridge, MA, USA) in triplicate at 10^5, 5×10^4, 2.5×10^4, 1.25×10^4 cells per well and with 5×10^3 target cells. After incubation at 37 °C for 4 h followed by centrifugation, 50 µl aliquots of cell-free supernatant were harvested and counted with Topcount NXT (PerkinElmer, Waltham, MA, USA). The percent of specific cytolysis was calculated from the release of ^{51}Cr as follows:

$$\frac{(\text{Experimental}\,^{51}\text{Cr}) - (\text{Control}\,^{51}\text{Cr})}{(\text{Maximal}\,^{51}\text{Cr}) - (\text{Control}\,^{51}\text{Cr})} \times 100$$

Control wells contained target cells incubated in media. The maximal ^{51}Cr was determined by measuring the ^{51}Cr content released by target cells lysed with 1% Triton X-100.

Statistical analysis

The Student's *t*-test was employed to determine statistical significance and $P<0.05$ was considered significant. Where applicable, the data are reported as an average and s.d. Electroporations were performed on two different donors while Q-PCR reactions were carried out in triplicate.

CONFLICT OF INTEREST

The authors declare no conflict of interest.

ABBREVIATIONS

SB, *Sleeping Beauty*; CAR, chimeric antigen receptor; aAPC, artificial antigen presenting cell; PBMC, peripheral blood mononuclear cells.

ACKNOWLEDGEMENTS

We thank Dr Perry Hackett University of Minnesota for *Sleeping Beauty* system and Dr Carl June from University of Pennsylvania for assistance generating the K562-aAPC. We are grateful to the Flow Cytometry Core Laboratory at MDACC. Cancer Prevention Research Institute of Texas, Department of Defense, PO1 (CA100265), CCSG (CA16672), RO1s (CA124782, CA120956), R33 (CA116127), Alex's Lemonade Stand Foundation, Alliance for Cancer Gene Therapy, Burroughs Wellcome Fund, Gillson Longenbaugh Foundation, Harry T Mangurian, Jr, Foundation, Institute of Personalized Cancer Therapy, Leukemia and Lymphoma Society, Lymphoma Research Foundation, Miller Foundation, National Foundation for Cancer Research, Pediatric Cancer Research Foundation, National Marrow Donor Program, William Lawrence and Blanche Hughes Foundation.

1 Jena B, Dotti G, Cooper LJ. Redirecting T-cell specificity by introducing a tumor-specific chimeric antigen receptor. *Blood* 2010; **116**: 1035–1044.
2 Tan PH, Tan PL, George AJ, Chan CL. Gene therapy for transplantation with viral vectors—how much of the promise has been realized? *Expert Opin Biol Ther* 2006; **6**: 759–772.
3 Ciuffi A. Mechanisms governing lentivirus integration site selection. *Curr Gene Ther* 2008; **8**: 419–429.
4 Hacein-Bey-Abina S, Von Kalle C, Schmidt M, McCormack MP, Wulffraat N, Leboulch P *et al.* LMO2-associated clonal T cell proliferation in two patients after gene therapy for SCID-X1. *Science* 2003; **302**: 415–419.
5 Liang Q, Kong J, Stalker J, Bradley A. Chromosomal mobilization and reintegration of *Sleeping Beauty* and *PiggyBac* transposons. *Genesis* 2009; **47**: 404–408.
6 Grabundzija I, Irgang M, Mátés L, Belay E, Matrai J, Gogol-Döring A *et al.* Comparative analysis of transposable element vector systems in human cells. *Mol Ther* 2010; **18**: 1200–1209.
7 Huang X, Wilber AC, Bao L, Tuong D, Tolar J, Orchard PJ *et al.* Stable gene transfer and expression in human primary T cells by the *Sleeping Beauty* transposon system. *Blood* 2006; **107**: 483–491.
8 Singh H, Manuri PR, Olivares S, Dara N, Dawson MJ, Huls H *et al.* Redirecting specificity of T-cell populations for CD19 using the *Sleeping Beauty* system. *Cancer Res* 2008; **68**: 2961–2971.
9 Peng PD, Cohen CJ, Yang S, Hsu C, Jones S, Zhao Y *et al.* Efficient nonviral *Sleeping Beauty* transposon-based TCR gene transfer to peripheral blood lymphocytes confers antigen-specific antitumor reactivity. *Gene Therapy* 2009; **16**: 1042–1049.
10 Geurts AM, Yang Y, Clark KJ, Liu G, Cui Z, Dupuy AJ *et al.* Gene transfer into genomes of human cells by the *Sleeping Beauty* transposon system. *Mol Ther* 2003; **8**: 108–117.
11 Williams DA. *Sleeping Beauty* vector system moves toward human trials in the United States. *Mol Ther* 2008; **16**: 1515–1516.
12 Hackett PB, Largaespada DA, Cooper LJ. A transposon and transposase system for human application. *Mol Ther* 2010; **18**: 674–683.
13 Mátés L, Chuah MK, Belay E, Jerchow B, Manoj N, Acosta-Sanchez A *et al.* Molecular evolution of a novel hyperactive *Sleeping Beauty* transposase enables robust stable gene transfer in vertebrates. *Nat Genet* 2009; **41**: 753–761.
14 Xue X, Huang X, Nodland SE, Mátés L, Ma L, Izsvák Z *et al.* Stable gene transfer and expression in cord blood-derived CD34+ hematopoietic stem and progenitor cells by a hyperactive *Sleeping Beauty* transposon system. *Blood* 2009; **114**: 1319–1330.
15 Kowolik CM, Topp MS, Gonzalez S, Pfeiffer T, Olivares S, Gonzalez N *et al.* CD28 costimulation provided through a CD19-specific chimeric antigen receptor enhances *in vivo* persistence and antitumor efficacy of adoptively transferred T cells. *Cancer Res* 2006; **66**: 10995–11004.
16 Geurts AM, Yang Y, Clark KJ, Liu G, Cui Z, Dupuy AJ *et al.* Gene transfer into genomes of human cells by the *Sleeping Beauty* transposon system. *Mol Ther* 2003; **8**: 108–117.
17 Manuri PV, Wilson MH, Maiti SN, Mi T, Singh H, Olivares S *et al. piggyBac* transposon/transposase system to generate CD19-specific T cells for treatment of B-lineage malignancies. *Hum Gene Ther* 2010; **21**: 427–437.
18 Izsvák Z, Chuah MK, Vandendriessche T, Ivics Z. Efficient stable gene transfer into human cells by the *Sleeping Beauty* transposon vectors. *Methods* 2009; **49**: 287–297.
19 Liu G, Aronovich EL, Cui Z, Whitley CB, Hackett PB. Excision of *Sleeping Beauty* transposons: parameters and applications to gene therapy. *J Gene Med* 2004; **6**: 574–583.
20 Szilagyi A, Blasko B, Szilassy D, Fust G, Sasvari-Szekely M, Ronai Z. Real-time PCR quantification of human complement C4A and C4B genes. *BMC Genet* 2006; **7**: 1.
21 Nakazawa Y, Huye LE, Dotti G, Foster AE, Vera JF, Manuri PR *et al.* Optimization of the *PiggyBac* transposon system for the sustained genetic modification of human T lymphocytes. *J Immunother* 2009; **32**: 826–836.
22 Huang X, Guo H, Kang J, Choi S, Zhou TC, Tammana S *et al. Sleeping Beauty* transposon-mediated engineering of human primary T cells for therapy of CD19+ lymphoid malignancies. *Mol Ther* 2008; **16**: 580–589.
23 Wilber A, Frandsen JL, Geurts JL, Largaespada DA, Hackett PB, McIvor RS. RNA as a source of transposase for *Sleeping Beauty*-mediated gene insertion and expression in somatic cells and tissues. *Mol Ther* 2006; **13**: 625–630.
24 Staunstrup NH, Moldt B, Mátés L, Villesen P, Jakobsen M, Ivics Z *et al.* Hybrid lentivirus-transposon vectors with a random integration profile in human cells. *Mol Ther* 2009; **17**: 1205–1214.
25 Vink CA, Gaspar HB, Gabriel R, Schmidt M, McIvor RS, Thrasher AJ *et al.* Sleeping beauty transposition from nonintegrating lentivirus. *Mol Ther* 2009; **17**: 1197–1204.

Supplementary Information accompanies the paper on Gene Therapy website (http://www.nature.com/gt)

Published OnlineFirst May 15, 2011; DOI:10.1158/0008-5472.CAN-10-3843

Cancer Research

Reprogramming CD19-Specific T Cells with IL-21 Signaling Can Improve Adoptive Immunotherapy of B-Lineage Malignancies

Harjeet Singh, Matthew J. Figliola, Margaret J. Dawson, et al.

Cancer Res 2011;71:3516-3527. Published OnlineFirst May 15, 2011.

Published OnlineFirst May 15, 2011; DOI:10.1158/0008-5472.CAN-10-3843

Cancer Research

Reprogramming CD19-Specific T Cells with IL-21 Signaling Can Improve Adoptive Immunotherapy of B-Lineage Malignancies

Harjeet Singh[1], Matthew J. Figliola[1], Margaret J. Dawson[1], Helen Huls[1], Simon Olivares[1], Kirsten Switzer[1], Tiejuan Mi[1], Sourindra Maiti[1], Partow Kebriaei[2], Dean A. Lee[1,3], Richard E. Champlin[2], and Laurence J.N. Cooper[1,3]

Abstract

Improving the therapeutic efficacy of T cells expressing a chimeric antigen receptor (CAR) represents an important goal in efforts to control B-cell malignancies. Recently an intrinsic strategy has been developed to modify the CAR itself to improve T-cell signaling. Here we report a second extrinsic approach based on altering the culture milieu to numerically expand CAR^+ T cells with a desired phenotype, for the addition of interleukin (IL)-21 to tissue culture improves CAR-dependent T-cell effector functions. We used electrotransfer of *Sleeping Beauty* system to introduce a CAR transposon and selectively propagate CAR^+ T cells on $CD19^+$ artificial antigen-presenting cells (aAPC). When IL-21 was present, there was preferential numeric expansion of CD19-specific T cells which lysed and produced IFN-γ in response to CD19. Populations of these numerically expanded CAR^+ T cells displayed an early memory surface phenotype characterized as $CD62L^+CD28^+$ and a transcriptional profile of naïve T cells. In contrast, T cells propagated with only exogenous IL-2 tended to result in an overgrowth of CD19-specific $CD4^+$ T cells. Furthermore, adoptive transfer of CAR^+ T cells cultured with IL-21 exhibited improved control of $CD19^+$ B-cell malignancy in mice. To provide coordinated signaling to propagate CAR^+ T cells, we developed a novel mutein of IL-21 bound to the cell surface of aAPC that replaced the need for soluble IL-21. Our findings show that IL-21 can provide an extrinsic reprogramming signal to generate desired CAR^+ T cells for effective immunotherapy. *Cancer Res; 71(10); 3516–27. ©2011 AACR.*

Introduction

Adoptive transfer of antigen-specific T cells has been used to treat and prevent malignancies and opportunistic infections. To overcome immune tolerance to human tumor-associated antigens (TAA), investigators have redirected specificity through the introduction of immunoreceptors. An initial clinical trial showed the safety and feasibility of redirecting T cell specificity to CD19, a TAA expressed on B-cell malignancies (1–3). These clinical data demonstrated that infused T cells were short lived due, in part, to the use of a first-generation chimeric antigen receptor (CAR) that recognized CD19 independent of MHC via chimeric CD3-ζ (signal 1). In response, we developed a second-generation CD19-specific CAR to activate T cells through both CD3-ζ and CD28 endodomains (signals 1 and 2, respectively) to improve T-cell activation (4). To translate this CAR to clinical trials, we established a platform for nonviral gene transfer using the *Sleeping Beauty* (SB) system and subsequent selective expansion of CAR^+ T cells recursively cocultured upon $CD19^+$ artificial antigen-presenting cells (aAPC) modified from K562 to express CD19 and desired costimulatory molecules (5–7).

In addition to modifying the CAR itself to augment therapeutic potential, we have now manipulated the tissue culture environment to alter the types of CAR^+ T cells that can be generated. We investigated whether cytokines could be added to cultures to provide a "signal 3" to improve the CAR^+ T cells response to B-cell malignancies.

One attractive cytokine to use in the culturing of T cells is interleukin (IL)-21, which like IL-2, signals through the cytokine receptor common γ chain (IL-2Rγ). This was selected to be tested on the basis of the published work showing that this cytokine increases tumor-specific T cells (8) and/or natural killer (NK) cells (9, 10) leading to antitumor immunity in animal models. Further, IL-21 provides a T-cell survival signal and can act in conjunction with CD28 to support proliferation and acquisition of effector functions (11). T cells genetically modified to have enforced secretion of IL-21 exhibited improved antitumor effect compared to T cells not modified

Authors' Affiliations: [1]Division of Pediatrics, Children's Cancer Hospital, [2]Department of Stem Cell Transplantation and Cellular Therapy, and [3]The University of Texas Graduate School of Biomedical Sciences at Houston, University of Texas MD Anderson Cancer Center, Houston, Texas

Note: Supplementary data for this article are available at Cancer Research Online (http://cancerres.aacrjournals.org/).

Corresponding Author: Laurence J. N. Cooper, University of Texas MD Anderson Cancer Center, Pediatrics-Research, Unit 907, 1515 Holcombe Blvd., Houston, TX 77030. Phone: 713-563-3208; Fax: 713-792-9832; E-mail: ljncooper@mdanderson.org

doi: 10.1158/0008-5472.CAN-10-3843

Published OnlineFirst May 15, 2011; DOI:10.1158/0008-5472.CAN-10-3843

to secrete cytokines (12). Recombinant soluble IL-21 has been intravenously administered in patients with metastatic renal cell carcinoma, melanoma, and lymphoma, and antitumor activity has been observed (13). In contrast to IL-2, IL-21 also inhibits generation of human regulatory T cells *in vitro* (14).

We hypothesized that altering the culture environment by the addition of IL-21 will lead to improved numeric expansion and functionality of CD19-specific CAR$^+$ T cells. When IL-21 was present with or on aAPC, we found there was a preferential numeric expansion of CAR$^+$ T cells with a preference to propagate subpopulations of (i) CD8$^+$ T cells, (ii) memory T cells, and (iii) naïve T cells, which lysed and produced IFN-γ in response to CD19. This resulted in improved control of CD19$^+$ tumor in a mouse model of human T-cell immunotherapy.

Materials and Methods

Plasmids

The SB transposon $_{CoOp}$CD19RCD28/pSBSO expresses the human codon optimized (CoOp) second generation $_{CoOp}$CD19RCD28 CAR under human elongation factor 1-α (hEF-1α) promoter, flanked by the SB inverted repeats (6). To generate membrane-bound IL-21 (mIL-21), the GM-CSF (granulocyte macrophage-colony-stimulating factor) signal peptide sequence was directly fused to the coding sequence of mature human IL-21 which was attached via a modified [amino acid (aa) 108, Ser → Pro] 12 aa IgG4 hinge region (aa 99–110), to the 5′ end of a human immunoglobulin γ-4 chain C_H2 and C_H3 regions (aa 111–327, UniProtKB P01861), that was fused in frame to human CD4 transmembrane domain (aa 397–418, UniProtKB P01730). After validating the sequence, the human codon optimized cDNA (GENEART) was cloned as a transposon into a SB expression plasmid, pT-MNDU3-eGFP (5) replacing the eGFP sequence to obtain $_{CoOp}$IL-21-Fc/pT-MNDU3 (Fig. 6A). The SB transposase, SB11 is expressed *in cis* from the plasmid pCMV-SB11 (6).

Cell lines and their propagation

Daudi coexpressing β_2-microglobulin (15; Daudiβ_2m, a kind gift from Dr Brian Rabinovich, University of Texas MD Anderson Cancer Center (MDACC)), NALM-6 [pre–B cell; ATCC (American Type Culture Collection)], U251T (glioblastoma; a kind gift from Dr Walder Debinksi, Wake Forest University, NC), CD19$^+$U251T [ref. 6; expressing truncated CD19, ref. 16] were cultured as described previously (5, 6). NALM-6 cells were transduced using a murine stem cell virus–based retroviral vector encoding enhanced firefly luciferase (effLuc; ref. 17) fused with enhanced green fluorescent protein (EGFP; a kind gift from Dr Brian Rabinovich, MDACC). Retrovirus was packaged as previously described (17), concentrated 50× using Amicon Ultra-15 100,000 NMWL centrifugal concentration units (Millipore), mixed with NALM-6 cells in the presence of 8 μg/mL polybrene (Sigma) and spinfected for 90 minutes at 2200 RPM/30°C. One week later, EGFP$^+$NALM-6 cells were sorted on a FACSAria (BD Biosciences). Selective *in vitro* expansion of genetically modified T cells was carried out using K562-derived aAPC (clone no. 4) coexpressing CD19, CD64, CD86, CD137L, and a membrane-bound IL-15 (mIL-15; coexpressed with EGFP; ref. 15). Clone no. 4 was further modified to express mIL-21 using the construct $_{CoOp}$IL-21-Fc/pT-MNDU3. Briefly, 10^6 aAPC were resuspended in 100 μL Amaxa Cell Line Nucleofector Solution V (catalogue no. VPA-1003) along with transposon ($_{CoOp}$IL-21-Fc/pT-MNDU3, 2 μg) and SB transposase (pCMV-SB11, 2 μg) DNA supercoiled plasmids, transferred to a cuvette and electroporated (Program T-16) using Nucleofector II (Lonza). The transfectants were cultured for a week in complete media and a clone (D2) was obtained by plating at limited dilution after FACS (fluorescence-activated cell sorter) sorting. All cell lines were verified by morphology and/or flow cytometry, tested for *Mycoplasma*, and conserved in research cell bank on reception.

Generation of CAR$^+$ T cells

CD19-specific CAR$^+$ T cells were generated from peripheral blood mononuclear cells (PBMC) using SB transposition as previously described and depicted in Figure 1 (5). Briefly, 10^7 to 2×10^7 mononuclear cells, isolated from blood by Ficoll-Paque density gradient centrifugation (GE Healthcare Bio-Sciences AB), were resuspended in 100 μL of Amaxa Nucleofector solution (Human T cell Kit, catalogue no. VPA-1002), along with CAR transposon (CD19RCD28/pSBSO, 15 μg) and SB transposase (pCMV-SB11, 5 μg) DNA plasmids, transferred to a single cuvette and electroporated (Program U-14) on day 0 using Nucleofector II. The cells were rested for 2 to 3 hours at 37°C in incomplete phenol-free RPMI (HyClone) and subsequently cultured overnight in phenol-free RPMI containing 10% FBS and stimulated the next day (day 1) with γ-irradiated (100 Gy) K562-aAPC at a 1:2 T cell/aAPC ratio. Additional γ-irradiated aAPC clone no. 4 were added every 7 days at the same ratio. When used, soluble recombinant human IL-21 (catalogue no. 34-8219-85, eBioscience) was added at a concentration of 30 ng/mL beginning the day after electroporation, and soluble recombinant human IL-2 (IL-2; Chiron) was added to the cultures at 50 U/mL beginning 7 days after electroporation. For experiments where CAR$^+$ T cells were cocultured on mIL-21$^+$ K562-aAPC (T cell/aAPC clone D2 ratio 1:2), IL-2 (50 U/mL) was added to the cultures on day 7 after electroporation. All exogenous cytokines continued to be supplemented on a Monday-Wednesday-Friday schedule for 7-day stimulation cycles marked by the addition of aAPC. The cultures were monitored by flow cytometry for the unwanted presence of a CD3^{neg}CD56$^+$ cell population and if the percentage exceeded approximately 10% of the total population, which usually occurred between 10 and 14 days of initial coculture with aAPC, a depletion for (CD3^{neg}) CD56$^+$ NK cells was carried out using CD56 beads (catalogue no. 130-050-401, Miltenyi Biotech Inc.) on LS column (catalogue no. 130-042-401, Miltenyi Biotech Inc.) according to the manufacturer's instructions. T cells were enumerated every 7 days and viable cells counted based on Trypan blue exclusion using Cellometer automated cell counter (Auto T4 Cell Counter, Nexcelom Bioscience). At the time of electroporation and during the course of coculture, programs "PBMC_human_frozen" and "activated T cell," respectively, were used for counting cells on the Cellometer. The fold expansion (as compared to day 1) of total, CD3$^+$, and CAR$^+$ cells at the end of 7, 14, 28 days of

Published OnlineFirst May 15, 2011; DOI:10.1158/0008-5472.CAN-10-3843

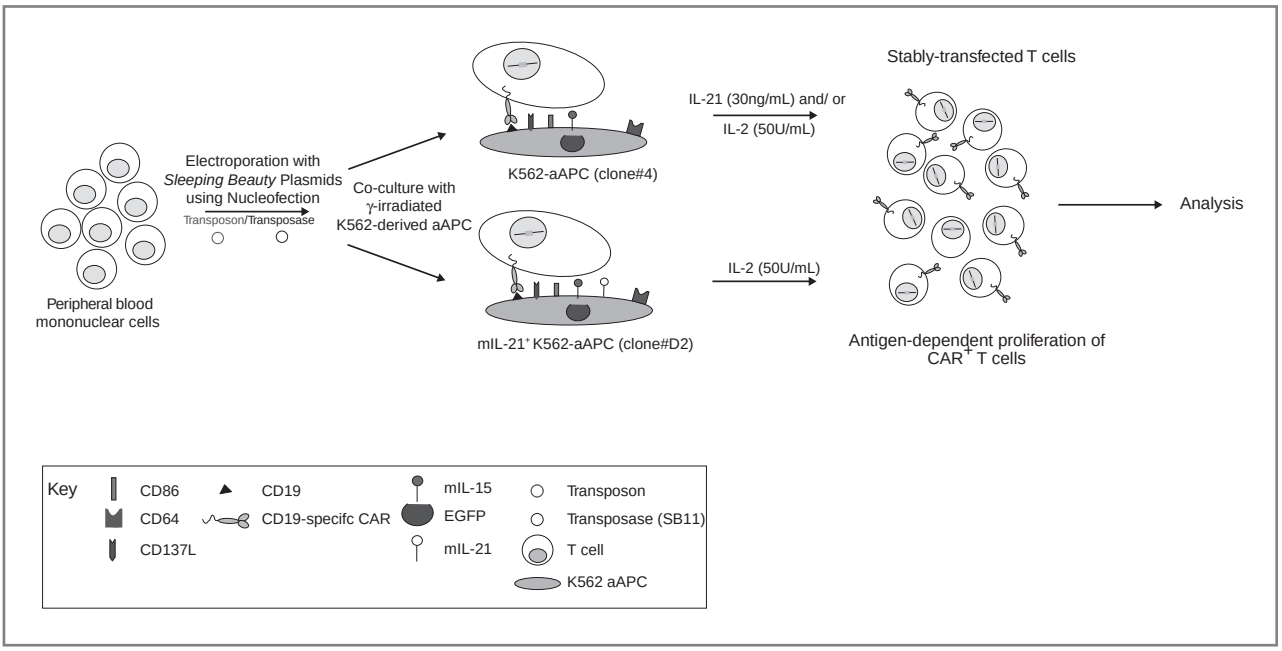

Figure 1. Generation of CAR$^+$ T cells on γ-irradiated aAPC. PBMC were electroporated with SB transposon and transposase. Cells were subsequently cocultured on K562-derived aAPC [modified to coexpress CD19, CD64, CD86, CD137L (4-1BBL), mIL-15, with and without mIL-21] in the presence of soluble IL-21 and/or IL-2.

coculture for individual experiments was calculated and the average compared between culture conditions using a Student's *t* test.

Flow cytometry

Up to 10^6 cells in 100 μL volume were stained with fluorochrome-conjugated [fluorescein isothiocyanate (FITC), phycoerythrin (PE), peridinin chlorophyll protein conjugated to cyanine dye (PerCPCy5.5), allophycocyanin (APC)] reagents which unless otherwise stated, were obtained from BD Biosciences: anti–CD3 FITC (catalogue no. 349201, 5 μL), anti–CD3 PerCPCy5.5 (catalogue no. 340949, 4 μL), anti–CD4 APC (catalogue no. 555349, 2.5 μL), anti–CD8 PerCPCy5.5 (catalogue no. 341051, 4 μL), anti–CD19 PE (catalogue no. 555413, 10 μL), anti–CD28 PerCPCy5.5 (catalogue no. 337181, 4 μL), anti–CD62L APC (catalogue no. 559772, 2.5 μL), anti–CD45RA FITC (catalogue no. 555488, 5 μL), anti–CD45RO APC (catalogue no. 559865, 2.5 μL), anti–IL7Rα Alexa Fluor 647 (catalog no. 558598, 10 μL), anti–PD1 APC (catalogue no. 558694, 2.5 μL), anti–PDL1 PE (catalogue no. 557924, 2.5 μL), anti–NKG2D PE (catalogue no. 557940, 2.5 μL), anti–Granzyme B Alexa Fluor 647 (catalogue no. 560212, 3 μL), anti–Perforin PE (Reagent Set no. 556437, 3 μL), anti–HLA (human leukocyte antigen)-ABC APC (catalogue no. 555555, 2.5 μL), anti–CD86 PE (catalogue no. 555658, 2.5 μL), anti–CD64 PE (catalogue no. 558592, 2.5 μL), anti–CD137L PE (catalogue no. 559446, 2.5 μL), anti–IFN-γ APC (catalogue no. 554702, 2 μL), anti-pSTAT3 (pY705) PE (catalogue no. 612569, 20 μL), anti–IL-21 PE (catalogue no. 12 7219-73, 2.5 μL, eBiosciences), anti–CCR7 PE (catalogue no. FAB197P, 10 μL, R&D Systems) and anti–CXCR4 PE (catalogue no. FAB173P, 10μL, R&D Systems). FITC-conjugated (catalogue no. H10101C, 3 μL, Invitrogen) and PE-conjugated (catalogue no. H10104, 2.5 μL, Invitrogen) F(ab′)$_2$ fragment of goat anti-human Fcγ was used to detect cell surface expression of the CD19-specific CAR. Blocking of nonspecific antibody binding was achieved using FACS wash buffer (2% FBS and 0.1% Sodium azide in PBS). Data acquisition was on a FACSCalibur (BD Biosciences) using CellQuest version 3.3 (BD Biosciences). Analyses and calculation of median fluorescence intensity (MFI) was undertaken using FCS Express version 3.00.007 (Thornhill).

Chromium release assay

The cytolytic activity of T cells was determined in a standard 4-hour chromium release assay (CRA) as described previously (5, 18).

Intracellular IFN-γ production

10^5 T cells were incubated with 0.5×10^6 stimulator cells in 200 μL culture media along with protein transport inhibitor (BD Golgi Plug containing Brefeldin A, catalogue no. 555028) in a round-bottom, 96-well plate. Following a 4 to 6 hour incubation at 37°C, the cells were stained for expression of CAR at 4°C for 30 minutes. After washing, the cells were fixed, permeabilized (for 20 minutes at 4°C with 100 μL of Cytofix/Cytoperm Buffer, catalogue no. 555028) and stained with APC-conjugated monoclonal antibody (mAb) specific for IFN-γ. Cells were further washed and analyzed by FACSCalibur. T cells treated with a leukocyte activation cocktail [PMA (phorbol 12 myristate 13 acetate) and ionomycin, catalogue no. 550583, BD Biosciences] were used as a positive control.

Induction of STAT3 phosphorylation

10^6 CAR$^+$ T cells were incubated with and without aAPC for 30 minutes at 37°C in a V-bottom 96-well plate. The cells were then fixed with 20 excess volumes of 37°C pre-warmed 1 × PhosFlow Lyse/Fix Buffer (catalogue no. 558049, BD

Published OnlineFirst May 15, 2011; DOI:10.1158/0008-5472.CAN-10-3843

Biosciences) diluted in water at 37°C for 10 minutes to prevent dephosphorylation. Thereafter, pelleted cells were permeabilized by adding BD PhosFlow Perm Buffer III (catalogue no. 55850, BD Biosciences) for 20 minutes on ice, followed by washing with BD Pharmingen Staining Buffer (catalogue no. 554656). Resuspended cells were then stained with antibodies for pSTAT3, CD3, and CAR for 20 minutes in the dark, washed once with BD Pharmingen Staining Buffer, and resuspended in the same buffer for flow cytometry analysis.

nCounter analysis digital gene expression system

Genetically modified T cells (10,000) were lysed in RNeasy lysis buffer (RLT; 5 μL, Qiagen) and frozen for single-use aliquots at −80°C. Lysates were thawed and the selected mRNA content analyzed using the nCounter Analysis System (model no. NCT-SYST-120, NanoString Technologies; ref. 19) after hybridization with a designer reporter code set and capture probe set for 12 hours at 65°C. The probes were designed, synthesized, and hybridized using the nCounter Gene Expression Assay Kit. The posthybridization processing was undertaken using the nCounter Prep Station. Nanominer software was used to carry out normalization compared to internal control and basic statistical analysis on the data. The normalized results are expressed as the relative mRNA level.

In vivo efficacy of CAR$^+$ T cells

On day 0, 7-week-old NOD.Cg-*Prkdc*^{scid}*Il2rg*^{tm1wjl}/SzJ (NSG) mice were intravenously (i.v.) injected via a tail vein with 10^5 EGFP$^+$effLuc$^+$ NALM-6 cells. Mice (n = 5/group) in the 2 treatment cohorts received via tail vein injection (on days 1 and 9) 2×10^7 of CAR$^+$ T cells grown in the presence of IL-2 or CAR$^+$ T cells grown in the presence of IL-2 and IL-21. One group of mice (n = 5) bearing tumor received no T cells. Anesthetized mice underwent bioluminescent imaging (BLI) in an anterior–posterior position using a Xenogen IVIS 100 series system (Caliper Life Sciences) 10 minutes after subcutaneous injection (at neck and shoulder) of 150 μL (200 μg/mouse) freshly thawed aqueous solution of D-Luciferin potassium salt (Caliper Life Sciences) as previously described (20). Photons emitted from NALM-6 xenografts were serially quantified using the Living Image 2.50.1 (Caliper Life Sciences) program. At the end of the experiment, mice were euthanized and tissues harvested. Bone marrow was flushed from the femurs using 30Gx$^1/_2$inch needles (BD, catalogue no. 305106) with 2% FBS in PBS. Spleens were disrupted using a syringe in 2% FBS/PBS and passed through a 40 μm nylon cell strainer (BD, catalogue no. 352340) to obtain single cell suspension. Red blood cells from bone marrow, spleen, and peripheral blood were lysed using ACK lysing buffer (Gibco-Invitrogen, A10492) and remaining cells stained for presence of tumor (CD19 and EGFP) by flow cytometry. Statistical analysis of photon flux and tumor burden was accomplished using Student's t test.

Results

Propagation of CAR$^+$ T cells with IL-21

A master cell-bank of clinical-grade K562-derived aAPC, designated clone no. 4, has been generated through the Production Assistance for Cellular Therapies (PACT) to propagate CD19-specific CAR$^+$ T cells to clinically sufficient numbers. These γ-irradiated aAPC selectively propagate CAR$^+$ T cells after the electrotransfer of SB plasmids coding for CD19RCD28 CAR (5). To investigate extrinsic factors that might improve the therapeutic potential of CAR$^+$ T cells, a role for IL-21 was examined in the culturing process on aAPC. We added this soluble cytokine, in addition to soluble IL-2 and mIL-15 on aAPC, and showed selective expansion of CAR$^+$ T cells (Fig. 2A). This resulted in a greater number of CD3$^+$ and CAR$^+$ T cells at 28 days of coculture on clone no. 4 ($P < 0.05$) compared with T cells receiving IL-2 alone, with differences between the 2 groups already apparent within 2 weeks after electroporation (Fig. 2B and C). Indeed, the average fold expansion of CAR$^+$ T cells at 7 (2.75 ± 1.1 fold, $n = 7$) and 14 (39.2 ± 36.2 fold, $n = 7$) days after electroporation were significantly higher ($P < 0.05$) compared to T cells that only received IL-2 (day 7, 0.29 ± 0.3 fold, $n = 4$; day 14, 0.49 ± 0.36 fold, $n = 4$). After 4 weeks of coculture on aAPC, the group that received IL-21 had an average 19,800 ± 11,313 ($n = 7$) fold expansion of CD3$^+$ T cells and there was a 35,800 ± 23,285 ($n = 7$) fold expansion of CAR$^+$ T cells. In contrast, T cells that only received IL-2 had an average CD3$^+$ fold expansion of 2,280 ± 4,227 ($n = 4$) and CAR$^+$ T cells expanded by an average of 2,680 ± 4,919 ($n = 4$) fold. The average total cell numbers at 7 (4.1×10^7 vs. 4.7×10^6) and 14 (3.1×10^8 vs. 2.7×10^7) days after electroporation were significantly higher ($P < 0.05$) in cultures receiving IL-21, as compared to cultures receiving only IL-2, which was due to an increased average number of average CD3$^+$ T cells (day 7, 4.1×10^7 vs. 3.0×10^6; day 14, 3.5×10^8 vs. 2.4×10^7; $P < 0.05$). These data suggest the addition of soluble recombinant IL-21 to the culture environment augments the propagation of CD3$^+$CAR$^+$ T cells on aAPC clone no. 4.

IL-21 results in qualitative differences in CAR$^+$ T cells

CAR$^+$ T cells cultured only in the presence of IL-2 produced low amounts of IFN-γ in response to CAR binding CD19 and expressed low levels of granzyme B. Expression of this cytokine and granzyme is associated with improved antitumor activity, therefore we investigated whether the presence of IL-21 could augment expression of these factors as T cells were propagated on aAPC. We measured mRNA levels using the nCounter Analysis System and IFN-γ and Granzyme B were found to be significantly elevated in populations of T cells receiving IL-21 (Fig. 3A). At day 28 of culture, we observed a 3-fold increase in IFN-γ (313 vs. 100) and 40-fold increase in granzyme B (4,458 vs. 110) mRNA transcript levels in T cells grown in IL-2 and IL-21, as compared to those grown in soluble IL-2. We demonstrated a significant increase in granzyme B protein levels (mean 89.5% vs. 17%) and CD19-dependent IFN-γ production (mean 55% vs. 0.1%) in the CAR$^+$ T cells receiving IL-21, as compared to those grown in soluble IL-2 (Fig. 3B). Thus, the mRNA measurements are consistent with the phenotype data showing an increase in expression of IFN-γ and granzyme B after coculture of CAR$^+$ T cells with IL-2 and IL-21. We have previously generated CD19RCD28$^+$ T cells on CD19$^+$ aAPC in the presence of soluble IL-2 which tended

Published OnlineFirst May 15, 2011; DOI:10.1158/0008-5472.CAN-10-3843

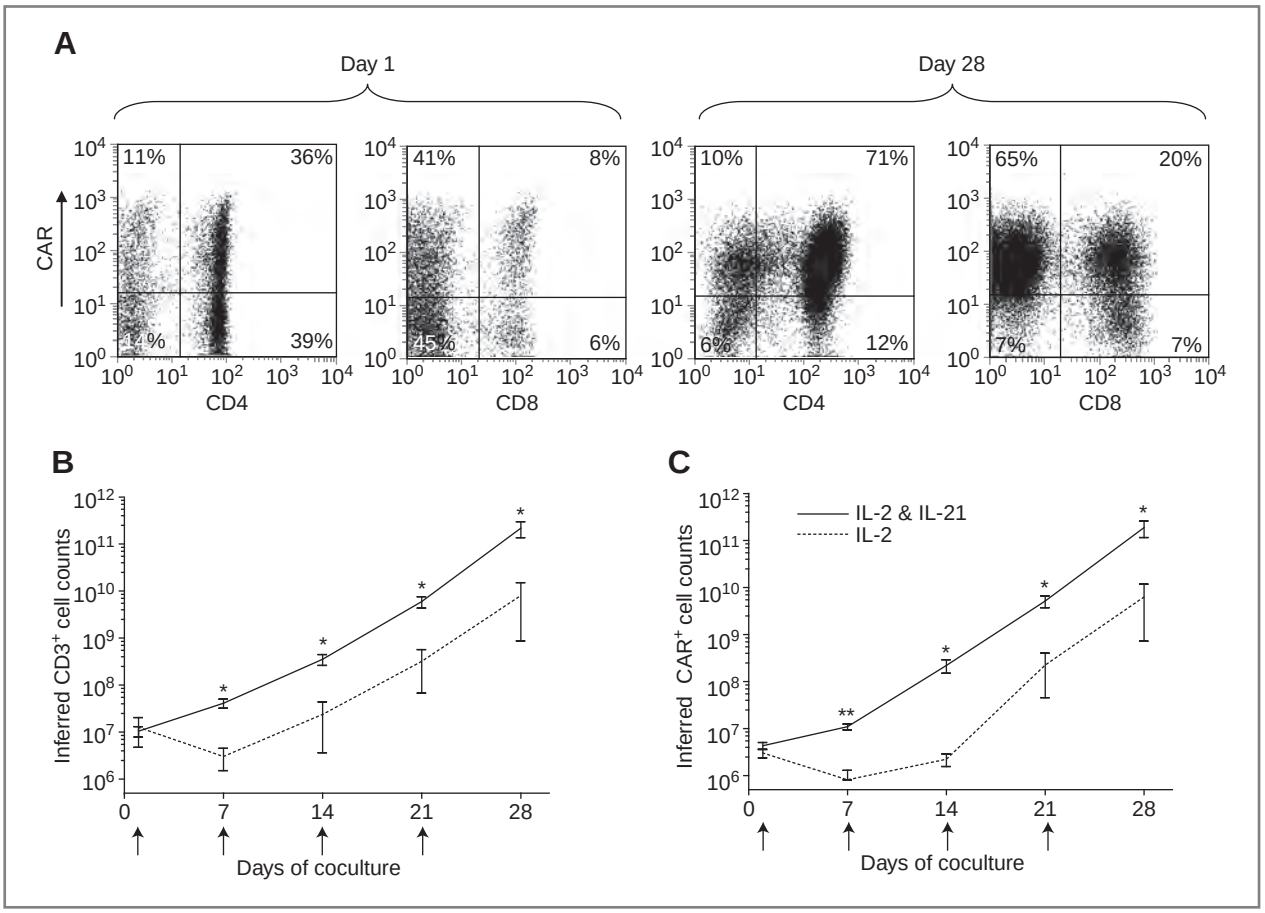

Figure 2. Propagation of genetically modified T cells on aAPC. A, T-cell expression of CAR before and after propagation on aAPC. The rate of T-cell growth cultured on γ-irradiated aAPC for 28 days in the presence of IL-2 ($n = 4$) or IL-2 and IL-21 ($n = 7$). The total number of B, $CD3^+$ cells, and C, CAR^+ T cells propagated over time. Small upward arrows indicate the addition of γ-irradiated aAPC to the culture. Inferred cell counts were calculated assuming all viable cells were carried forward through each stimulation cycle. Mean ± SD is shown; *, $P < 0.05$; **, $P < 0.001$.

to result in a preferential outgrowth of CAR^+ T cells with a predominance of $CD4^+$ T cells (5). Recognizing that $CD8^+$ T cells contribute to antitumor immunity, we sought a method to improve the outgrowth of $CD8^+CAR^+$ T cells on aAPC. IL-21 has been shown to help propagate $CD8^+$ effector T cells (21), therefore the genetically modified T cells were cocultured with aAPC in the presence of exogenous IL-21 and IL-2 for 28 days which resulted in a trend toward improved outgrowth of $CD8^+CAR^+$ compared with $CD4^+CAR^+$ T cells. Day 28 was selected as an endpoint for tissue culture and subsequent analyses since over this time period CAR^+ T cells expand to numbers sufficient for clinical translation (Fig. 2). The T cells receiving IL-21 had 1.8-fold higher number of average $CD8^+$ T cells (24.2 ± 25.3) compared to the T cells receiving just IL-2 (13.4 ± 0.9) at day 28 of coculture (Fig. 3D). At the time of analysis, there was increased CAR expression on the T cells exposed to IL-21 compared to T cells cultured with only IL-2 (mean 90% ± 7.5 vs. 66% ± 7; $P < 0.01$) which indicates that manipulating the cytokine milieu can improve the outgrowth of T cells with increased expression of CAR (Fig. 3C). In aggregate, the addition of IL-21 compared to culturing only with IL-2, results in T cells containing subpopulations that have improved effector function, a trend toward $CD8^+$ phenotype, and augmented CAR expression.

IL-21 results in propagation of subpopulations of CAR^+ T cells with memory and naïve phenotypes

T cells propagated over a prolonged time in tissue culture tend to mature to a differentiated phenotype which may compromise their therapeutic potential. To determine if IL-21 can curtail this differentiation of genetically modified T cells, we examined the expression of (i) eomesodermin (EOMES) which controls cytolytic development and function of T cells, and has recently been shown to be reduced in naïve-derived effector cells (22–24) and (ii) killer cell lectin-like receptor subfamily G, member 1 (KLRG1), an inhibitory receptor that is expressed by senescent T cells (25, 26). At day 28, the T cells cultured only with IL-2 had increased levels of mRNA species coding for EOMES and KLRG1 showing that this cytokine promoted differentiation of CAR^+ T cells on aAPC. However, when IL-21 was added there was a 7-fold and 54-fold reduction in EOMES and KLRG1, respectively (Fig. 3A). To expand on the mRNA data, we examined the cell surface expression for flow

Published OnlineFirst May 15, 2011; DOI:10.1158/0008-5472.CAN-10-3843

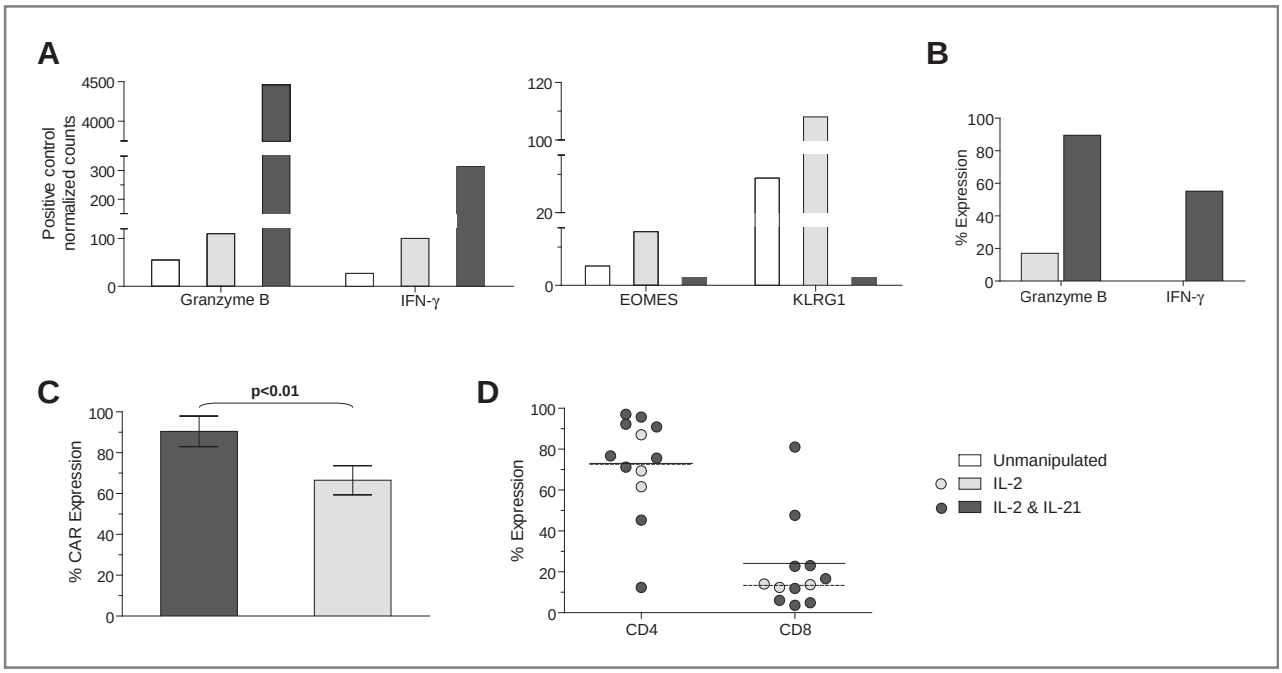

Figure 3. IL-21 supports outgrowth of T cells with improved CAR expression and desired phenotype. CAR$^+$ T cells grown in the presence of IL-2, or IL-21 and IL-2, at the end of 28 days of coculture on aAPC were evaluated for: A, the amount of mRNA transcripts coding for Granzyme B, IFN-γ, EOMES, and KLRG1 using NanoString nCounter analysis, and B, expression of Granzyme B and CD19-specific IFN-γ (percent IFN-γ production when cells were stimulated with CD19$^+$U251T as compared to CD19^{neg} U251T) using flow cytometry. C, total CAR expression (mean ± SD). D, percent CD4 and CD8 T cells in cultures receiving IL-2 and IL-2 & IL-21 at the end of 28 days of coculture over aAPC. Each circle represents individual experiment, horizontal bars represent mean expression, solid (IL-2 and IL-21) and dotted (IL-2).

cytometry markers of naïve, memory, and differentiated T cells. A naïve phenotype was defined by the presence of CD62L and CD45RA, whereas a central memory (T_{CM}) phenotype can be defined by the expression of CD28, CD62L, CCR7, and CD45RO on T cells (27–29). Differentiated effector cells typically lose expression of these markers upon prolonged culturing, and exhausted cells upregulate expression of PD-1 and PDL-1 (30). CAR$^+$ T cells grown in the presence of IL-2 and IL-21 exhibited markers consistent with both naïve and memory cells and lacked expression of PD-1/PDL-1 (Fig. 4A). In addition, the lack of (2%) CD57 expression supports absence of exhaustion among the CAR$^+$ T cells (31). At day 28 of culture, the CAR$^+$ T cells expressed CD28 (mean 69%, range: 22%–88%), CCR7 (mean 16%, range: 0.9%–60.5%), CD62L (mean 50%, range: 22%–75%), CD45RO (93%, range: 84%–98%), and IL7Rα (mean 26%, range: 9%–37%). Among the CAR$^+$ cells were T cells with a T_{CM} phenotype exemplified by the coexpression of CD28$^+$CD62L$^+$ (34%, range: 11%–59%), CD28$^+$CCR7$^+$ (mean 18%, range: 0.8%–56.5%), CD62L$^+$,CCR7$^+$ (10%, range: 0.5%–48%), CD45RO$^+$CD45RA$^+$ (mean 19%, range: 2%–63%). In summary, the addition of IL-21 supports the numeric expansion of CAR$^+$ T cells on aAPC that contain memory and naïve subpopulations.

Redirected specificity of CAR$^+$ T cells numerically expanded with IL-21

T cells expressing CAR and propagated in the presence of IL-2 and IL-21 were able to specifically lyse CD19$^+$ tumor targets (Fig. 4B). At an effector:target ratio of 5:1, the CAR$^+$ T cells could lyse an average 51% (range: 32%–66%) of CD19$^+$ Daudiβ_2m cells and an average 38% (range: 25%–60%) of CD19$^+$ NALM-6. The Daudi cells used as targets were genetically modified to express β_2 microglobulin and thus re-express classical HLA class I (Supplementary Fig. 1) to decrease unwanted killing by contaminating NK or lymphokine-activated killer cells. Specificity for CD19 was shown by a 4.5-fold (range: 1.3–12.6) increased killing of genetically modified CD19$^+$ U251T (glioma) targets as compared to parental CD19^{neg} U251T targets at an effector:target ratio of 5:1. We further assessed the function of CAR$^+$ T cells by evaluating their ability to produce IFN-γ in response to CD19 (Fig. 4C). When CAR$^+$ T cells were stimulated with CD19$^+$ Daudiβ_2m cells there was an average 29.6-fold (range: 4.6–114.9) increase in IFN-γ production. The specificity for production of CD19 was shown by a 12.6-fold (range: 3.2–45.5) increase in IFN-γ production by CAR$^+$ T cells when cocultured with CD19$^+$ U251T cells in comparison to CD19^{neg} U251T cells. These data show that CAR$^+$ T cells cultured in the presence of IL-21 exhibit CD19-dependent redirected effector functions.

Efficacy of CAR$^+$ T cells propagated on aAPC to treat B-lineage malignancy

We investigated whether CAR$^+$ T cells numerically expanded in the presence of IL-2 and IL-21 were able to show an improved antitumor effect compared with CAR$^+$ T cells cultured with only IL-2. Mice injected with NALM-6 were longitudinally measured by BLI for tumor-associated effLuc activity. We observed that CAR$^+$ T cells grown in the presence

Published OnlineFirst May 15, 2011; DOI:10.1158/0008-5472.CAN-10-3843

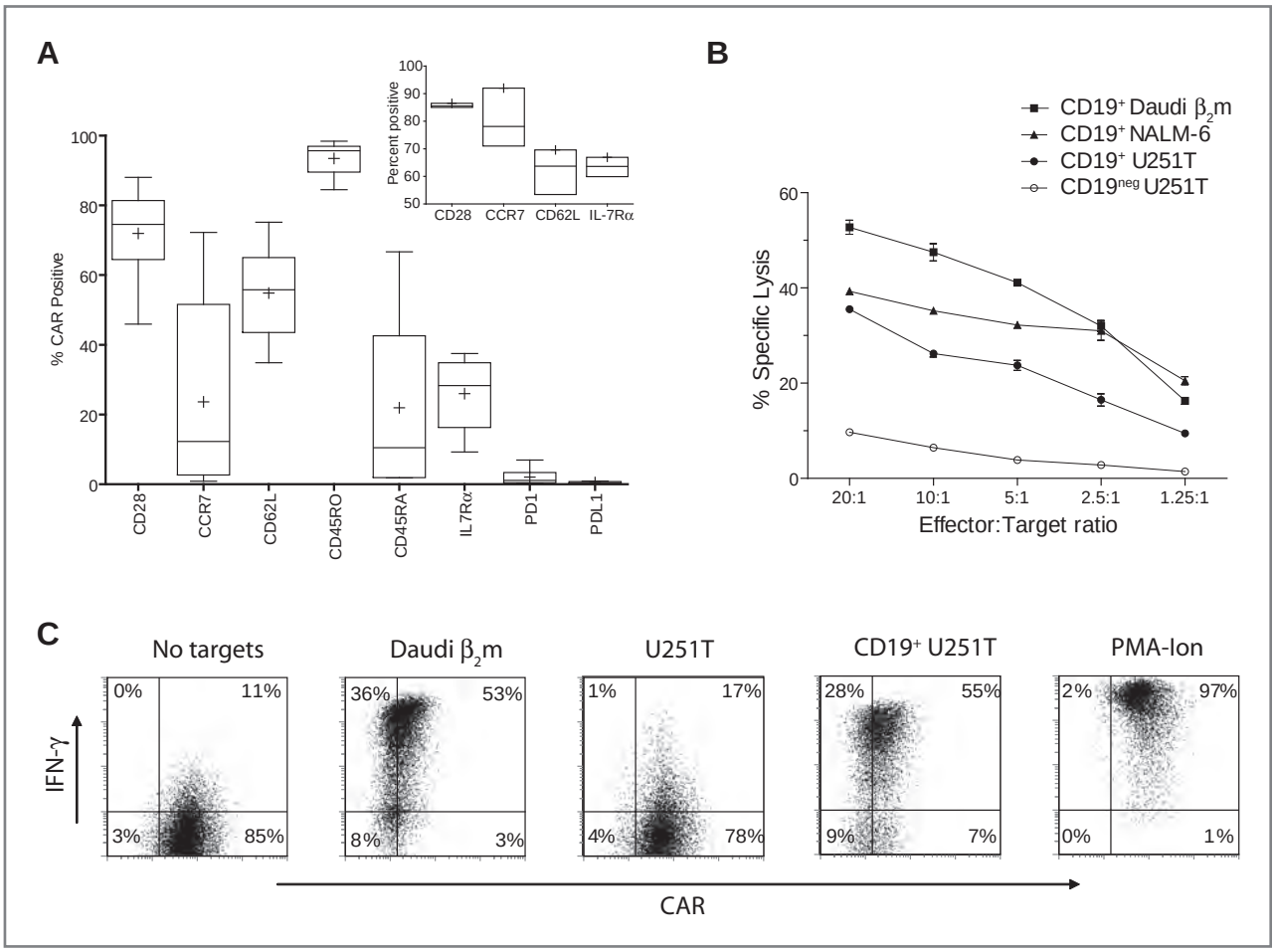

Figure 4. IL-21 supports outgrowth of sub-populations of naïve and memory CD19-specific CAR$^+$ T cells. A, immunophenotype of genetically modified T cells numerically expanded in the presence of IL-2 and IL-21. Inset shows expression of selected cell-surface proteins before electroporation on T cells obtained from PBMC ($n = 3$). Data are presented as "Box-and-Whiskers" plot and in inset as "low-high-bar" plot. Horizontal bar within boxes represents median and "+" represents the means. B, four-hour CRA shows killing of CD19$^+$ Daudiβ_2m, NALM-6, and CD19$^+$U251T cells. Lysis of CD19^{neg}U251T cells demonstrates background killing. Mean ± SD for triplicate wells is represented. C, IFN-γ production by CAR$^+$ T cells upon incubation with targets. PMA-ionomycin is used as a positive control.

of IL-2 and IL-21 were more effective in controlling tumor growth as compared to CAR$^+$ T cells grown in the presence of IL-2 (day 8, $P < 0.01$; day 13, $P < 0.05$; day 17, $P < 0.05$) and as compared to mice that did not receive T cells (days 8, 13, 17, $P < 0.01$; Fig. 5A and B). Groups of mice receiving no T cells or CAR$^+$ T cells grown in the presence of IL-2 showed similar rates of tumor growth (day 8, $P = 0.11$; day 13, $P = 0.2$; day 17, $P = 0.07$). Tissues from mice were assessed for EGFP$^+$CD19$^+$ NALM-6 and consistent with the BLI data, we observed that the tumor burden was significantly reduced in mice receiving CAR$^+$ T cells grown in the presence of IL-2 and IL-21, as compared to mice receiving no T cells or CAR$^+$ T cells grown in the presence of IL-2 (Fig. 5C and D). The presence of NALM-6 blasts in peripheral blood was lower in the IL-2 and IL-21 (1.8 ± 0.92, mean ± SD) group as compared to mice that received CAR$^+$ T cells cultured with IL-2 (20.4 ± 20.3, $P < 0.05$) or no T cells (3.8 ± 0.6, $P < 0.01$). There was also a significant reduction in average tumor burden in the bone marrow after administration of T cells that were cultured with IL-2 and IL-21 group (48.5 ± 4.2) as compared to IL-2 group (86.6 ± 7.8, $P < 0.00001$) or no T-cell group (86.6 ± 7.9, $P < 0.001$). The difference in average splenic tumor burden was more apparent ($P < 0.0001$) comparing mice that received CAR$^+$ T cells cultured with IL-2 and IL-21 (30.9 ± 18.8) vs. mice that were infused with CAR$^+$ cells cultured with IL-2 (88.3 ± 4). The tumor burden was similar in the blood ($P = 0.07$) and bone marrow ($P = 0.49$) between the mice that received no T cells and mice that received CAR$^+$ T cells cultured with IL-2. Thus, these *in vivo* data confirm that CD19-specific CAR$^+$ cells propagated on aAPC in presence of IL-2 and IL-21 are superior in controlling tumor growth.

A membrane-bound mutein of IL-21 can replace soluble recombinant IL-21

Signaling through 2nd generation CAR and cytokine receptor(s) occurs in the tissue culture environment enabling aAPC to selectively propagate T cells that receive signals 1, 2, and 3. To improve the coordination between these sig-

Published OnlineFirst May 15, 2011; DOI:10.1158/0008-5472.CAN-10-3843

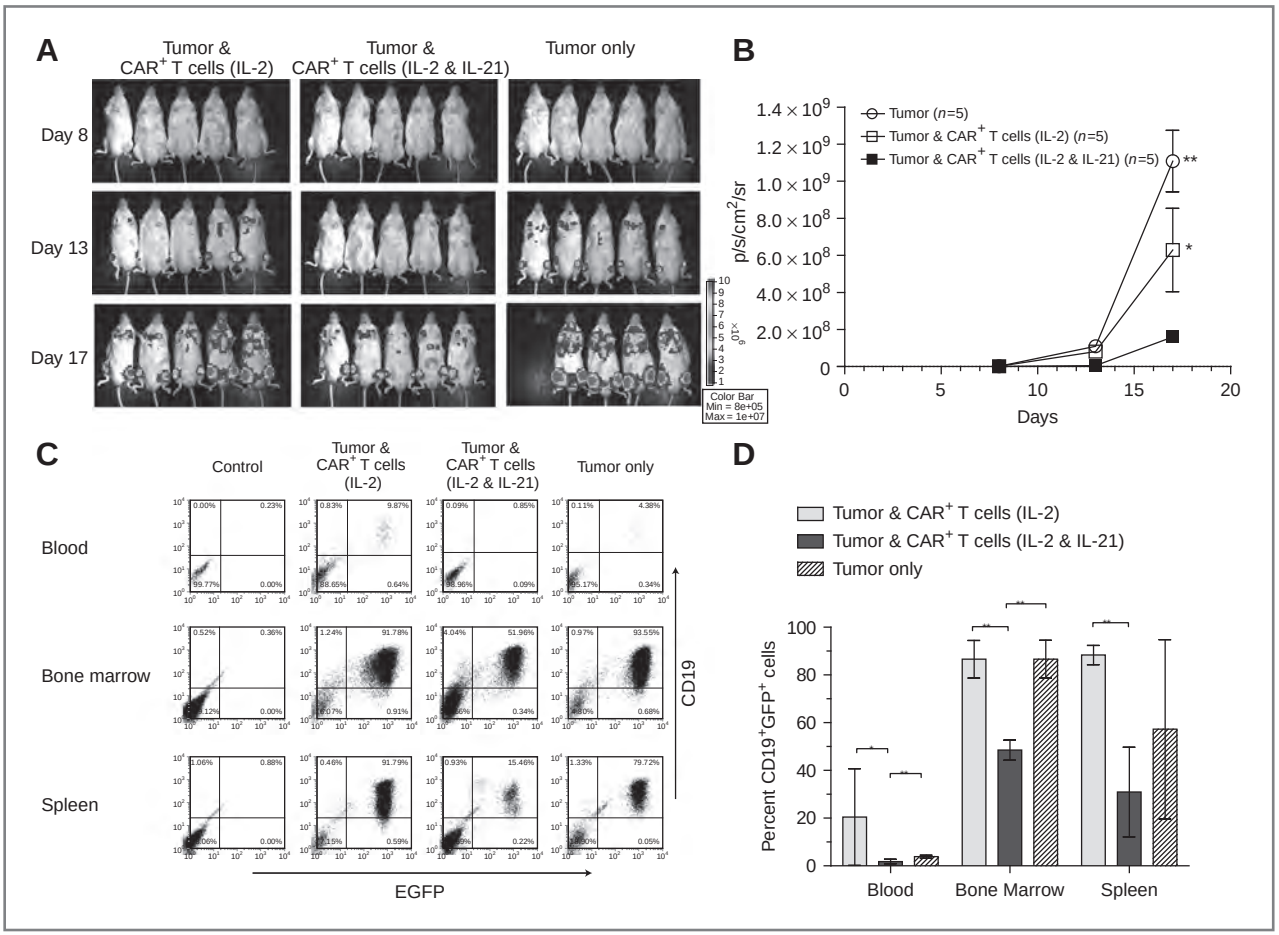

Figure 5. Efficacy of CAR$^+$ T cells in mice. NSG mice i.v. injected (day 0) with 10^5 EGFP$^+$effLuc$^+$ NALM-6 tumor received, on days 1 and 9, 2×10^7 CAR$^+$ T cells grown in the presence of IL-2 or IL-2 & IL-21, or received no T cells. A, false-colored images representing photon flux from NALM-6–derived ffLuc activity. B, time course of longitudinal measurements of tumor-derived mean photon flux $\pm$ SD from 3 groups of mice ($n = 5$). Background luminescence (10^6 p/s/cm^2/sr) was defined from mice with no tumor imaged after receiving D-Luciferin in parallel with mice in treatment groups. *In vitro* ffLuc-derived activity of genetically modified EGFP$^+$effLuc$^+$ NALM-6 was 2.8 $\pm$ 0.2 cpm/cell (mean $\pm$ SD) compared with 0.003 $\pm$ 0.001 cpm/cell (mean $\pm$ SD) for parental NALM-6 cells that do not express ffLuc. C, at the end of the experiment (day 21) mice were euthanized and tissues (blood, bone marrow, spleen) were harvested and analyzed by flow cytometry for expression of CD19 and EGFP. Representative flow cytometry dot plots for tumor at various sites are shown. E, the percentage of CD19$^+$EGFP$^+$ cells present in mice from the 3 groups (mean $\pm$ SD) is shown along with statistical significance (*, $P < 0.05$, **, $P < 0.01$).

nals, we altered the aAPC to not only provide the CD19 antigen and associated costimulatory molecules, but to express a novel mutein of membrane-bound of IL-21 (Fig. 6A). This enabled us to test the hypothesis that expressing IL-21 on the cell surface of the aAPC could replace the need for providing IL-21 as a soluble recombinant cytokine. To accomplish this, the aAPC clone no. 4 were electroporated with the SB plasmid $_{CoOp}$IL-21-Fc/pT-MNDU3 and a subclone (D2) was selected based on uniform expression of mIL-21 and the other introduced cell surface markers (Fig. 6B). PBMC electroporated with SB system to express CD19R-CD28 and propagated on γ-irradiated mIL-21$^+$ aAPC in the absence of soluble IL-21, but in the presence of soluble IL-2 resulted in an outgrowth of CAR$^+$ T cells (Fig. 7A). The CAR expression (81% vs. 79%) was similar to when T cells were grown in the presence of exogenous IL-21 or with aAPC expressing mIL-21. The average fold expansion at the end of 28 days of coculture as assessed by expression of CD3 (11,700; $P = 0.27$, not significant, NS) and CAR (14,000; $P = 0.17$, NS) on T cells numerically expanded with mIL-21$^+$ aAPC was similar to the T cells propagated with soluble IL-21 (Fig. 7B). The CAR$^+$ T cells numerically expanded on mIL-21$^+$ aAPC showed specific lysis of CD19$^+$ target cells and a 13-fold increase in IFN-γ production when cells were stimulated with CD19$^+$ U251T targets over control CD19^{neg}U251T cells (Fig. 7D). To examine if mIL-21 can directly activate T cells, we evaluated the phosphorylation status of STAT3. CAR$^+$ T cells that were propagated for 28 days with IL-2 plus mIL-21^{neg} aAPC (clone no. 4) and IL-2 plus mIL-21$^+$ aAPC (clone no. D2), were stimulated for 30 minutes on aAPC with (clone no. D2) or without mIL-21 (clone no. 4). T cells cultured with IL-2 and soluble IL-21 stimulated with aAPC (clone no. 4) along with soluble IL-21 were used as positive controls. CAR$^+$ T cells cultured on mIL-21$^+$ aAPC in

Published OnlineFirst May 15, 2011; DOI:10.1158/0008-5472.CAN-10-3843

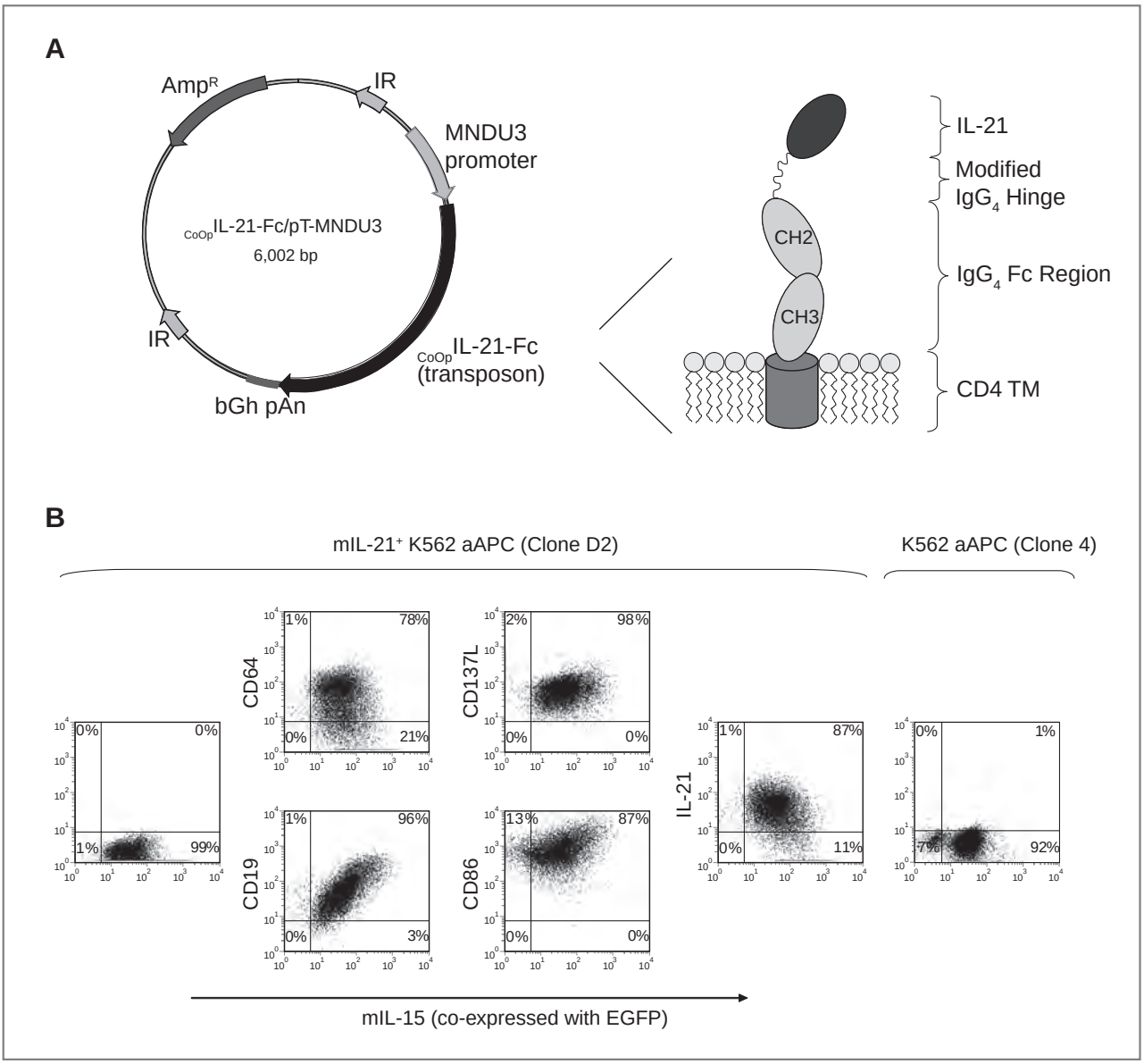

Figure 6. Expression of membrane-bound IL-21 (mIL-21). A, schematic of the DNA plasmid, $_{CoOp}$IL-21-Fc/pT-MNDU3, expressing mIL-21 along with a cartoon showing the folded mIL-21 protein. Abbreviations: MNDU3 promoter, promoter from U3 region of the MND retrovirus; $_{CoOp}$IL-21-Fc, codon-optimized mIL-21 (IL-21-Fc fusion); IR, SB-inverted/direct repeats; bGh pAn, polyadenylation signal from bovine growth hormone; Amp^R, ampicillin resistance gene. B, dot plots showing the presence of mIL-21 (detected by mAb against IL-21) and cell surface markers (CD19, CD64, CD86, CD137, mIL-15) on the aAPC.

the presence of IL-2 when stimulated with mIL-21$^+$ aAPC resulted in an increase in MFI of pSTAT3 (27.1), over the unstimulated control T cells (11.6), or when stimulated with aAPC lacking mIL-21 (13.2; Fig. 7C). When CAR$^+$ T cells which had been propagated on aAPC (clone no. 4) in the presence of IL-2 (and had not seen IL-21 in any form) were exposed to mIL-21$^+$ aAPC, there was a similar increase in MFI of pSTAT3 (25.2) compared to the controls (unstimulated, 11.1; aAPC lacking mIL-21, 14.3). These data show that mIL-21 on aAPC is functional and capable of activating T cells through the STAT3 pathway. In aggregate, these data suggest that mIL-21$^+$ aAPC can replace soluble recombinant IL-21 to selectively propagate CAR$^+$ T cells with redirected specificity.

Discussion

The tissue culture environment can be modified to play a critical role in the growth and function of T cells propagated *in vitro*. In the current study, we show that the addition of IL-21 to the culture milieu in soluble form or presented in conjunction with antigen on aAPC results in improved effector function and preservation of naïve/memory phenotype of CAR$^+$ T cells which predicts for improved therapeutic effect in clinical trials.

Published OnlineFirst May 15, 2011; DOI:10.1158/0008-5472.CAN-10-3843

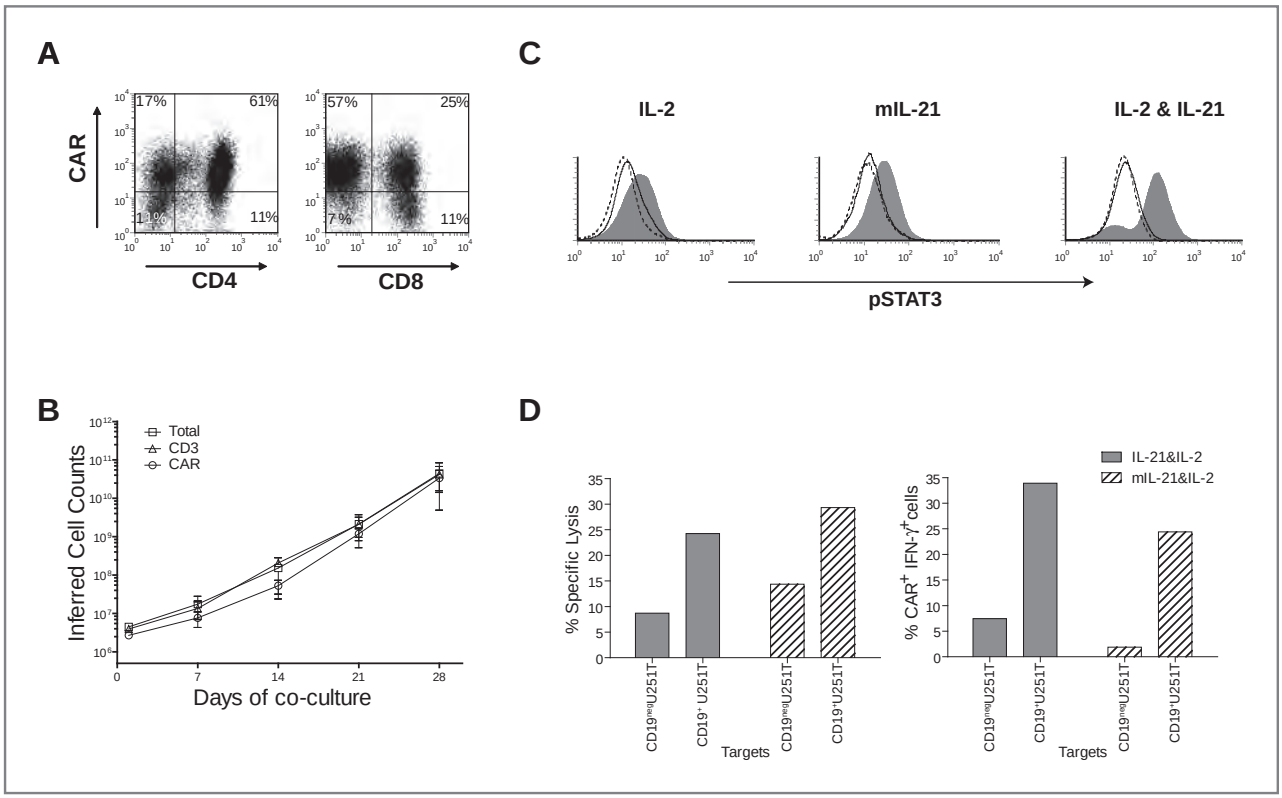

Figure 7. Characterization of T cells grown on mIL-21+ aAPC. A, CAR expression on CD4+ and CD8+ T cells after 28 days of coculture on mIL-21+ aAPC (clone no. D2) along with exogenous IL-2. B, expansion of total, CD3+, and CAR+ T cells over 28 days of culture period. C, induction of STAT3 phosphorylation was measured in T cells grown with IL-2 or mIL-21 & IL-2. These propagated T cells were subsequently stimulated by aAPC with (Clone D2, filled grey histograms) or without (Clone 4, black histograms) mIL-21 for 30 minutes, then fixed, permeabilized, and stained for flow cytometry. Cells grown in presence of IL-2 and soluble IL-21 stimulated with aAPC (Clone 4) with (filled grey histogram) and without (black histogram) soluble IL-21 were used as control. Histograms (dotted, unstimulated cells) represent phosphoSTAT3 staining and indicate a shift in MFI. D, redirected specificity of CAR+ T cells grown on mIL-21+ aAPC with IL-2 as measured by 4-hour CRA and flow cytometry for IFN-γ production.

Initial (first generation) CARs commonly link a scFv to a single signaling moiety (e.g., CD3-ζ) and these typically showed a lack of sustained persistence *in vivo* (2). Therefore, the CAR design was modified to add one or more costimulatory signaling domains of CD28 (4), 4-1BB (32, 33), OX40 (34) to generate "second" or "third" generation CARs. We have previously described our second generation CAR, CD19RCD28, which provides CD19-dependent signaling through CD3ζ and CD28 resulting in improved persistence and antitumor effect (4). Operating under the premise that T cells propagated in a CAR-dependent manner *ex vivo* may select for T cells with sustained proliferation *in vivo*, we developed a culturing system based on aAPC to selectively numerically expand CAR+ T cells. Such aAPC derived from K562 can be tailored to express cell-surface antigen (35) or intracellular antigen presented by restricting MHC (36, 37) in the context of desired and introduced T-cell costimulatory molecules (37–40). Our aAPC (clone no. 4) were also engineered to express mIL-15 and this membrane-bound cytokine is present throughout our culturing process in addition to the addition of soluble cytokines. The addition of IL-21–mediated signaling during the culturing process to selectively propagate T cells expressing a second generation CD19-specific CAR resulted in an outgrowth of T cells on aAPC with a desired phenotype and improved function when assessed *in vitro* and *in vivo*. Thus, from the perspective of manufacturing CAR+ T cells for clinical application it appears beneficial to include IL-21 in the culturing process.

It has been previously shown that the tissue culture microenvironment can be altered with cytokines for improved T-cell function. For example, T cells can be primed using cytokines to augment immune responses after adoptive transfer. In some cases, this is dependent on generation of memory phenotype which requires the presence of IL-15 and IL-21 (41, 42). This memory phenotype predicts for improved persistence as shown for T cells cultured with IL-7, IL-15, and IL-21, compared to T cells propagated with IL-2 (8, 43, 44). Our data provide supportive evidence that not only can the CAR be manipulated, but the choice of additional cytokines influences the number and character of the propagated CAR+ T cells.

Membrane-bound cytokines (45, 46) offer an attractive approach for delivering a desired cytokine to the immediate microenvironment of the T cell-aAPC synapse along with alleviating the need to add the soluble recombinant (expensive) cytokine to the culture system and avoiding the need to procure clinical-grade cytokine for clinical applications. Membrane-bound IL-15 has been used to propagate

Published OnlineFirst May 15, 2011; DOI:10.1158/0008-5472.CAN-10-3843

T cells (6, 47) and NK cells (48, 49) on aAPC derived from K562 cells. Our aAPC (clone no. 4) used in this study express mIL-15 and is being used in our clinical trials infusing patient- and donor-derived CD19-specific CAR$^+$ T cells after autologous and allogeneic hematopoietic stem-cell transplantation. Building upon the success of aAPC expressing mIL-15, we further modified the aAPC clone no. 4 to coexpress mIL-21 and suggest that this genetic approach to aAPC design may avoid the need to add soluble recombinant IL-21 to the culture.

Our data show that the SB system and aAPC platform can be manipulated to culture T cells to receive 3 coordinated signals. This was achieved by influencing intrinsic (CAR) and now extrinsic (tissue culture) factors to improve the therapeutic potential of genetically modified and propagated T cells. Activation through second generation CAR, triggered by CD3ζ (signal 1) and CD28 (signal 2), and common γ_c receptor (triggered by IL-21, signal 3) results in generation of CAR$^+$ T cells that have an improved ability to respond to CD19 compared to T cells cultured without IL-21. The ability to augment signal 3 leads to an outgrowth of CAR$^+$ T cells on aAPC that have desired properties for use in clinical trials.

Disclosure of Potential Conflicts of Interest

No potential conflicts of interest were disclosed.

Acknowledgments

The authors thank Karen Ramirez and David He from Flow Cytometry Core Laboratory (NIH grant no. 5P30CA016672-32) for their help with flow cytometry. The authors also thank Brian Rabinovich for assistance with transduction of NALM-6 tumor cells.

Grant Support

The work was supported by Cancer Center Core Grant (CA16672); DOD PR064229; PO1 (CA100265); RO1 (CA124782, CA120956, CA141303); R33 (CA116127); Mr. and Mrs. Joe H. Scales; The Alex Lemonade Stand Foundation; The Burroughs Wellcome Fund; The Cancer Prevention Research Institute of Texas; The Gillson Longenbaugh Foundation; The Harry T. Mangurian Jr, Foundation, The Institute of Personalized Cancer Therapy; The Leukemia and Lymphoma Society; The Lymphoma Research Foundation; The Miller Foundation; The National Foundation for Cancer Research; The Pediatric Cancer Research Foundation; and The William Lawrence and Blanche Hughes Children's Foundation.

The costs of publication of this article were defrayed in part by the payment of page charges. This article must therefore be hereby marked *advertisement* in accordance with 18 U.S.C. Section 1734 solely to indicate this fact.

Received October 20, 2010; revised March 9, 2011; accepted March 15, 2011; published OnlineFirst May 10, 2011.

References

1. Jensen MC, Popplewell L, DiGiusto DL, Kalos M, Cooper L JN, Raubitschek A, et al. A first-in-human clinical trial of adoptive therapy using CD19-specific chimeric antigen receptor re-directed T cells for recurrent/refrctory follicular lymphoma. Mol Ther 2007; 15:S142.
2. Jensen MC, Popplewell L, Cooper LJ, DiGiusto D, Kalos M, Ostberg JR, et al. Antitransgene rejection responses contribute to attenuated persistence of adoptively transferred CD20/CD19-specific chimeric antigen receptor redirected T cells in humans. Biol Blood Marrow Transplant 2010;16:1245–56.
3. Jena B, Dotti G, Cooper LJ. Redirecting T-cell specificity by introducing a tumor-specific chimeric antigen receptor. Blood 2010;116: 1035–44.
4. Kowolik CM, Topp MS, Gonzalez S, Pfeiffer T, Olivares S, Gonzalez N, et al. CD28 costimulation provided through a CD19-specific chimeric antigen receptor enhances *in vivo* persistence and antitumor efficacy of adoptively transferred T cells. Cancer Res 2006;66:10995–1004.
5. Singh H, Manuri PR, Olivares S, Dara N, Dawson MJ, Huls H, et al. Redirecting specificity of T-cell populations for CD19 using the Sleeping Beauty system. Cancer Res 2008;68:2961–71.
6. Davies JK, Singh H, Huls H, Yuk D, Lee DA, Kebriaei P, et al. Combining CD19 redirection and alloanergization to generate tumor-specific human T cells for allogeneic cell therapy of B-cell malignancies. Cancer Res 2010;70:3915–24.
7. Hackett PB, Largaespada DA, Cooper LJ. A transposon and transposase system for human application. Mol Ther 2010;18:674–83.
8. Moroz A, Eppolito C, Li Q, Tao J, Clegg CH, Shrikant PA. IL-21 enhances and sustains CD8$^+$ T cell responses to achieve durable tumor immunity: comparative evaluation of IL-2, IL-15, and IL-21. J Immunol 2004;173:900–9.
9. Ma HL, Whitters MJ, Konz RF, Senices M, Young DA, Grusby MJ, et al. IL-21 activates both innate and adaptive immunity to generate potent antitumor responses that require perforin but are independent of IFN-gamma. J Immunol 2003;171:608–15.
10. Brady J, Hayakawa Y, Smyth MJ, Nutt SL. IL-21 induces the functional maturation of murine NK cells. J Immunol 2004;172:2048–58.
11. Casey KA, Mescher MF. IL-21 promotes differentiation of naive CD8 T cells to a unique effector phenotype. J Immunol 2007;178: 7640–8.
12. Markley JC, Sadelain M. IL-7 and IL-21 are superior to IL-2 and IL-15 in promoting human T cell-mediated rejection of systemic lymphoma in immunodeficient mice. Blood 2010;115:3508–19.
13. Hashmi MH, Van Veldhuizen PJ. Interleukin-21: updated review of Phase I and II clinical trials in metastatic renal cell carcinoma, metastatic melanoma and relapsed/refractory indolent non-Hodgkin's lymphoma. Expert Opin Biol Ther 2010;10:807–17.
14. Li Y, Yee C. IL-21 mediated Foxp3 suppression leads to enhanced generation of antigen-specific CD8$^+$cytotoxic T lymphocytes. Blood 2008;111:229–35.
15. Manuri PV, Wilson MH, Maiti SN, Mi T, Singh H, Olivares S, et al. piggyBac transposon/transposase system to generate CD19-specific T cells for the treatment of B-lineage malignancies. Hum Gene Ther 2010;21:427–37.
16. Serrano LM, Pfeiffer T, Olivares S, Numbenjapon T, Bennitt J, Kim D, et al. Differentiation of naive cord-blood T cells into CD19-specific cytolytic effectors for posttransplantation adoptive immunotherapy. Blood 2006;107:2643–52.
17. Rabinovich BA, Ye Y, Etto T, Chen JQ, Levitsky HI, Overwijk WW, et al. Visualizing fewer than 10 mouse T cells with an enhanced firefly luciferase in immunocompetent mouse models of cancer. Proc Natl Acad Sci U S A 2008;105:14342–6.
18. Cooper LJ, Topp MS, Serrano LM, Gonzalez S, Chang WC, Naranjo A, et al. T-cell clones can be rendered specific for CD19: toward the selective augmentation of the graft-versus-B-lineage leukemia effect. Blood 2003;101:1637–44.
19. Geiss GK, Bumgarner RE, Birditt B, Dahl T, Dowidar N, Dunaway DL, et al. Direct multiplexed measurement of gene expression with color-coded probe pairs. Nat Biotechnol 2008;26:317–25.
20. Singh H, Serrano LM, Pfeiffer T, Olivares S, McNamara G, Smith DD, et al. Combining adoptive cellular and immunocytokine therapies to improve treatment of B-lineage malignancy. Cancer Res 2007;67: 2872–80.
21. Li Y, Bleakley M, Yee C. IL-21 influences the frequency, phenotype, and affinity of the antigen-specific CD8 T cell response. J Immunol 2005;175:2261–9.
22. Pearce EL, Mullen AC, Martins GA, Krawczyk CM, Hutchins AS, Zediak VP, et al. Control of effector CD8$^+$ T cell function by the transcription factor Eomesodermin. Science 2003;302:1041–3.

Published OnlineFirst May 15, 2011; DOI:10.1158/0008-5472.CAN-10-3843

23. Intlekofer AM, Takemoto N, Wherry EJ, Longworth SA, Northrup JT, Palanivel VR, et al. Effector and memory CD8$^+$ T cell fate coupled by T-bet and eomesodermin. Nat Immunol 2005;6:1236–44.
24. Hinrichs CS, Borman ZA, Gattinoni L, Yu Z, Burns WR, Huang J, et al. Human effector CD8$^+$ T cells derived from naive rather than memory subsets possess superior traits for adoptive immunotherapy. Blood 2011;117:808–14.
25. Henson SM, Franzese O, Macaulay R, Libri V, Azevedo RI, Kiani-Alikhan S, et al. KLRG1 signaling induces defective Akt (ser473) phosphorylation and proliferative dysfunction of highly differentiated CD8$^+$ T cells. Blood 2009;113:6619–28.
26. Voehringer D, Koschella M, Pircher H. Lack of proliferative capacity of human effector and memory T cells expressing killer cell lectinlike receptor G1 (KLRG1). Blood 2002;100:3698–702.
27. Dutton RW, Bradley LM, Swain SL. T cell memory. Annu Rev Immunol 1998;16:201–23.
28. Sallusto F, Lenig D, Forster R, Lipp M, Lanzavecchia A. Two subsets of memory T lymphocytes with distinct homing potentials and effector functions. Nature 1999;401:708–12.
29. Sallusto F, Geginat J, Lanzavecchia A. Central memory and effector memory T cell subsets: function, generation, and maintenance. Annu Rev Immunol 2004;22:745–63.
30. Barber DL, Wherry EJ, Masopust D, Zhu B, Allison JP, Sharpe AH, et al. Restoring function in exhausted CD8 T cells during chronic viral infection. Nature 2006;439:682–7.
31. Brenchley JM, Karandikar NJ, Betts MR, Ambrozak DR, Hill BJ, Crotty LE, et al. Expression of CD57 defines replicative senescence and antigen-induced apoptotic death of CD8$^+$ T cells. Blood 2003;101:2711–20.
32. Imai C, Mihara K, Andreansky M, Nicholson IC, Pui CH, Geiger TL, et al. Chimeric receptors with 4–1BB signaling capacity provoke potent cytotoxicity against acute lymphoblastic leukemia. Leukemia 2004;18:676–84.
33. Brentjens RJ, Santos E, Nikhamin Y, Yeh R, Matsushita M, La Perle K, et al. Genetically targeted T cells eradicate systemic acute lymphoblastic leukemia xenografts. Clin Cancer Res 2007;13:5426–35.
34. Pulè MA, Straathof KC, Dotti G, Heslop HE, Rooney CM, Brenner MK. A chimeric T cell antigen receptor that augments cytokine release and supports clonal expansion of primary human T cells. Mol Ther 2005;12:933–41.
35. Numbenjapon T, Serrano LM, Singh H, Kowolik CM, Olivares S, Gonzalez N, et al. Characterization of an artificial antigen-presenting cell to propagate cytolytic CD19-specific T cells. Leukemia 2006;20:1889–92.
36. Latouche JB, Sadelain M. Induction of human cytotoxic T lymphocytes by artificial antigen-presenting cells. Nat Biotechnol 2000;18:405–9.
37. Hirano N, Butler MO, Xia Z, Berezovskaya A, Murray AP, Ansén S, et al. Efficient presentation of naturally processed HLA class I peptides by artificial antigen-presenting cells for the generation of effective antitumor responses. Clin Cancer Res 2006;12:2967–75.
38. Maus MV, Thomas AK, Leonard DG, Allman D, Addya K, Schlienger K, et al. *Ex vivo* expansion of polyclonal and antigen-specific cytotoxic T lymphocytes by artificial APCs expressing ligands for the T-cell receptor, CD28 and 4-1BB. Nat Biotechnol 2002;20:143–8.
39. Suhoski MM, Golovina TN, Aqui NA, Tai VC, Varela-Rohena A, Milone MC, et al. Engineering artificial antigen-presenting cells to express a diverse array of co-stimulatory molecules. Mol Ther 2007;15:981–8.
40. Hirano N, Butler MO, Xia Z, Ansén S, von Bergwelt-Baildon MS, Neuberg D, et al. Engagement of CD83 ligand induces prolonged expansion of CD8$^+$ T cells and preferential enrichment for antigen specificity. Blood 2006;107:1528–36.
41. Neeson P, Shin A, Tainton KM, Guru P, Prince HM, Harrison SJ, et al. *Ex vivo* culture of chimeric antigen receptor T cells generates functional CD8$^+$ T cells with effector and central memory-like phenotype. Gene Ther 2010;17:1105–16.
42. Zeng R, Spolski R, Finkelstein SE, Oh S, Kovanen PE, Hinrichs CS, et al. Synergy of IL-21 and IL-15 in regulating CD8$^+$ T cell expansion and function. J Exp Med 2005;201:139–48.
43. Hinrichs CS, Spolski R, Paulos CM, Gattinoni L, Kerstann KW, Palmer DC, et al. IL-2 and IL-21 confer opposing differentiation programs to CD8$^+$ T cells for adoptive immunotherapy. Blood 2008;111:5326–33.
44. Schluns KS, Lefrancois L. Cytokine control of memory T-cell development and survival. Nat Rev Immunol 2003;3:269–79.
45. Kim YS. Tumor therapy applying membrane-bound form of cytokines. Immune Netw 2009;9:158–68.
46. Cimino AM, Palaniswami P, Kim AC, Selvaraj P. Cancer vaccine development: protein transfer of membrane-anchored cytokines and immunostimulatory molecules. Immunol Res 2004;29:231–40.
47. Wu Z, Xu Y. IL-15R alpha-IgG1-Fc enhances IL-2 and IL-15 anti-tumor action through NK and CD8$^+$ T cells proliferation and activation. J Mol Cell Biol 2010;2:217–22.
48. Fujisaki H, Kakuda H, Imai C, Mullighan CG, Campana D. Replicative potential of human natural killer cells. Br J Haematol 2009;145:606–13.
49. Gong W, Xiao W, Hu M, Weng X, Qian L, Pan X, et al. *Ex vivo* expansion of natural killer cells with high cytotoxicity by K562 cells modified to co-express major histocompatibility complex class I chain-related protein A, 4–1BB ligand, and interleukin-15. Tissue Antigens 2010;76:467–75.

Published OnlineFirst April 27, 2010; DOI:10.1158/0008-5472.CAN-09-3845

Cancer Research

Combining CD19 Redirection and Alloanergization to Generate Tumor-Specific Human T Cells for Allogeneic Cell Therapy of B-Cell Malignancies

Jeff K. Davies, Harjeet Singh, Helen Huls, et al.

Cancer Res 2010;70:3915-3924. Published OnlineFirst April 27, 2010.

Published OnlineFirst April 27, 2010; DOI:10.1158/0008-5472.CAN-09-3845

Cancer Research

Combining CD19 Redirection and Alloanergization to Generate Tumor-Specific Human T Cells for Allogeneic Cell Therapy of B-Cell Malignancies

Jeff K. Davies[1], Harjeet Singh[4], Helen Huls[4], Dongin Yuk[1], Dean A. Lee[4,6], Partow Kebriaei[5], Richard E. Champlin[5], Lee M. Nadler[1], Eva C. Guinan[2,3], and Laurence J.N. Cooper[4,6]

Abstract

Allogeneic hematopoietic stem-cell transplantation can cure some patients with high-risk B-cell malignancies, but disease relapse following transplantation remains a significant problem. One approach that could be used to augment the donor T-cell–mediated antitumor effect is the infusion of allogeneic donor–derived T cells expressing a chimeric antibody receptor (CAR) specific to the B-cell antigen CD19. However, the use of such cells might result in toxicity in the form of graft-versus-host disease mediated by CD19-specific (CD19-CAR) T cells possessing alloreactive endogenous T-cell receptors. We therefore investigated whether nonalloreactive tumor-specific human T cells could be generated from peripheral blood mononuclear cells of healthy donors by the combination of CD19 redirection via CAR expression and subsequent alloanergization by allostimulation and concomitant blockade of CD28-mediated costimulation. Alloanergization of CD19-CAR T cells resulted in efficient and selective reduction of alloresponses in both $CD4^+$ and $CD8^+$ T cells, including allospecific proliferation and cytokine secretion. Importantly, T-cell effector functions including CAR-dependent proliferation and specific target cytolysis and cytokine production were retained after alloanergization. Our data support the application of CD19 redirection and subsequent alloanergization to generate allogeneic donor T cells for clinical use possessing increased antitumor activity but limited capacity to mediate graft-versus-host disease. Immunotherapy with such cells could potentially reduce disease relapse after allogeneic transplantation without increasing toxicity, thereby improving the outcome of patients undergoing allogeneic transplantation for high-risk B-cell malignancies. *Cancer Res; 70(10); 3915–24. ©2010 AACR.*

Introduction

Disease recurrence is a major cause of mortality after allogeneic hematopoietic stem-cell transplantation (HSCT) for patients with poor-risk B-lineage malignancies (1–3). Adoptive transfer of allogeneic donor–derived T cells possessing additional antitumor activity has the potential to reduce relapse after allogeneic HSCT. The combination of such an approach with a strategy to selectively control alloresponses to limit toxicity from graft-versus-host disease (GvHD) might improve the outcome of allogeneic HSCT for patients with B-cell malignancies.

Authors' Affiliations: Departments of [1]Medical Oncology and [2]Pediatric Oncology, Dana-Farber Cancer Institute; [3]Division of Hematology/Oncology, Children's Hospital, Boston, Massachusetts; and Division of [4]Pediatrics and [5]Cancer Medicine and [6]Graduate School of Biomedical Sciences, The University of Texas M.D. Anderson Cancer Center, Houston, Texas

Note: J.K. Davies and H. Singh contributed equally to this work.

Corresponding Author: Laurence J.N. Cooper, Pediatrics-Research, Unit 907, The University of Texas M.D. Anderson Cancer Center, 1515 Holcombe Boulevard, Houston, TX 77030. Phone: 713-563-3208; Fax: 713-792-9832; E-mail: ljncooper@mdanderson.org.

doi: 10.1158/0008-5472.CAN-09-3845

The introduction of a chimeric antibody receptor (CAR; ref. 4) to redirect human T-cell specificity is one strategy to enhance desired T-cell–mediated antitumor activity (5). CARs typically consist of an HLA-independent high-affinity antigen recognition domain formed from extracellular single-chain immunoglobulin variable fragments, linked to one or more cytoplasmic T-cell activation domains, including CD3-ζ. Infusion of patient-derived T cells expressing a tumor-associated antigen–specific CAR has resulted in some disease responses in early clinical trials for $CD20^+$ B-cell lymphomas and GD_2^+ neuroblastoma, but in other trials, apparently limited *in vivo* persistence of CAR T cells restricted their therapeutic potential (6–10).

CD19, an early cell-surface B-lineage–restricted molecule, is expressed on both normal B cells and a wide range of human B-cell malignancies (11). Therefore, human CD19-specific CAR^+ T cells have been developed to redirect a T-cell–mediated antitumor effect (12, 13). Second-generation CD19-CAR cells possessing modified costimulatory signaling domains fused to chimeric CD3-ζ have improved *in vivo* persistence and antitumor efficacy in mice (14, 15). To facilitate the clinical use of CAR^+ T cells, we and others have recently used an augmented nonviral gene insertion strategy [the Sleeping Beauty (SB) transposon/transposase system] to introduce a second-generation CD19-CAR into primary human T cells (16–19).

Published OnlineFirst April 27, 2010; DOI:10.1158/0008-5472.CAN-09-3845

CAR$^+$ T cells have not yet been infused in the human allogeneic setting. Allogeneic CAR$^+$ T cells could provide an additional donor-derived T-cell–mediated antitumor effect to protect against tumor relapse after allogeneic HSCT. The use of allogeneic rather than patient-derived CAR$^+$ T cells would also eliminate the risk of tumor cell contamination. Additionally, reconstituting donor-derived T cells that have not undergone CD19 redirection but are reactive to recipient hematopoietic tissue–restricted minor histocompatibility antigens could provide protection against CD19^{neg} tumor precursors (20, 21), which would not be selectively targeted by CD19-CAR cells.

However, CAR$^+$ T cells possess endogenous αβ T-cell receptors (TCR), and infused allogeneic CAR$^+$ T cells bearing αβ TCR specific to recipient alloantigens could potentially mediate GvHD. Nonselective approaches to reducing alloreactivity after allogeneic HSCT (such as pharmacologic immunosuppression) would likely reduce the ability of allogeneic CAR to expand and function *in vivo*. Strategies have been developed to selectively reduce alloreactivity in donor T cells after allogeneic HSCT (22–24). We and others have previously shown that one such strategy, alloanergization by allostimulation concomitant with blockade of CD28-mediated costimulation, effectively and selectively reduces alloreactivity of HLA-mismatched human peripheral blood mononuclear cells (PBMC; refs. 25–27). Furthermore, we have successfully applied this strategy in two prior clinical trials to selectively reduce alloreactivity of HLA-mismatched donor-derived T cells in the setting of haploidentical bone marrow trans plantation (28, 29). A significant proportion of SB-modified CD19-CAR cells propagated on artificial CD19$^+$ antigen-presenting cells (aAPC) bearing the costimulator ligand CD86 express CD28 (18), suggesting that alloanergization would be a suitable technique to selectively reduce alloreactivity in such cells.

To develop a clinical strategy to increase antitumor activity in allogeneic donor T cells while controlling alloreactivity, we investigated whether our established strategy of alloanergization could abrogate alloresponses of second-generation CD19-CAR cells without loss of viability, phenotype, and CAR-dependent T-cell effector functions.

Materials and Methods

Plasmids. The SB transposon contains the codon-optimized (CoOp) second-generation *CD19RCD28* CAR, specific for human CD19, flanked by the SB inverted repeats. The ampicillin resistance gene (*Amp^R*) and origin of replication from the plasmid $_{CoOp}$CD19RCD28/pT-MNDU3 (18) were replaced with the DNA fragment encoding the kanamycin resistance gene (*Kan^R*) and origin of replication (*ColE1*) from the pEK vector (30), and the human elongation factor-1α (*hEF-1α*) promoter fragment from pVitro4 vector (InvivoGen) was swapped with *MNDU3* promoter to generate CD19RCD28/pSBSO [also referred to as CD19RCD28mZ(CoOp)/pSBSO]. The SB hyperactive transposase *SB11*, under the control of cytomegalovirus (*CMV*) promoter from the plasmid pCMV-SB11 (18), was ligated with the pEK vector fragment encoding *Kan^R* and *ColE1* to generate pKan-CMV-SB11.

Cell lines. CD19$^+$ Daudi (Burkitt lymphoma) and CD19^{neg} K562 (erythroleukemia) cells were obtained from American Type Culture Collection. CD19$^+$ NALM-6 (pre-B cell) and CD19$^+$ Granta 519 (B-cell non–Hodgkin lymphoma) cells were from DSMZ. CD19^{neg} LM7 (osteosarcoma) was a kind gift from Dr. Eugenie Kleinerman (M.D. Anderson Cancer Center, Houston, TX). Cell lines, including aAPC, were maintained in HyQ RPMI 1640 (Hyclone) supplemented with 2 mmol/L Glutamax-1 (Invitrogen) and 10% heat-inactivated FCS (Hyclone; 10% RPMI). CD19$^+$ K562 targets were maintained in 10% RPMI with HygroGold (hygromycin B, 0.4 mg/mL; InvivoGen) as described (31). CD19^{neg} U251T (glioblastoma) was a kind gift from Dr. Waldemar Debinski (Wake Forest University, Winston-Salem, NC). U251T were transfected with SB DNA plasmid (pSBSO) expressing truncated CD19 (ΔCD19/pSBSO) to generate CD19$^+$ U251T. The U251T cell lines were maintained in 10% RPMI with G418 (0.2 mg/mL; InvivoGen).

Generation of CD19-CAR cells. PBMC isolated by Ficoll-Paque (GE Healthcare) density gradient centrifugation of peripheral blood obtained from healthy adult volunteer donors after informed consent from Gulf Coast Regional Center (Houston, TX) were cultured in HyQ RPMI 1640 (Hyclone) supplemented with 2 mmol/L Glutamax-1 (Life Technologies-Invitrogen) and 10% heat-inactivated defined FCS (Hyclone). The SB transposon/transposase were electrotransferred (Amaxa/Lonza) into T cells derived from PBMC and a population of CD19-CAR cells were numerically expanded on γ-irradiated (100 Gy) K562-artificial antigen-presenting cells (aAPC; ref. 32) expressing CD19, 4-1BBL, CD86, CD64, and membrane-bound interleukin (IL)-15 as previously described (Fig. 1A and B; ref. 18).

Alloanergization of CD19-CAR cells and measurement of secondary alloresponses. Equal numbers of CD19-CAR cells and γ-irradiated (3.5 Gy) first-party allostimulator PBMC (isolated from healthy unrelated adult volunteers after consent on an Institutional Review Board–approved protocol) were cocultured in culture medium (RPMI containing penicillin/streptomycin and 10% human AB serum; Sigma-Aldrich) with or without humanized monoclonal anti-B7.1 (clone h1F1) and anti-B7.2 (h3D1) antibodies (10 μg/10^6 cells; Wyeth) as described (26) and outlined in Fig. 1C. After 72 hours, cocultures with anti-B7 antibodies ("alloanergized") and without anti-B7 antibodies ("nonanergized") were washed and resuspended. Secondary alloresponses were measured after restimulation with γ-irradiated first- or third-party allostimulator PBMC or soluble CD3 and CD28 antibodies (10 μg/mL; Beckman Coulter). Proliferation was determined by thymidine incorporation as described (26). Alloanergization efficiency (AE) was calculated as AE = 100 – {100 × [secondary alloproliferation (alloanergized cells)/secondary alloproliferation (nonanergized cells)]}.

Additionally, CD19-CAR cells were labeled with carboxyfluorescein diacetate succinimidyl ester (CFSE; Invitrogen) before restimulation (26). Allospecific precursor frequency was calculated as previously described (33), using Flowjo V4 software. Cytokine responses after allorestimulation were also measured using intracellular cytokine flow cytometry (ICC;

Published OnlineFirst April 27, 2010; DOI:10.1158/0008-5472.CAN-09-3845

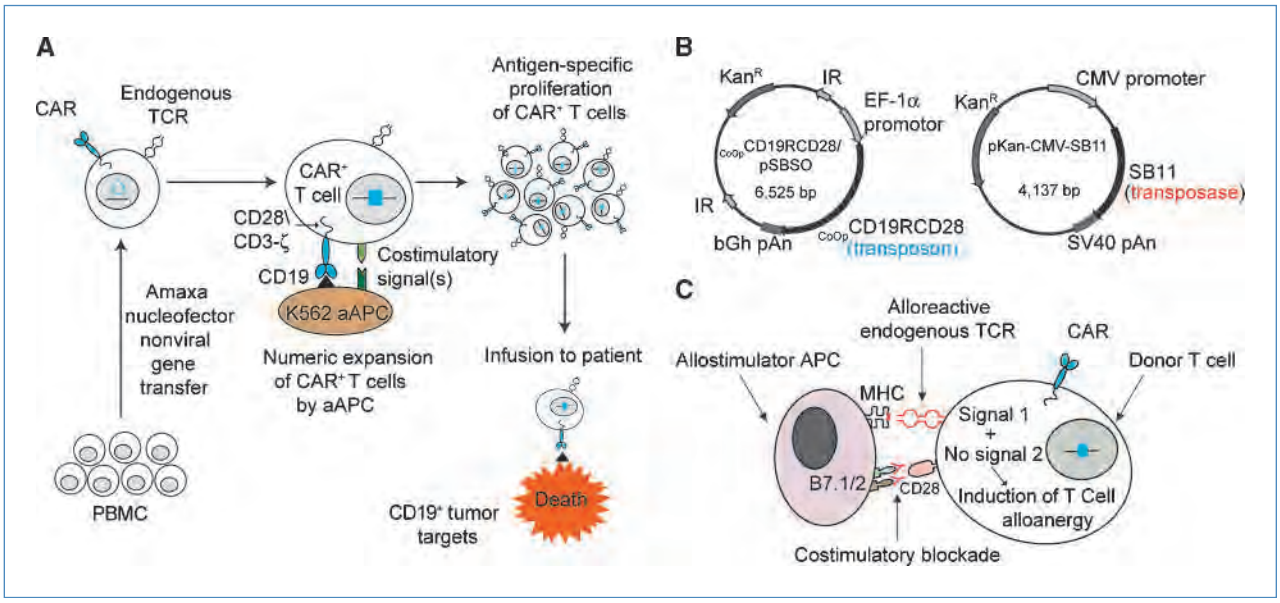

Figure 1. Generation and alloanergization of adult donor–derived CD19-CAR cells. A, electroporation of human T cells with SB DNA plasmids and propagation on CD19+ K562-derived aAPC. After electroporation, T cells were cocultured with γ-irradiated K562 (genetically modified to coexpress CD19, CD64, CD86, 4-1BBL, and surface membrane–bound IL-15) with addition of soluble IL-2 every alternate weekday, resulting in expansion of stably transfected CAR+ T cells to numbers suitable for use in adoptive cell therapy trials. B, schematic of the SB DNA plasmids. $_{CoOp}$CD19RCD28/pSBSO (transposon): *hEF-1α* promoter, human elongation factor-1α promoter; $_{CoOp}$*CD19RCD28*, codon-optimized CD19RCD28 CAR; IR, SB-inverted/direct repeats; bGh pAn, polyadenylation signal from bovine growth hormone; *KanR*, kanamycin resistance gene. pKan-CMV-SB11 (transposase): *SB11*, SB-transposase; CMV promoter, CMV enhancer/promoter; SV40pAn, polyadenylation signals from SV40. C, alloanergization of human CD19-CAR cells by allostimulation with costimulatory blockade. T cells are cocultured with γ-irradiated allostimulator PBMC in the presence of antibody-mediated blockade of CD28-mediated costimulation. T cells possessing alloreactive endogenous αβ TCR receive signal 1 (alloantigenic stimulus), but not signal 2 (CD28-mediated costimulation). This triggers intracellular events rendering the alloreactive T-cell hyporesponsive (anergic) to subsequent alloantigenic challenge, even in the presence of CD28-mediated costimulation.

ref. 34). Positive controls were stimulated with staphylococcal enterotoxin B (SEB; 10 μg/mL; Sigma-Aldrich). Stimulus-specific responses were calculated by subtracting values for unstimulated cells from values for stimulated cells.

CD19 depletion of allostimulator PBMC. Allostimulator PBMC were depleted of CD19+ B cells by labeling with conjugated anti-CD19 paramagnetic microbeads (Miltenyi Biotec, Gladbach, Germany) and passaged through an LD column and midiMACS magnetic device before irradiation. PBMC were analyzed by flow cytometry to assess efficiency of depletion.

Flow cytometry. Unless stated, antibodies were from Beckman Coulter. For alloresponses assessment, cells were stained with anti-CD3 (clone UCHT1), anti-CD4 (13B8.2), anti-CD8 (SFCI21Thy2D3), anti-CD14 [M5E2, Becton Dickinson (BD)], and anti-CD19 (RMO52) antibodies conjugated to FITC, phycoerythrin (PE), energy-coupled dye, PE-Cy5, and/or PE-Cy7. Viability was assessed with 7-amino actinomycin D (BD). For ICC, cells were stained for surface molecules, fixed, permeabilized, and then stained with IFN-γ-FITC (4S.B3, BD) and tumor necrosis factor-α (TNF-α)-PE-Cy7 (MAb11, BD). Events were acquired on a Cytomics FC500 flow cytometer and analyzed using Flowjo version 4. For detection of cell-surface expression of CD19-CAR, goat $F(ab')_2$ anti-human IgG (γ)-PE (Invitrogen) or goat $F(ab')_2$ anti-human IgG (γ)-FITC (Jackson ImmunoResearch Laboratories, Inc.) was used (1/20 dilution) with anti-CD4 (RPA-T4, BD), anti-CD8 (SK1, BD), and anti-CD3 (SK7, BD). Anti-CD27 (M-T271), anti-CD28 (L293), anti-CD45RO (UCHL1), anti-CD62L (Dreg 56), and anti-CD95 (DX2) were used for memory cell phenotyping (all BD). Nonspecific antibody binding was blocked using 2% fetal bovine serum in PBS (with sodium azide). For CAR-dependent IFN-γ secretion, 10^5 CD19-CAR cells were incubated for 4 to 6 hours with 0.5×10^6 stimulator cells or phorbol 12-myristate 13-acetate (5 ng/mL) and ionomycin (500 ng/mL) in 200 μL of culture medium with Golgi Plug (BD), fixed, permeabilized, and stained for intracellular IFN-γ (B27, BD). Events were acquired on a FACSCalibur flow cytometer and analyzed using CellQuestversion 3.3 (both from BD).

Measurement of cytotoxicity. The cytolytic activity of CD19-CAR cells was determined by a 4-hour chromium release assay (13). CD19-CAR cells were incubated with 5×10^3 ^{51}Cr-labeled target cells in V-bottomed 96-well plates (Costar). The percentage of specific cytolysis was calculated from the release of ^{51}Cr, as described, using a TopCount NXT (Perkin-Elmer).

Statistics. Statistical analysis was done with GraphPad Prism v4. A P value of <0.05 was used to reject the null hypothesis. Data are presented as mean (±SD) unless otherwise stated. P values are for two-tailed paired t tests.

Results

Proliferative alloresponses of CD19-CAR cells were specifically reduced after alloanergization. We screened CD19-CAR T-cell lines from six adult donors for secondary

Published OnlineFirst April 27, 2010; DOI:10.1158/0008-5472.CAN-09-3845

(recall) alloproliferative responses after allostimulation (priming) and subsequent allorestimulation with γ-irradiated PBMC from 18 different unrelated adult volunteers. Secondary alloproliferative responses were detectable in all CD19-CAR T-cell lines. We next examined the efficacy and specificity of alloanergization in reducing secondary alloresponses. Viability of CD19-CAR cells was similar before (87 ± 7%, $CD4^+$ and 92 ± 4%, $CD8^+$) and after alloanergization (83 ± 11%, $CD4^+$ and 90 ± 5%, $CD8^+$). Alloanergized CD19-CAR cells were hyporesponsive to first-party allorestimulation. This was not due to a change in kinetics of the alloproliferative response (Fig. 2A). Reduction of peak first-party–specific alloproliferation after alloanergization was seen in all CD19-CAR cell lines, whereas there was no significant change in third-party–specific alloproliferation or mitogen-stimulated proliferation, showing that hyporesponsiveness was specific to alloantigens used during alloanergization (Fig. 2B). The median efficiency of alloanergization was 82% (range, 33–96%) with a median 5.4-fold (range, 1.5–26) reduction in first-party alloproliferative responses. Third-party and mitogen-stimulated proliferation were not reduced (Fig. 2C). These data show that alloanergization specifically reduced alloproliferation of CD19-CAR cells, consistent with our previous data for alloanergization of nongenetically modified human PBMC (26, 35).

The use of CD19-depleted allostimulators resulted in a further reduction of residual alloresponses after alloanergization of CD19-CAR cells. Proliferation of CD19-CAR cells after stimulation with allogeneic PBMC containing $CD19^+$ cells could result either from alloantigen-specific stimulation via endogenous TCR or from direct CD19-mediated stimulation via introduced CAR. The latter could provide a confounding factor in our proliferation assays. Therefore, we sought to determine whether the presence of $CD19^+$ cells within allostimulator PBMC affected the residual proliferation of alloanergized CD19-CAR cells. We depleted $CD19^+$ cells from allostimulator PBMC before γ-irradiation, resulting in a median 500-fold reduction in $CD19^+$ cells. Proliferative responses after allorestimulation of nonanergized CAR^+ T cells were retained using CD19-depleted allostimulator PBMC, consistent with retention of allostimulatory capacity. However, the use of CD19-depleted allostimulator PBMC resulted in a lower residual proliferation after allorestimulation of alloanergized CAR^+ T cells compared with the use of unsorted allostimulator PBMC, suggesting that a direct stimulatory effect mediated by $CD19^+$ cells within allostimulator PBMC contributed to the

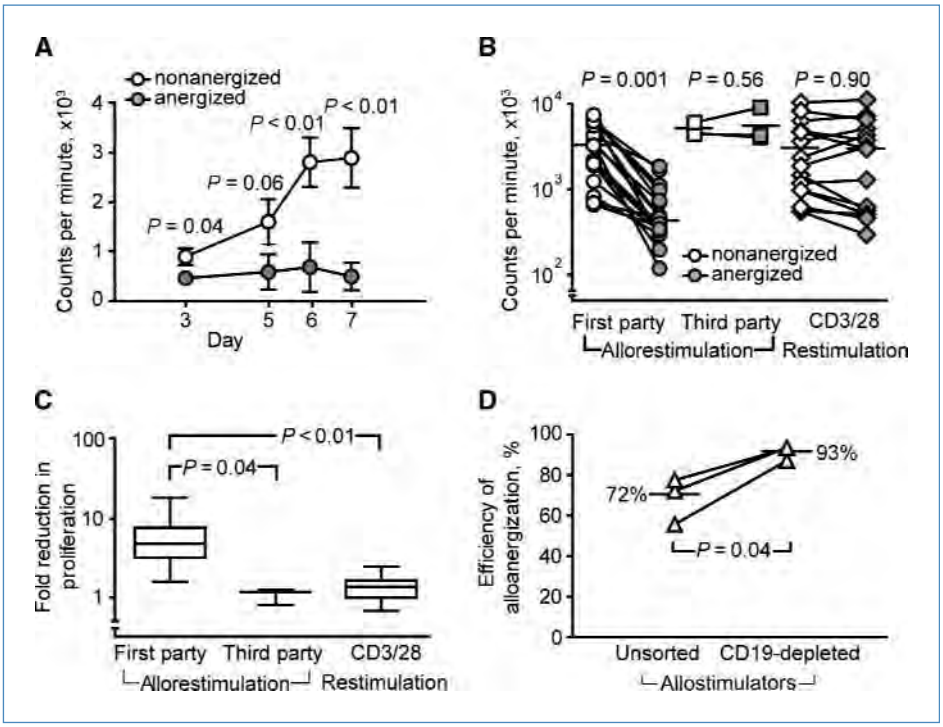

Figure 2. Alloproliferation of CD19-CAR cells is specifically reduced by alloanergization. A, mean values for proliferation ([^{3}H]thymidine incorporation) of nonanergized and alloanergized CD19-CAR cells after allorestimulation for 18 stimulator-responder pairs; bars, SD. B, peak proliferation in nonanergized and alloanergized CD19-CAR cells after restimulation with first- or third-party allostimulators or mitogenic CD3 and CD28 antibodies. Symbols, means of triplicate values for unique stimulator-responder pairs; horizontal bars, mean values for all pairs. C, fold reduction in proliferation of alloanergized CD19-CAR cells (compared with nonanergized cells) after restimulation with allostimulators or mitogen is shown as box-and-whisker plots. Horizontal bars, medians; boxes, interquartile range; whiskers, minimum and maximum values. D, efficiency of alloanergization of CD19-CAR cells using unsorted PBMC or $CD19^+$ B-cell–depleted PBMC as allostimulators. Results depict three separate experiments; horizontal bars and adjacent numbers depict median values.

Published OnlineFirst April 27, 2010; DOI:10.1158/0008-5472.CAN-09-3845

residual proliferation after alloanergization. As a result, measured efficiency of alloanergization was significantly higher (median, 93%; range, 87–94%) using CD19-depleted allostimulator PBMC when compared with unsorted allostimulator PBMC (median, 72%; range, 55–77%; $P = 0.04$; Fig. 2D).

Alloanergization reduced alloproliferation in both CD4$^+$ and CD8$^+$ CD19-CAR cells. As the propagated CD19-CAR cells contained both CD4$^+$ and CD8$^+$ T cells, we next determined whether alloanergization reduced alloproliferation in both cellular subsets. We labeled CD19-CAR cells with CFSE before allorestimulation and measured proliferation by CFSE dilution. After 6 days of allorestimulation, 21% (±6.2%) and 15% (±6.1%) of nonanergized CD4$^+$ and CD8$^+$ CD19-CAR cells had proliferated. This represented median CD4$^+$ and CD8$^+$ alloprecursor frequencies of 1.5% (range, 1.0–1.8%) and 1.4% (range, 1.3–1.9%), respectively. In contrast, the mean percentages of CD4$^+$ and CD8$^+$ T cells proliferating after allorestimulation of alloanergized CD19-CAR cells were significantly lower at 6.9% (±4.7%) and 4.1% (±3.6%), respectively. Importantly, proliferation of both CD4$^+$ and CD8$^+$ CD19-CAR cells after mitogenic stimulation was unaffected by alloanergization (Table 1). Thus, CD19-CAR cells contain both alloproliferative CD4$^+$ and CD8$^+$ T cells, and alloproliferation in both these subsets was specifically reduced after alloanergization.

Alloanergization of CD19-CAR cells reduced allospecific cytokine production. Alloreactive human CD4$^+$ and CD8$^+$ T cells secrete proinflammatory cytokines (predominantly IFN-γ and TNF-α) after HLA-mismatched allostimulation (34). Therefore, we used ICC to examine the effect of alloanergization on allospecific cytokine responses of CD19-CAR cells. Allospecific cytokine$^+$ T cells were detected within CD19-CAR T-cell populations with cell frequencies of 3.8% (±2.7%, CD4$^+$IFN-γ$^+$), 0.8% (±0.7%, CD8$^+$IFN-γ$^+$), 2.5% (±1.4%, CD4$^+$TNF-α$^+$), and 0.8% (±0.7%, CD8$^+$TNF-α$^+$). Allospecific cytokine$^+$ T-cell frequencies were reduced in alloanergized CD19-CAR cells to cell frequencies of 0.4% (±0.2%, CD4$^+$IFN-γ$^+$), 0.15% (±0.1%, CD8$^+$IFN-γ$^+$), 0.20% (±0.1%, CD4$^+$TNF-α$^+$), and 0.17% (±0.02% CD8$^+$ TNF-α$^+$). This represented median fold reductions of 11 (range, 3–17; CD4$^+$IFN-γ$^+$), 15 (range, 5–25; CD4$^+$TNF-α$^+$), 2.3 (range, 1.7–19; CD8$^+$IFN-γ$^+$), and 2.6 (range, 1.8–10; CD8$^+$TNF-α$^+$). In contrast, CD19-specific cytokine responses after stimulation with CD19$^+$ Daudi and U251T targets were only modestly reduced after alloanergization. CD19-specific IFN-γ$^+$ cell frequencies were 49% (nonanergized) and 26% (anergized; Daudi) and 50% (nonanergized) and 38% (alloanergized; CD19$^+$ U251T), representing 1.9- and 1.3-fold reductions, respectively (Fig. 3). This showed that alloanergization preferentially reduced allospecific cytokine responses within CD19-CAR cells while maintaining the majority (but not all) of CD19-specific responses.

Phenotypic characteristics of CD19-CAR cells after alloanergization. Although the proportion of CD8$^+$ CD19-CAR cells expressing surface CAR was not affected by alloanergization, the proportion of CD4$^+$ CD19-CAR cells expressing surface CAR was temporarily reduced by up to 50%. The majority of CD19-CAR cells were CD45RO$^+$CD27^{neg} memory cells both before and after alloanergization. Using coexpression patterns of CD28 and Fas (CD95) to distinguish CD28^{neg}CD95$^+$ effector memory T cells (T_{EM}) from CD28$^+$CD95$^+$ central memory (T_{CM}) cells (36), we were able to identify similar proportions of T_{CM} (24.2% and 37.2%) and T_{EM} (75.8% and 62.8%) cells before and after alloanergization of CD19-CAR cells. Using coexpression patterns of CD45RO and CD62L (37), CD19-CAR cells also contained similar proportions of T_{CM} cells (31.0% and 45.7%) and T_{EM} cells (69.0% and 53.8%) before and after alloanergization (Fig. 4A). This is consistent with CAR transgene expression in T_{CM} cells and preservation of these cells after alloanergization.

Table 1. Percent of CD4$^+$ and CD8$^+$ subsets of nonalloanergized and alloanergized CD19-specific CAR$^+$ T cells proliferating after restimulation with alloantigens or mitogenic CD3 and CD28 antibodies

	Allorestimulation		Mitogen restimulation	
	CD4$^+$	CD8$^+$	CD4$^+$	CD8$^+$
Nonalloanergized cells	21 (±6.2)	15 (±6.1)	53 (±5.1)	48 (±3.6)
Alloanergized cells	6.9 (±4.7)	4.1 (±3.6)	61 (±8.4)	59 (±9.7)
*P**	0.01	0.02	0.30	0.22

NOTE: Numbers in parentheses indicate SD.
*Two-tailed paired *t* test comparing values for nonalloanergized and alloanergized cells.

CD19-specific cytolytic function of CD19-CAR cells was preserved after alloanergization. CD19-CAR cells were evaluated for redirected killing before and after alloanergization in a 4-hour ^{51}Cr release assay (Fig. 4B). CD19-CAR cells effectively lysed CD19$^+$ B-cell lines before and after alloanergization (Daudi: before, 59.4%; after, 56.7%; NALM-6: before, 29%; after, 26.7% at an effector/target ratio of 20:1). Retention of CD19 specificity was shown by the 1.8-fold (before alloanergization) and 2.2-fold (after alloanergization) increased killing of CD19$^+$ targets when compared with CD19^{neg} K562 targets at an effector/target ratio of 20:1. In comparison, alloanergization resulted in a 5-fold reduction in lysis of cultured first-party allogeneic target cells at an effector/target ratio of 20:1 (Fig. 4C).

CD19-specific proliferation of CD19-CAR cells after alloanergization. We next compared the capacity for CAR-dependent proliferation of nonanergized and alloanergized CD19-CAR cells using CD19$^+$ aAPC without or with CD64 (FcγRI)-loaded OKT3 (to provide an additional CD3-dependent antigen-independent proliferative signal). The numbers of nonanergized CD19-CAR cells were expanded by 3 to 4 log over 21 days on both CD19$^+$ aAPC and OKT3-loaded CD19$^+$ aAPC. Alloanergized CD19-CAR cells retained the capacity to expand on both CD19$^+$ aAPC and OKT3-loaded CD19$^+$ aAPC, with a 2- to 2.5-log expansion over 21

Published OnlineFirst April 27, 2010; DOI:10.1158/0008-5472.CAN-09-3845

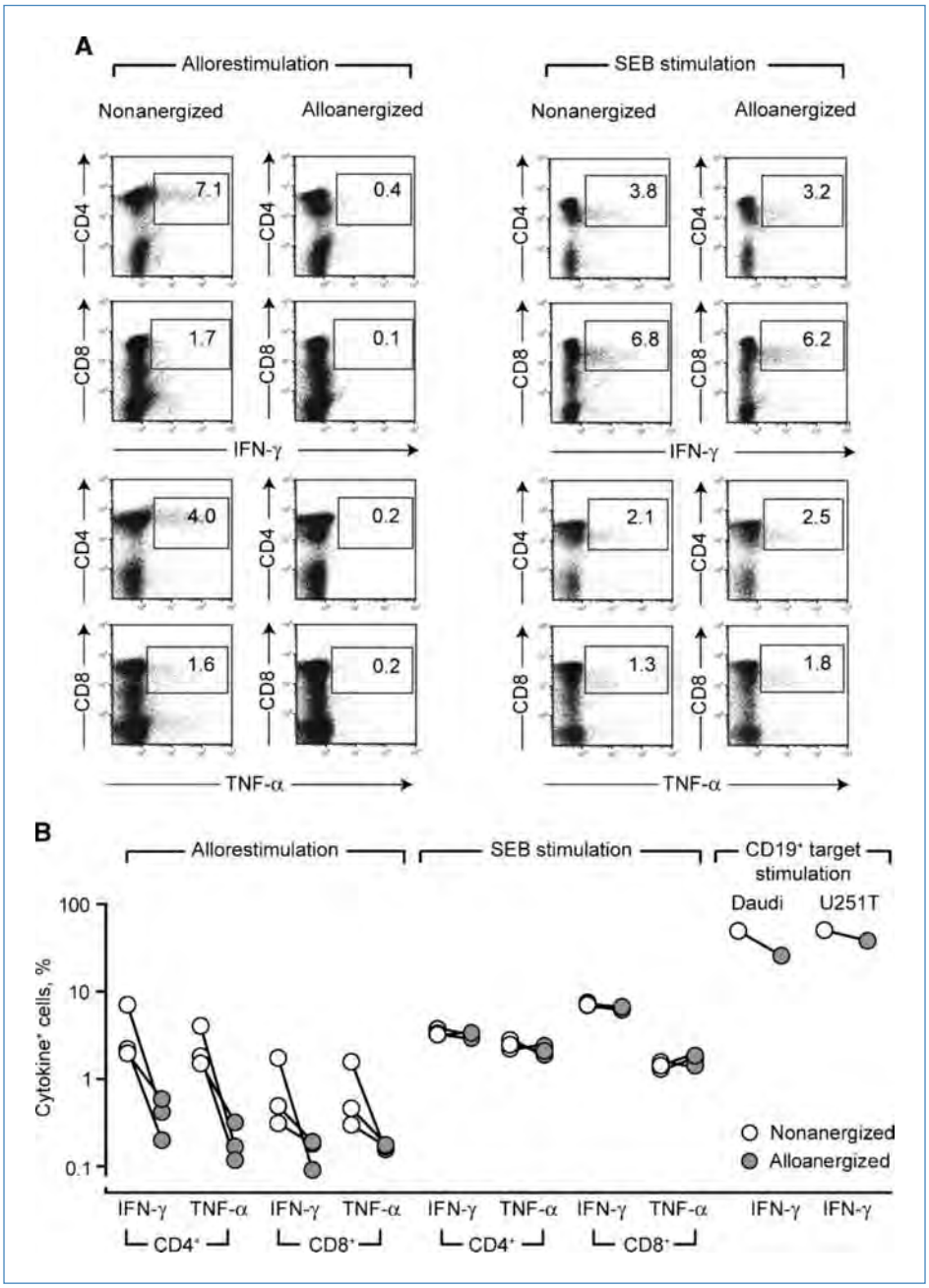

Figure 3. Alloanergization of CD19-CAR cells results in reduced allospecific cytokine production. A, cytokine secretion by nonanergized and alloanergized CD19-CAR cells after restimulation with allostimulators or SEB. Flow cytometer dot plots are shown depicting intracellular cytokine production in $CD4^+$ and $CD8^+$ cells, gated on $CD3^+$ events excluding irradiated stimulator cells. Boxed regions represent $cytokine^+$ events and numbers represent frequency of $cytokine^+$ events expressed as a percentage of $CD4^+$ or $CD8^+$ cells. Results are shown for a representative experiment of three. B, frequencies of $cytokine^+$ cells in nonanergized and alloanergized CD19-CAR cells after restimulation with allostimulators, SEB, or $CD19^+$ target cells.

days. Although CD19-dependent expansion was 1 to 2 log less than that seen in nonanergized CD19-CAR cells, the retention of capacity to proliferate in a CAR-dependent manner implies that alloanergization did not substantially interfere with the ability of the CAR to provide and sustain a proliferative signal. In contrast, alloanergized CD19-CAR cells could not be expanded by repeat stimulation with first-party allostimulators (Fig. 5A). Furthermore, expansion of alloanergized CD19-CAR cells on OKT3-loaded $CD19^+$ aAPC restored the proportion of $CD4^+$ CD19-CAR cells expressing surface CAR to similar levels seen in nonalloanergized cells (Fig. 5B). Importantly, alloanergized CD19-CAR cells remained hyporesponsive to allostimulation after *in vitro* expansion on $CD19^+$ aAPC (Fig. 5C). Finally, to confirm that CD19-expanded alloanergized CAR^+ cells retained effector function, we again examined CD19-specific IFN-γ production. *In vitro* expanded alloanergized CD19-CAR cells retained up to 70% of their capacity to produce IFN-γ after contact with cell-surface CD19 when compared with expanded nonanergized CD19-CAR cells. Intracellular cytokine staining showed a 3-fold increase in IFN-γ production when alloanergized CD19-CAR cells were stimulated with a $CD19^+$ B-cell line (Daudi). IFN-γ production

Published OnlineFirst April 27, 2010; DOI:10.1158/0008-5472.CAN-09-3845

was 1.6-fold greater when alloanergized cells were stimulated with CD19$^+$ transfected U251T glioma cells in comparison with CD19^{neg} U251T cells, showing the CD19 specificity of IFN-γ production (Fig. 5D). These data are consistent with retention of capacity of expanded alloanergized CD19-CAR cells to be activated via the introduced CD19-CAR.

Discussion

Disease relapse remains a major cause of treatment failure after allogeneic HSCT, especially in patients with advanced B-cell malignancies. A significant unmet need, therefore, is a clinically applicable strategy to enhance the antitumor effect of allogeneic donor T cells. In the present study, we have developed such a strategy by combining the approaches of redirection of human donor T cells to the B-cell antigen CD19 and alloanergization to reduce the potential of such cells to mediate GvHD. We show that the strategy of alloanergization effectively reduces alloresponses without adversely affecting the CD19-specifc effector functions of CD19-CAR cells. This combined approach could be used to reduce relapse without increasing toxicity after allogeneic HSCT for patients with B-lineage leukemias and lymphomas.

A major concern with the infusion of allogeneic CAR$^+$ T cells is their potential to mediate toxicity in the form of GvHD. CAR$^+$ T cells can be activated by pathogen-specific antigens via their endogenous αβ TCR, indicating that these receptors and their associated intracellular pathways remain functionally intact (7, 30, 38). We have previously shown that CD19-CAR cells generated using the *SB* technology retain broad endogenous αβ TCR Vβ distribution (18), in apparent contrast to some other strategies used to enrich antigen-specific T cells using repetitive antigenic stimulation (39). It has also been shown that murine and human folate-binding protein–specific CAR$^+$ T cells can be activated via endogenous αβ TCR by stimulation with alloantigens, supporting the potential of such cells to mediate alloresponses (40). In our current study, we detected CD4$^+$ alloprecursor frequencies within human CD19-CAR cells at comparable levels to those detected by CFSE dye dilution in unmanipulated human CD4$^+$ T cells by Martins and colleagues (1.1%), who, in common with our strategy, used single-donor allostimulator PBMC (34). This suggests that alloproliferative CD4$^+$ T cells occur at a similar frequency within human CD19-CAR cells and unmanipulated T cells.

Alloanergization of CD19-CAR cells effectively and specifically reduced proliferative and cytokine alloresponses in these cells. When the confounding effect of CD19-driven proliferation was removed (by using CD19-depleted allostimulators in both the alloanergization step and in assays to detect

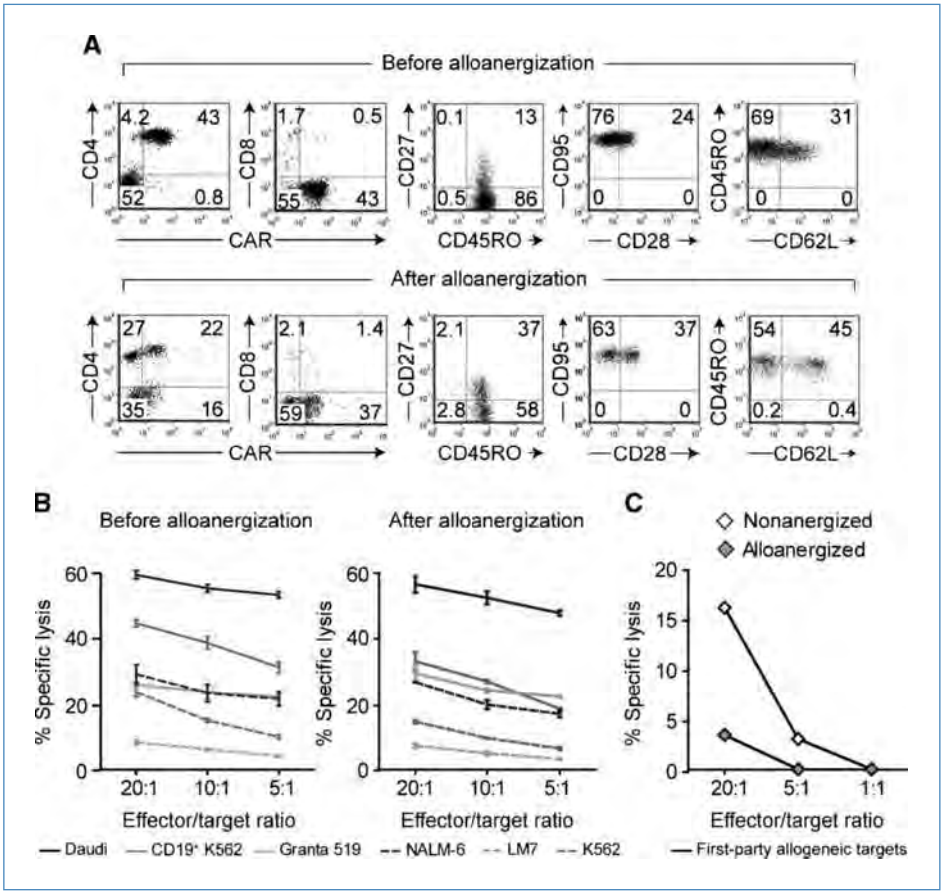

Figure 4. Characterization of CD19-CAR cells before and after alloanergization. A, representative flow cytometry dot plots showing cell-surface expression of CD19-CAR on CD4$^+$ and CD8$^+$ T cells and proportions of CD19-CAR cells with memory T cells (CD27^{neg}CD45RO$^+$) and central memory cells (T_{CM}, defined as CD28$^+$CD95$^+$ or CD62L$^+$CD45RO$^+$) before and after alloanergization. Numbers represent percentages of cells in each quadrant. B, killing of CD19$^+$ target cells (Granta 519; NALM-6; HLA class I^{neg} Daudi; HLA class I/II^{neg} K562 cells transfected to express truncated CD19) in a 4-hour ^{51}Cr release assay by nonanergized and alloanergized CD19-CAR cell effectors. Background lysis of CD19^{neg} (parental K562 and LM7) cells is also shown. Points, mean specific lysis of triplicate wells; bars, SD. C, killing of cultured first-party allogeneic targets by CD19-CAR cell effectors in a 4-hour ^{51}Cr release assay. Results from a representative experiment of two are shown.

Published OnlineFirst April 27, 2010; DOI:10.1158/0008-5472.CAN-09-3845

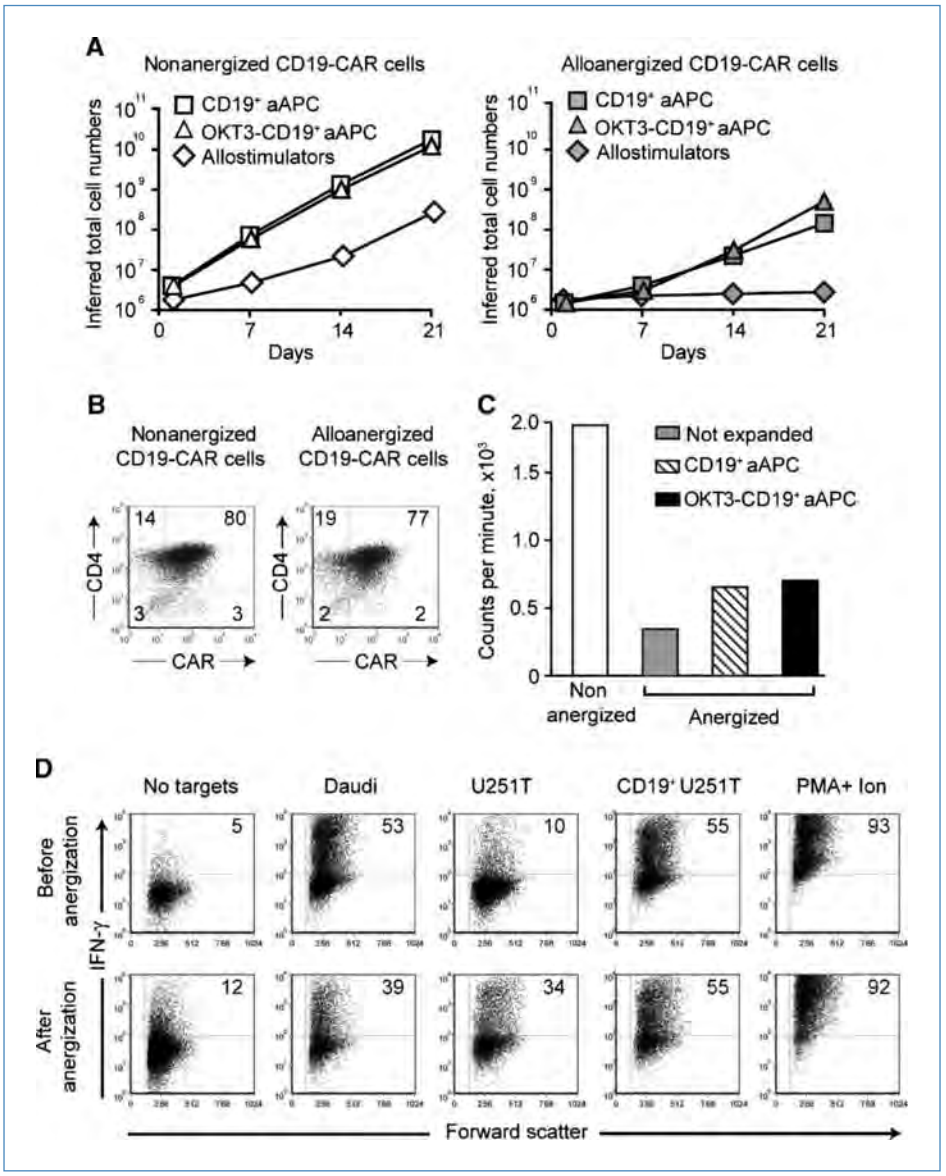

Figure 5. CD19-dependent expansion of alloanergized CD19-CAR cells. A, expansion of nonanergized and alloanergized CD19-CAR cells on $CD19^+$ aAPC, OKT3-loaded $CD19^+$ aAPC, and first-party allostimulators. B, expression of surface CAR on nonanergized and alloanergized $CD4^+$ CD19-CAR cells after 21 days of expansion on OKT3-loaded $CD19^+$ aAPC. Numbers represent percentages of cells in each quadrant. C, first-party alloproliferation ($[^3H]$ thymidine incorporation) of nonanergized, alloanergized, and alloanergized then aAPC-expanded CD19-CAR cells after first-party allostimulation. D, CD19-specific intracellular IFN-γ secretion of aAPC-expanded CD19-CAR cells before and after alloanergization following incubation with $CD19^-$ and $CD19^+$ stimulator cells. Events are gated on $CD3^+$ lymphocytes. Numbers represent percentages of cells in each quadrant.

residual alloreactivity), the efficiency of alloanergization of CD19-CAR cells was >90%. This was consistent with both our previous published data and other effective strategies used to reduce alloreactivity of HLA-mismatched PBMC (23, 26). Because our strategy of alloanergization only directly affects $CD28^+$ T cells, the strategy could theoretically be less effective at reducing alloresponses in $CD8^+$ CD19-CAR cells than in $CD4^+$ CD19-CAR cells, as human $CD8^+$ T cells typically contain a lower proportion of $CD28^+$ cells compared with human $CD4^+$ T cells. However, alloanergization reduced alloproliferative responses effectively in both $CD4^+$ and $CD8^+$ CD19-CAR cells. This may reflect an indirect effect on $CD8^+$ T cells consequent to alloanergization of $CD4^+$ T cells, consistent with reports that alloproliferative $CD4^+$ T cells are required for alloreactive $CD8^+$ T cells to proliferate (34, 41). The concern remains that $CD4^+CD28^{neg}$ T_{EM}–mediated alloresponses may persist after alloanergization. However, clinically significant GvHD mediated by such cells is likely to be limited. T_{EM} cells are less potent mediators of proliferative alloresponses *in vitro* than T_{CM} or naïve human T cells (42), and human $CD28^{neg}$ T cells typically have shortened telomeres compared with $CD28^+$ T cells (43), predicting a restricted life span *in vivo* after infusion (44).

Alloanergization did not reduce the proportion of $CD8^+$ CD19-CAR cells expressing surface CAR, and CD19-specific redirected target cell cytolysis was preserved, demonstrating retained functionality and specificity. However, alloanergization resulted in modest reductions in the proportion of $CD4^+$ CD19-CAR cells expressing surface CAR, frequencies of CD19-specific IFN-γ^+ cells, and capacity for CD19-CAR cells to expand *in vitro* after stimulation on $CD19^+$ aAPC. These findings suggest that the *in vivo* efficacy of alloanergized

Published OnlineFirst April 27, 2010; DOI:10.1158/0008-5472.CAN-09-3845

CD19-CAR cells could be reduced in comparison with nonanergized cells. However, more than half of $CD4^+$ CD19-CAR cells expressing cell-surface CAR and 50% to 70% of the proportion of CD19-CAR cells secreting IFN-γ^+ after CD19 stimulation were retained after alloanergization, and CD19-specific proliferation was still demonstrable, consistent with retention of significant capacity for CD19-specific expansion and target cell lysis. Furthermore, it is likely that homeostatic expansion resulting from the lymphopenic environment created after allogeneic HSCT would augment expansion and persistence of infused alloanergized donor CD19-CAR cells. This is supported by the data from *in vitro* expansion of alloanergized CD19-CAR cells on CD19-aAPC loaded with OKT3, which restored the proportion of $CD4^+$ CD19-CAR cells expressing surface CAR to levels seen in nonalloanergized cells without loss of allospecific hyporesponsiveness, suggesting that CD19-specific function and alloanergy might be maintained after expansion. Further studies using an immunodeficient tumor-bearing mouse model could be used to compare the *in vivo* persistence and antitumor efficacy of nonanergized and alloanergized human CD19-CAR cells.

Allogeneic CD19-CAR cells could be used to augment antitumor effects in a variety of allogeneic HSCT settings. These data support the application of a clinical strategy in which CD19-CAR cells are generated from allogeneic donors and subsequently anergized to recipient alloantigens before infusion after allogeneic HSCT. The broad endogenous TCR Vβ subfamily distribution retained by CD19-CAR cells generated using the SB system (18) suggests that these cells could also contribute to pathogen-specific immunity after allogeneic HSCT via their endogenous αβ TCR. Therefore, allogeneic HSCT approaches using T-cell–depleted hematopoietic stem cell sources or umbilical cord blood cells, both of which are associated with delayed immune reconstitution and increased infectious complications (45–47), would be particularly suitable platforms for the use of allogeneic donor CD19-CAR cells. Although we are developing approaches to limit off-target effects, one consequence of allogeneic CD19-CAR T-cell therapy might be destruction of healthy donor–derived $CD19^+$ B cells. Intravenous immunoglobulin could be used to correct clinically significant hypogammaglobulinemia in such an event. Another potential limitation to our approach is that repeated *in vivo* stimulation may contribute to replicative senescence of CD19-CAR cells via telomere erosion (48) and preclude their long-term persistence. In this case, repeat infusions of alloanergized CD19-CAR cells could provide a persistent antitumor effect.

In summary, we describe the successful application of alloanergization to selectively reduce alloreactivity in human CD19-specific T cells without significant impairment of CAR-dependent effector functions. Nonviral gene transfer of CAR, propagation on aAPC, and induction of alloanergy all use methods currently individually in use in phase 1/2 clinical trials. These approaches could therefore be readily applied in combination at a clinical scale to generate donor-derived T cells engineered to contain enhanced antitumor activity, but reduced alloreactivity, suitable for use after allogeneic HSCT to reduce disease relapse while limiting toxicity from GvHD.

Disclosure of Potential Conflicts of Interest

No potential conflicts of interest were disclosed.

Acknowledgments

We thank Dr. Perry Hackett (University of Minnesota, Minneapolis, MN) for the *Sleeping Beauty* system, Dr. Carl June (University of Pennsylvania, Philadelphia, PA) for assistance in generating the K562-aAPC, and Karen Ramirez and David He (Flow Cytometry Core Laboratory, M.D. Anderson Cancer Center; NIH grant 5P30CA016672-32) for technical assistance.

Grant Support

PO1 (CA100265), CCSG (CA16672), RO1s (CA124782, CA120956), R21s (CA129390, CA116127, CA137645), DOD (PR064229), Alex Lemonade Stand Foundation, Alliance for Cancer Gene Therapy, Burroughs Wellcome Fund, Department of Veterans Affairs, Gillson Longenbaugh Foundation, Leukemia and Lymphoma Society, Lymphoma Research Foundation, Miller Foundation, National Foundation for Cancer Research, Pediatric Cancer Research Foundation, National Marrow Donor Program, and William Lawrence and Blanche Hughes Foundation.

The costs of publication of this article were defrayed in part by the payment of page charges. This article must therefore be hereby marked *advertisement* in accordance with 18 U.S.C. Section 1734 solely to indicate this fact.

Received 10/19/2009; revised 02/04/2010; accepted 03/01/2010; published OnlineFirst 04/27/2010.

References

1. Kiehl MG, Kraut L, Schwerdtfeger R, et al. Outcome of allogeneic hematopoietic stem cell transplantation in adult patients with acute lymphoblastic leukemia: no difference in related compared with unrelated transplant in first complete remission. J Clin Oncol 2004;22:2816–25.
2. MacMillan ML, Davies SM, Nelson GO, et al. Twenty years of unrelated donor bone marrow transplantation for pediatric acute leukemia facilitated by the National Marrow Donor Program. Biol Blood Marrow Transplant 2008;14:16–22.
3. Levine JE, Harris RE, Loberiza FR, Jr., et al. A comparison of allogeneic and autologous bone marrow transplantation for lymphoblastic lymphoma. Blood 2003;101:2476–82.
4. Eshhar Z, Waks T, Gross G, Schindler DG. Specific activation and targeting of cytotoxic lymphocytes through chimeric single chains consisting of antibody-binding domains and the γ or ζ subunits of the immunoglobulin and T-cell receptors. Proc Natl Acad Sci U S A 1993;90:720–4.
5. Sadelain M, Riviere I, Brentjens R. Targeting tumours with genetically enhanced T lymphocytes. Nat Rev Cancer 2003;3:35–45.
6. Till BG, Jensen MC, Wang J, et al. Adoptive immunotherapy for indolent non-Hodgkin lymphoma and mantle cell lymphoma using genetically modified autologous CD20-specific T cells. Blood 2008;112:2261–71.
7. Pule MA, Savoldo B, Myers GD, et al. Virus-specific T cells engineered to coexpress tumor-specific receptors: persistence and antitumor activity in individuals with neuroblastoma. Nat Med 2008;14:1264–70.
8. Kershaw MH, Westwood JA, Parker LL, et al. A phase I study on adoptive immunotherapy using gene-modified T cells for ovarian cancer. Clin Cancer Res 2006;12:6106–15.

Published OnlineFirst April 27, 2010; DOI:10.1158/0008-5472.CAN-09-3845

9. Lamers CH, Sleijfer S, Vulto AG, et al. Treatment of metastatic renal cell carcinoma with autologous T-lymphocytes genetically retargeted against carbonic anhydrase IX: first clinical experience. J Clin Oncol 2006;24:e20–2.
10. Park JR, Digiusto DL, Slovak M, et al. Adoptive transfer of chimeric antigen receptor re-directed cytolytic T lymphocyte clones in patients with neuroblastoma. Mol Ther 2007;15:825–33.
11. Nadler LM, Anderson KC, Marti G, et al. B4, a human B lymphocyte-associated antigen expressed on normal, mitogen-activated, and malignant B lymphocytes. J Immunol 1983;131:244–50.
12. Brentjens RJ, Latouche JB, Santos E, et al. Eradication of systemic B-cell tumors by genetically targeted human T lymphocytes costimulated by CD80 and interleukin-15. Nat Med 2003;9:279–86.
13. Cooper LJ, Topp MS, Serrano LM, et al. T-cell clones can be rendered specific for CD19: toward the selective augmentation of the graft-versus-B-lineage leukemia effect. Blood 2003;101:1637–44.
14. Kowolik CM, Topp MS, Gonzalez S, et al. CD28 costimulation provided through a CD19-specific chimeric antigen receptor enhances *in vivo* persistence and antitumor efficacy of adoptively transferred T cells. Cancer Res 2006;66:10995–1004.
15. Milone MC, Fish JD, Carpenito C, et al. Chimeric receptors containing CD137 signal transduction domains mediate enhanced survival of T cells and increased antileukemic efficacy *in vivo*. Mol Ther 2009;17:1453–64.
16. Huang X, Guo H, Kang J, et al. Sleeping Beauty transposon-mediated engineering of human primary T cells for therapy of CD19+ lymphoid malignancies. Mol Ther 2008;16:580–9.
17. Peng PD, Cohen CJ, Yang S, et al. Efficient nonviral Sleeping Beauty transposon-based TCR gene transfer to peripheral blood lymphocytes confers antigen-specific antitumor reactivity. Gene Ther 2009;16:1042–9.
18. Singh H, Manuri PR, Olivares S, et al. Redirecting specificity of T-cell populations for CD19 using the Sleeping Beauty system. Cancer Res 2008;68:2961–71.
19. Williams DA. Sleeping beauty vector system moves toward human trials in the United States. Mol Ther 2008;16:1515–6.
20. Cox CV, Evely RS, Oakhill A, Pamphilon DH, Goulden NJ, Blair A. Characterization of acute lymphoblastic leukemia progenitor cells. Blood 2004;104:2919–25.
21. Hotfilder M, Rottgers S, Rosemann A, et al. Leukemic stem cells in childhood high-risk ALL/t(9;22) and t(4;11) are present in primitive lymphoid-restricted CD34+CD19– cells. Cancer Res 2005;65:1442–9.
22. Cavazzana-Calvo M, Fromont C, Le Deist F, et al. Specific elimination of alloreactive T cells by an anti-interleukin-2 receptor B chain-specific immunotoxin. Transplantation 1990;50:1–7.
23. Amrolia PJ, Muccioli-Casadei G, Yvon E, et al. Selective depletion of donor alloreactive T cells without loss of antiviral or antileukemic responses. Blood 2003;102:2292–9.
24. Mielke S, Nunes R, Rezvani K, et al. A clinical scale selective allodepletion approach for the treatment of HLA-mismatched and matched donor-recipient pairs using expanded T lymphocytes as antigen-presenting cells and a TH9402-based photodepletion technique. Blood 2007;111:4392–402.
25. Gimmi CD, Freeman GJ, Gribben JG, Gray G, Nadler LM. Human T-cell clonal anergy is induced by antigen presentation in the absence of B7 costimulation. Proc Natl Acad Sci U S A 1993;90:6586–90.
26. Davies JK, Yuk D, Nadler LM, Guinan EC. Induction of alloanergy in human donor T cells without loss of pathogen or tumor immunity. Transplantation 2008;86:854–64.
27. Tan P, Anasetti C, Hansen JA, et al. Induction of alloantigen-specific hyporesponsiveness in human T lymphocytes by blocking interaction of CD28 with its natural ligand B7/BB1. J Exp Med 1993;177:165–73.
28. Guinan EC, Boussiotis VA, Neuberg D, et al. Transplantation of anergic histoincompatible bone marrow allografts. N Engl J Med 1999;340:1704–14.
29. Davies JK, Gribben JG, Brennan LL, Yuk D, Nadler LM, Guinan EC. Outcome of alloanergized haploidentical bone marrow transplantation after *ex vivo* costimulatory blockade: results of 2 phase 1 studies. Blood 2008;112:2232–41.
30. Cooper LJ, Al-Kadhimi Z, Serrano LM, et al. Enhanced antilymphoma efficacy of CD19-redirected influenza MP1-specific CTLs by cotransfer of T cells modified to present influenza MP1. Blood 2005;105:1622–31.
31. Serrano LM, Pfeiffer T, Olivares S, et al. Differentiation of naive cord-blood T cells into CD19-specific cytolytic effectors for posttransplantation adoptive immunotherapy. Blood 2006;107:2643–52.
32. Manuri PV, Wilson MH, Maiti SN, et al. piggyBac transposon/transposase system to generate CD19-specific T cells for the treatment of B-lineage malignancies. Hum Gene Ther 2010;21:1–11.
33. Godfrey WR, Krampf MR, Taylor PA, Blazar BR. *Ex vivo* depletion of alloreactive cells based on CFSE dye dilution, activation antigen selection, and dendritic cell stimulation. Blood 2004;103:1158–65.
34. Martins SL, St John LS, Champlin RE, et al. Functional assessment and specific depletion of alloreactive human T cells using flow cytometry. Blood 2004;104:3429–36.
35. Gribben JG, Guinan EC, Boussiotis VA, et al. Complete blockade of B7 family-mediated costimulation is necessary to induce human alloantigen-specific anergy: a method to ameliorate graft-versus-host disease and extend the donor pool. Blood 1996;87:4887–93.
36. Berger C, Jensen MC, Lansdorp PM, Gough M, Elliott C, Riddell SR. Adoptive transfer of effector CD8+ T cells derived from central memory cells establishes persistent T cell memory in primates. J Clin Invest 2008;118:294–305.
37. Sallusto F, Geginat J, Lanzavecchia A. Central memory and effector memory T cell subsets: function, generation, and maintenance. Annu Rev Immunol 2004;22:745–63.
38. Savoldo B, Rooney CM, Di Stasi A, et al. Epstein Barr virus specific cytotoxic T lymphocytes expressing the anti-CD30ζ artificial chimeric T-cell receptor for immunotherapy of Hodgkin disease. Blood 2007;110:2620–30.
39. Peggs KS, Verfuerth S, Pizzey A, et al. Adoptive cellular therapy for early cytomegalovirus infection after allogeneic stem cell transplantation with virus-specific T-cell lines. Lancet 2003;362:1375–7.
40. Kershaw MH, Westwood JA, Hwu P. Dual-specific T cells combine proliferation and antitumor activity. Nat Biotechnol 2002;20:1221–7.
41. Nikolaeva N, Uss E, van Leeuwen EM, van Lier RA, ten Berge IJ. Differentiation of human alloreactive CD4+ and CD8+ T cells *in vitro*. Transplantation 2004;78:815–24.
42. Foster AE, Marangolo M, Sartor MM, et al. Human CD62L– memory T cells are less responsive to alloantigen stimulation than CD62L+ naive T cells: potential for adoptive immunotherapy and allodepletion. Blood 2004;104:2403–9.
43. Monteiro J, Batliwalla F, Ostrer H, Gregersen PK. Shortened telomeres in clonally expanded CD28–CD8+ T cells imply a replicative history that is distinct from their CD28+CD8+ counterparts. J Immunol 1996;156:3587–90.
44. Zhou J, Shen X, Huang J, Hodes RJ, Rosenberg SA, Robbins PF. Telomere length of transferred lymphocytes correlates with *in vivo* persistence and tumor regression in melanoma patients receiving cell transfer therapy. J Immunol 2005;175:7046–52.
45. Keever CA, Small TN, Flomenberg N, et al. Immune reconstitution following bone marrow transplantation: comparison of recipients of T-cell depleted marrow with recipients of conventional marrow grafts. Blood 1989;73:1340–50.
46. Chakrabarti S, Mackinnon S, Chopra R, et al. High incidence of cytomegalovirus infection after nonmyeloablative stem cell transplantation: potential role of Campath-1H in delaying immune reconstitution. Blood 2002;99:4357–63.
47. Barker JN, Hough RE, van Burik JA, et al. Serious infections after unrelated donor transplantation in 136 children: impact of stem cell source. Biol Blood Marrow Transplant 2005;11:362–70.
48. Epel ES, Blackburn EH, Lin J, et al. Accelerated telomere shortening in response to life stress. Proc Natl Acad Sci U S A 2004;101:17312–5.